

**TECTONIC EFFECTS ON GEOMORPHOLOGY AND
SEDIMENTATION IN PARTS OF WESTERN BASTAR
CRATON**

Ph.D. THESIS

by

VIJAY SHARMA



**DEPARTMENT OF EARTH SCIENCES
INDIAN INSTITUTE OF TECHNOLOGY ROORKEE
ROORKEE - 247 667 (INDIA)
JULY, 2017**

**TECTONIC EFFECTS ON GEOMORPHOLOGY AND
SEDIMENTATION IN PARTS OF WESTERN BASTAR
CRATON**

A THESIS

*Submitted in partial fulfilment of the
requirements for the award of the degree*

of

DOCTOR OF PHILOSOPHY

in

DEPARTMENT OF EARTH SCIENCES

by

VIJAY SHARMA



**DEPARTMENT OF EARTH SCIENCES
INDIAN INSTITUTE OF TECHNOLOGY ROORKEE
ROORKEE – 247 667 (INDIA)
JULY, 2017**

**©INDIAN INSTITUTE OF TECHNOLOGY ROORKEE, ROORKEE-2017
ALL RIGHTS RESERVED**



INDIAN INSTITUTE OF TECHNOLOGY ROORKEE ROORKEE

CANDIDATE'S DECLARATION

I hereby certify that the work which is being presented in the thesis entitled **“TECTONIC EFFECTS ON GEOMORPHOLOGY AND SEDIMENTATION IN PARTS OF WESTERN BASTAR CRATON”** in partial fulfilment of the requirements for the award of the degree of Doctor of Philosophy and submitted in the Department of Earth Sciences of the Indian Institute of Technology Roorkee, Roorkee, is an authentic record of my own work carried out during a period from July, 2011 to July, 2017 under the supervision of Dr. Pitambar Pati, Assistant Professor, Department of Earth Sciences, Indian Institute of Technology Roorkee, Roorkee.

The matter presented in this thesis has not been submitted by me for the award of any other degree of this or any other institution.

(VIJAY SHARMA)

This is to certify that the above statement made by the candidate is correct to the best of my knowledge.

Dated:

(Pitambar Pati)
Supervisor

ABSTRACT:

The Pranhita-Godavari basin is basically a rift basin between the western Bastar and Eastern Dharwar cratonic nuclei. The study area falls in the NE part of the eastern margin of the Pranhita-Godavari basin near Chandrapur, Maharashtra. Western Bastar craton, here, exhibits the peripheral Proterozoic sedimentary cover. This fossil rift has witnessed several phases of opening and closing in response to the Precambrian tectonics. This rift basin has various synthetic and antithetic faults which have shaped the basin-margin geomorphology and sedimentology by intermittent activities. The established stratigraphy of the region explains the Pakhal, Penganga and the Sullavai Group sediments which are discriminated by unconformable sequences. Multiple episodes of subsidence caused the sediments to adjust in the crustal spaces and deposition of some sedimentary sequences. Previously deposited sequences were very thin as they were just deposited over the Archaean basement.

The region has shown sub-dendritic to sub-parallel drainage patterns and it varies with rocktype and structure of the particular region. The central Neo-Proterozoic part of the region has also shown hydrothermal activity in the form of veins and has reduced the rock porosity and permeability. Therefore, exceptions in the drainage morphology has been recorded as compared to its adjacent regions. The previous westerly slope precluded the sedimentary sequences to move westerly which is supported by the imbricated clasts and palaeocurrent directions through cross bedding. However, the present drainage follows the southerly and easterly directions showing a complete inversion of the drainage in response to the major tectonic activities.

Upper part of the study area along the basin margin, there were closed sub-basinal areas during the Neo-Proterozoic time which has recorded the presence of paleosol embedded within a clastic sedimentary sequence. The magnetic susceptibility and the paleo- weathering data help in the reconstruction of paleoclimate during the formation of the paleosol. Its analysis has revealed low temperatures and high physical weathering which coincides with other parameters. In the middle of the area, lies about a 400m thick limestone sequence (Penganga limestone). Its equivalent has been reported in the western margin of the PG basin. The dolomitic limestone deposited along the basin

margin disintegrated due to various fault activities which caused mass flow on the westerly slope of the basin margin. There are many limestone facies documented in the three major mass-flow events which describe tectonic activities and flow parameters. However, *in-situ* stromatolitic formation in between the mass-flows indicates intermittent tectonically stable periods and origin of life in the basin.

The Ground Penetrating Radar (GPR) was used to acquire subsurface data in relation to unconformity or any fault trace and various profiles have given ample evidences of offlap, onlap and some unconformable surfaces which helped in basin interpretation as well as tectonics associated with it.

Some sedimentary sequences which are common along the basin margin are the fan-delta sequences. Dongargaon fan-delta within study area is one of them. Different sedimentary facies like fine grained sandstone, and intercalatory sandstone-conglomerate sequence and shale facies were mapped on 1:1000 scale to analyze the facies assembles in detail with respect to sea-level fluctuation and subsidence. Basic model for the evolution has been identified and explained on the basis of exhaustive field evidences and it has been correlated with the overall geology and geomorphology of the region to get some inference about the tectonic history and sedimentation of the area.

Eventually, various processes along the basin margin including the formation of fan-delta sequence or mass flow events or some paleosol formation during the period of non-deposition in the fossilized rift basin may conclude about the local basin-margin processes due to tectonism and sedimentation. Also, present geomorphology of the terrain is another manifestation of the same.

ACKNOWLEDGEMENTS

Sometimes words are not enough to say the thoughts or feelings but if anyone shares them, it becomes the cause of his cordial happiness which spreads. Therefore, at times we need to take more out of few words like here.

Paramount and primarily, it is my honour to express deep gratitude towards my *Aadarniya Guru*, **Dr. Pitambar Pati**, for their precious guidance and productive criticism during the tenure of my research work. His thorough knowledge of geology, invaluable advices and persistent support has shaped this thesis to its present form. I am immensely thankful to him for his strength, motivation and passion which took me here. His guidance helped me in all the time of research and writing of this thesis. To him, I shall remain, professionally and emotionally obliged. I could not have imagined having a better advisor and mentor for my Ph.D. work then him.

I am very grateful to the respected research committee members **Prof. R Krishnamurthy**, **Prof. A K Sen** and **Prof. J Das** for sparing their valuable time in monitoring the work progress and providing imperative comments and precious suggestions from time to time which helped me a lot to improve the work and way of thinking.

Respected **Prof. D C Srivastav** (Head, Department of Earth Sciences) is gratefully acknowledged for providing me the necessary research facilities and important ambience to complete this work.

I express my special gratitude to respected **Dr. M L Dora** (Director, Geological Survey of India) for his immense help during the work as well as deep interest in my work. I am also thankful to **Ramnath Barik** (Geologist, GSI) for help during the fieldwork

I am thankful to **Anna Ji** (Freedom Fighter) warden of Vishwa Hindu Aadiwasi Hostel (Gondpipri, Maharashtra) for providing me accommodation and other facilities during my field work. I am very much thankful to **Gajanan ji**, **Namdev ji** and **Jaypal** for their continuous support during the strenuous field work.

It's my fortune to gratefully acknowledge the immense support and help of my friends/labmates **Aditya Kumar Verma**, **Ankit Gupta**, **Narendra Kumar Patel** and

Chinmoy Dash throughout this work in and off the field. I would also like to thanks **Vikas Ahire, Nicky Nishad** and **Parvez Alam** who were my juniors and helped me a lot during my field work programs and off the field.

I feel very lucky to be blessed by the company of wonderful friends like **Keyur Rajpura, Sandan Sharma, Gajendra Gaurav, Neeraj Srivastav, Abhishek Rajput** who have shared their knowledge and wisdom, whenever I needed it most.

I cannot thank enough to my **Parents** and my sister, **Indu** for their everlasting care, huge patience, endless love and blessings in contemplation. They are the real form of God and source of encouragement for all I could do.

There are important persons without whose help, during my work period, made it easier to pull upon otherwise this would have been difficult. I specially thank **Nair ji, Rakesh ji, Bhim ji, Sarvesh ji, Babulal ji, Surendra bhai**, all office staff for being always there and helping me with all the official procedures, sample preparations, thin section preparations and other works for completion of this thesis. I would also like to thank all those who helped me directly or indirectly during various stages of this work.

Above all, to the **Great Almighty**, the imparter of knowledge and wisdom, for his everlasting love and strength that he poured upon me throughout this journey.

CONTENTS

	Page No.
ABSTRACT	i
ACKNOWLEDGEMENT	iii
CONTENTS	v
LIST OF FIGURES	ix
LIST OF TABLES	xv
CHAPTER 1: INTRODUCTION	1
1.1 General Introduction	1
1.2 Location and Accessibility	4
1.3 Physiography and Drainage	4
1.4 Geomorphology	6
1.5 Land Use	6
1.6 Significance of Research	6
1.7 Overview of the previous works	8
1.8 Research aims and objectives	9
1.9 Methodology	10
1.10 Organisation of Thesis	11
CHAPTER 2: REGIONAL GEOLOGY AND STRATIGRAPHY	13
2.1 Introduction	13
2.2 The Pranhita-Godavari rift and the Basin margin overview	14
2.3 Tectonic setup of the region and the study area	18
2.4 Stratigraphic Overview	19
2.5 Geochronology	21

CHAPTER 3: GEOMORPHOLOGICAL EVOLUTION OF THE REGION

3.1	Introduction	23
3.2	Study based on remote sensing	27
3.3	Digital Elevation Model	27
3.4	Hydrological Parameters	30
	3.4.1 Bifurcation ratio	30
	3.4.2 Drainage pattern/Density/Slope	30
	3.4.3 Drainage texture	31
	3.4.4 Stream frequency	31
	3.4.5 Infiltration number	31
	3.4.6 Channel sinuosity	32
3.5	Impact of tectonics on drainage and geomorphology	35
3.6	Lithology and relief interaction	37
3.7	Structural orientation and tectonics	38
3.8	Interpretations	39

CHAPTER 4: FACIES DISTRIBUTION AND THEIR ENVIRONMENTS 41

4.1	Introduction	41
4.2	Different facies observed along the basin margin	45
	Dubarpet region	45
	4.2.1 Conglomerate facies	46
	4.2.2 Sandstone facies	47
	4.2.3 Paleosol	48
	Methodology adopted for paleosol analysis	51
	4.2.3.1 Field mapping and recognition of paleosol	52
	4.2.3.2 Petrography	54
	4.2.3.3 Magnetic Susceptibility	56
	4.2.3.4 XRD analysis	57
	4.2.3.5 Major element geochemistry of the paleosol and its application	59

Chemical index of alteration	61
Clayeness	62
Salinization and Paleotemperature	62
Interpretations	63
Around Gojoli (middle part of the basin margin)	64
4.2.4 Limestone facies	66
4.2.5 Autoclastic massflow conglomerates	66
4.2.6 Massive cherty limestone	70
4.2.6.1 Mass flow associated facies and flow	71
Facies A: Massive cherty limestone	71
Facies B: Stromatolitic limestone	72
Autoclastic mass flow-1	74
Facies C: Tabular and rounded clast-supported conglomerate ungraded	74
Autoclastic mass flow-2	75
Facies D: Matrix supported ungraded conglomerate	75
Facies E: Clast-supported imbricated conglomerate	76
Facies F: Clast-supported conglomerate, normally graded	77
Facies G: Clast-supported conglomerate, reverse graded	78
Facies H: Conglomeratic limestone with rounded clasts	78
Facies I: Fine mud	80
Iron ore facies	81
Dongargaon fan-delta system	83
4.2.7 Facies and fan setting	85
4.2.7.1 Fine grained sandstone facies	87
4.2.7.2 Clast supported conglomerate with intercalating Sandstone facies	89
4.2.7.3 Shale facies	91
4.2.8 Controls and evolutionary pattern of Dongargaon fan delta	92

4.3	Depositional environments in the basin margin	93
4.3.1	Shallow marine environment: marginal swash zone detached, anoxic and cold	94
4.3.2	Shallow marine environment: Supratidal to near shore warm and alkaline	94
4.3.3	Continental shelf environment: Near shore to deep coast line warm and alkaline, below active wave base	95
4.3.4	Shallow marine continental shelf: Intertidal deltaic environment	95
4.3.5	Moderately deep marine continental shelf: Subtidal deltaic environment	96
 CHAPTER 5: SPECIFIC GPR PROFILE BASED ANALYSIS		97
5.1	Introduction	97
5.2	Basic principles about GPR and data collection	98
5.3	Methodology	101
5.3.1	Site selection	101
5.3.2	Instrumentation and data acquisition	102
5.3.3	Data acquisition in point mode	103
5.3.4	Data processing	104
5.3.5	Profiles and interpretation	104
5.3.5.1	Profile AB	105
5.3.5.2	Profile XY	106
5.3.5.3	Profile PQ	108
5.3.5.4	Profile RS	109
 CHAPTER 6: DISCUSSION		113
 CHAPTER 7: CONCLUSION		121
 BIBLIOGRAPHY		125

LIST OF FIGURES

Figure No.	Description	Page No.
Figure 1.1	Tectonic map of India showing distribution of Purana basins, including Vindhyan (V), Chhattisgarh (Ch), Khariar (K), Indravati (I), Pranhita–Godavari (PG), Cuddapah (Cu) and Kaladgi–Bhima (KBB) basins. (Redrawn after Rao & Reddy, 2002).	1
Figure 1.2	Major localities in the study area and their road linking as well as the various lithounit distributions in the study area.	3
Figure 1.3	Type of undulations in the terrain shown in the Digital Elevation Model (DEM) as well as the slope towards the South-East direction.	5
Figure 1.4	The concordant nature of higher order streams with the basin margin structures (Lineaments after Das et al., 2003)..	7
Figure 2.1	Geological map of the study area (after J.P. Dias and others. 1965-66, GSI) and the overall view of the Pranhita-Godavari valley in the inset (redrawn from Rao and Reddy, 2002).	15
Figure 3.1	Diagram showing modern drainage system, cratonic boundaries and inland terraines along with various faults and lineaments of Das et al., (2003) and seismotectonic atlas of India.	25
Figure 3.2	Landsat-TM image derived by stacking of the band 7-4-2 (P-143, R-047; 03/05/2011) prepared using software ArcGIS 10.2.2.	26
Figure 3.3	Various sets of lineaments of Das et al., (2003) of minor, medium and major range and structures are marked over Landsat-TM image for interpretation.	28
Figure 3.4	Digital Elevation Model (DEM) showing terrain and slope with lineaments prepared using softwares ArcGIS 10.2.2 and SURFER 8.0	29
Figure 3.5	Diagrammatic representation of the lithological and structural disposition of the area with variation of drainage parameters. Circles represent the position of photographs shown below the figure. (a) Gondwana sandstone at Kirmiri (b) Hydrothermal injections in the form of veins within the basin boundary limestone near Gojoli (c ¹) Hydrothermal veins within basin boundary sandstone surface at Dongargaon hill (c ²) at Dubarpet (below the surface) (d) Development of thick weathering profile on Archaean gneiss terrain near	32

Dongargaon.

Figure 3.6	Proterozoic channels were west flowing evidenced by (a) Cross-bedding of sandstone showing westward flowing channels near Dubarpet (b) near Dongargaon (c) & (d) imbricated pebbles (yellow lines) in the conglomerate beds at Dongargaon hill showing flow direction.	36
Figure 4.1	Regional map of the Pranhita-Godavari basin and its adjacent blocks showing convergence of Bastar and Dharwarcraton and the study area near Chandrapur near eastern margin of Pranhita-Godavari basin.	42
Figure 4.2	Dubarpet region in the toposheet clip showing elongated sandstone ridge in the NNW part (shown in yellow box)	45
Figure 4.3	Photographs shows (a) Gravel sized clast and coarse grained matrix (b) Thick elongated bodies of sandstone, conglomerate and their cyclicity (c) Loose clasts of conglomerate in the weathered matrix and soil.	47
Figure 4.4	Folk (1974) classification showing position of quartz arenite.	48
Figure 4.5	Field photographs showing (a) sandstone hosting paleosol (b) Alternating sandstone conglomerate sequence (c) Weathered chloritized zone in the sandstone and (d) Close view of chloritized sandstone.	49
Figure 4.6	The methodology adopted for paleosol analysis is shown in the given flowchart.	51
Figure 4.7	Geological map of the Dubarpet region on large scale of 1:1000	52
Figure 4.8	Model (schematic) showing development of paleosol and unconformity in the basin, prepared based on field evidences and literature reviews.	53
Figure 4.9	Photomicrograph of paleosol (a and b) show development of pedo features (marked as red dotted lines) and fractures are filled with silica veins in the upper part of the soil horizon, (c) shows crude lamination in the lower part of the soil horizon, (d) encrustation around the quartz grain and rock fragments as diagenetic changes.	55
Figure 4.10	Photomicrographs (a&b) shows the rounded and multiple grains containing grains of quartz with their outcrop images of sandstone below in (c&d).	56
Figure 4.11	Magnetic susceptibility of the paleosol profile shows bottomward decrease of susceptibility.	57

Figure 4.12	XRD analysis of paleosol samples named as PS-1, PS-2 and PS-3	58
Figure 4.13	Photograph showing iron ore bed resting over the dolomitic limestone.	64
Figure 4.14	Study area showing various locations near Gojoli and the nearby region of mass flow.	65
Figure 4.15	Large scale geological map of the region at 1:1000 where the autoclastic mass flow took place near village Gojoli and Dhaba.	66
Figure 4.16	Distribution of limestone facies (facies-C) representing the flow-1 as clasts within the flow-2 along the basin boundary (a, b&c) shows the clast in clast of flow-1 within flow-2 with tabular and elongated clasts in (a) and (c).	67
Figure 4.17	Map showing the fault originated activity in the region causing formation of autoclastic conglomerate (Dora et al., 2011; 2015).	69
Figure 4.18	A schematic model showing various facies assemblages of the autoclastic mass flow over the slope with various faults.	70
Figure 4.19	Diagram showing massive cherty limestone where (a&b) change in colour can be observed from pink to grey and dark grey (c&d) K-alteration due to hydrothermal activities in limestone facies due to volcanic activities juxtaposed.	72
Figure 4.20	Stromatolitic limestone (Facies-B) exposed in the study area. (a) Stratiform stromatolites (b) Stratiform stromatolites showing calcilutite and dolosiltite (c) micro-faults (arrow) in the stromatolitic bands developed due to lack of cohesion and increasing intergranular friction (d, e, f) biohermal stromatolites are found as clasts within the mass flow.	73
Figure 4.21	Structureless, matrix-supported conglomerate deposit (Facies-D) comprising large limestone clasts (10-20 cm) dispersed relatively uniformly through carbonate matrix (a, b for flow-2 & c, d for flow-3). (d) Sub-vertical broad based columns of small angular clasts cutting across the mass of assorted clasts possibly record of fluidization events.	76
Figure 4.22	(a) Clast-supported imbricated conglomerate (Facies-E) of flow-2 and (b) flow-3, respectively, is succeeded by bed-parallel and normally graded conglomerate (Facies-F). (c), (d) Massflow representing flow-2 and flow-3 respectively, shows reverse grading conglomerate (Facies-G).	77
Figure 4.23	Rounded clast conglomerate of facies H. (a), (b) representing	79

flow-2 and shows sense of rotation of the whole mass. (c), (d), (e) representing flow-3.

Figure 4.24	Fine-grained limestone representing the turbidite resting over the mass flow deposit.	80
Figure 4.25	Comparison of facies assemblages among the western and eastern margin of the basin. The western margin stratigraphic sequence have been developed by compiling Bose and sarkar, 1991; Amarasinghe et al., 2015).	81
Figure 4.26	(a) Iron ore sample with dark reddish tint (b) Iron ore resting over dolomitic limestone (c&d) Presence of colloform texture as well as presence of haematite with high reflectance in the 10X view of reflecting microscope.	82
Figure 4.27	Various rocktypes of Dongargaon fan-delta (a&b) shows massive fine grained sandstone and shale facies (c&d) clast supported conglomerate and the limestone sequence in the prodeltaic part of the region (e) Panoramic view of the exposed southern part of the fan delta.	83
Figure 4.28	Large scale geological map of the Dongargaon fan delta at 1:1000 showing lithological distribution.	84
Figure 4.29	Some important parameters given by Postma (1995) to explain the formation of fan delta.	85
Figure 4.30	Structurally controlled architecture of the Dongargaon fan delta with classic gilbert type fan delta (redrawn from Postma, 1995) and observed schematics of Dongargaon.	86
Figure 4.31	The rounded quartz in the photomicrographs show the level of reworking in the sediments of fine grained sandstone which is the initial stage of its formation.	88
Figure 4.32	Fe content in the sandstone can be observed with the grain to grain mutual cementing in the photomicrographs.	88
Figure 4.33	(a&b) Deposition of initially deposited thick fine grained sandstone facies which later went a deformation phase and folded (c&d) Conglomerate and sandstone intercalatory relation showing intermittent fluvio-marine energy variations due to tectonism (e&f) Matrix supported and clast supported conglomerate in the proximal and distal end of the fan delta.	90
Figure 4.34	(a) Shale facies can be observed with splintery shale (b) limestone without any laminations which is in the prodelta region beyond the deposition of shale.	91

Figure 4.35	Schematic shows the presence and disposition of various facies and gives the overview about the morphology of the delta with structural control.	92
Figure 5.1	Four main types of geophysical survey. T=Transmitter, R= Receiver, (Neal, 2004; Daniels, 1996).	100
Figure 5.2	GPR data acquisition and the resulting radar reflection profile (a) Data acquisition at a single survey point, showing GPR system components and subsurface reflector configuration. (b) Radar reflection profile resulting from sequential plotting of individual traces from adjacent survey points. Positions of air-wave, ground wave and primary reflections are indicated (Neal, 2004).	100
Figure 5.3	Google earth image showing the location and path of profile various profiles.	101
Figure 5.4	Image showing various parts of GPR.	102
Figure 5.5	Google earth image showing the location and path of profile A-B	105
Figure 5.6	(a&b) Reflection profile of path AB and indicating the bounding surfaces of sedimentary package on Archaean gneiss	105
Figure 5.7	Google earth image showing the location and path of profile X-Y	106
Figure 5.8	(a&b) Reflection profile of path XY and Positive reflections from GPR profile of path XY indicating cross-stratifications and bounding surfaces	107
Figure 5.9	Google earth image showing the location and path of profile P-Q	108
Figure 5.10	(a&b) Reflection profile of path P-Q and positive reflections from GPR profile of path PQ indicating cross-stratifications and bounding surfaces	108
Figure 5.11	Google earth image showing the location and path of profile R-S	109
Figure 5.12	(a&b) Reflection profile of path R-S and Positive reflections from GPR profile of path R-S indicating cross-stratifications and bounding surfaces	110
Figure 6.1	Frontal view of fan-delta model at Dongargaon (not to scale, after Pati, 2010)	115
Figure 6.2	Faulting and folding in Dongargaon fan-delta (not to scale)	118

LIST OF TABLES

Table No.	Description	Page No.
Table 2.1	Lithostratigraphic classification of the Purana rocks in the Pranhita-Godavari valley (Chaudhuri et al., 2015).	20
Table 2.2	Geochronological order of the Pakhal sediments worked out by various workers.	21
Table 3.1	Showing various parameters and their inferences based on actual values.	33
Table 4.1	Proxies used for chemical analysis and their outcome (Sheldon and Tabor, 2009)	59
Table 4.2	Oxide weight percentage obtained from XRF	60
Table 4.3	CIA value and representing mineral (Nesbitt and Young, 1982; Fedo et al., 1995)	61
Table 4.4	Chemical Index of Alteration (Al ₂ O ₃ /(Al ₂ O ₃ +Na ₂ O+K ₂ O+CaO)) for samples	61
Table 4.5	Clayeness values (Al ₂ O ₃ /SiO ₂)	62
Table 4.6	Paleotemperature calculated from salinization values	63
Table 5.1	Dielectric values for common materials used for various terrains (Desai et al., 2016)	99

1.1 General Introduction

Crustal perturbations in any region are the manifestations of tectonic disturbances caused by regional or local earth surface adjustments. Assistance to this by many other factors like sedimentary, igneous or metamorphic phenomena's is just an appendage of nature. The temporal and spatial distribution of various sedimentary

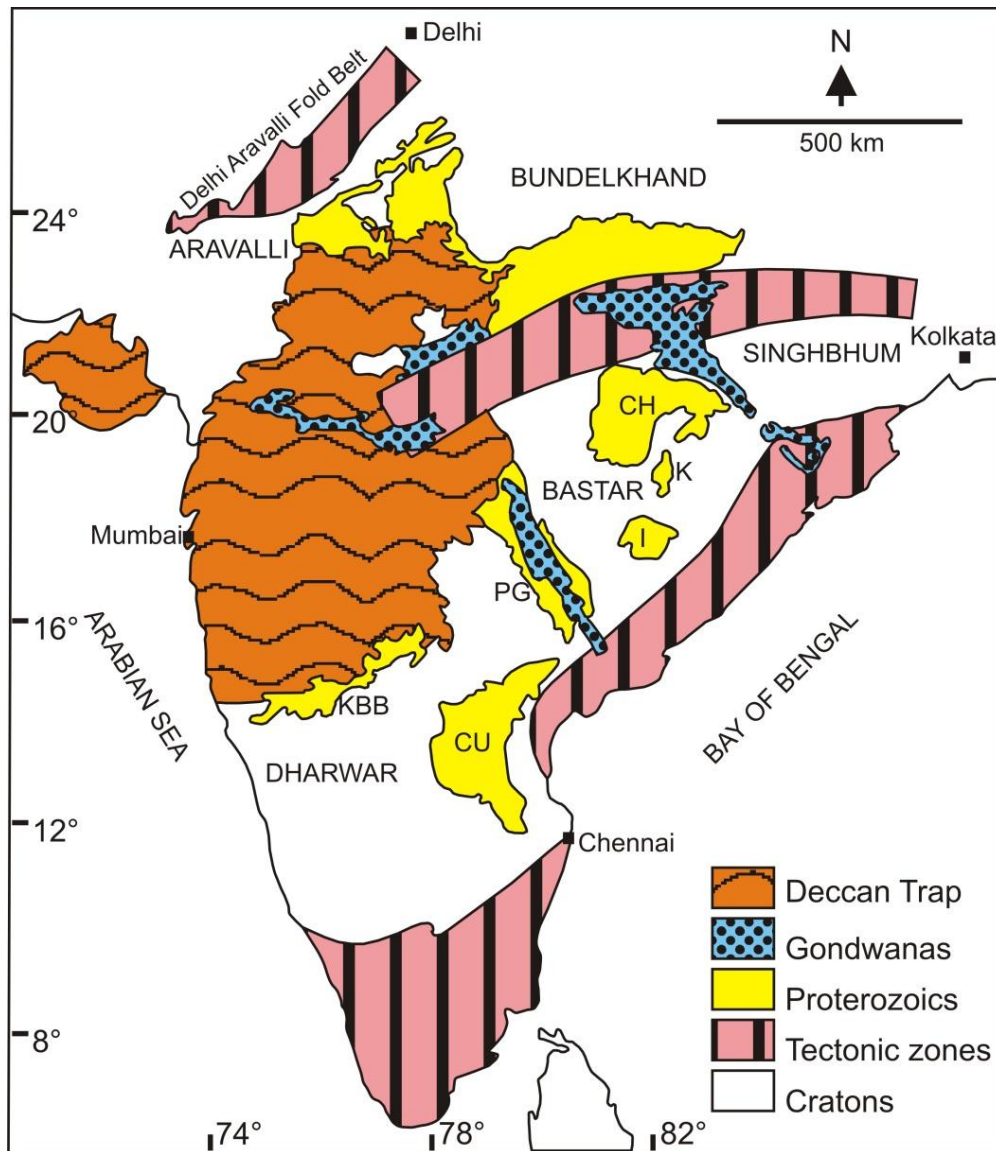


Figure 1.1: Tectonic map of India showing distribution of Purana basins, including Vindhyan (V), Chhattisgarh (Ch), Khariar (K), Indravati (I), Pranhita-Godavari (PG), Cuddapah (Cu) and Kaladgi-Bhima (KBB) basins. (Redrawn after Rao & Reddy, 2002).

cycles and sequences is thus a function of such activities which can be observed through the field traverses in different terrains.

India is a complex mosaic of sutured terrain which includes Archaean and Proterozoic rocks of low to high-grade metamorphism (Stein et al., 2004). Das et al. (2003) identified numerous major and minor lineaments along the sutured terrains of different cratons which are passing through for distances ranging from a few km to hundreds of km which cause them to interact and create various sedimentary basins along different locations depending upon the severity of perturbations. Proterozoic sedimentary basins occur as isolated patches within the Achaeans (Fig. 1.1). The linkage of these basins during their formation or later always became a debate among the geoscience community in India and abroad. As many of these basins are fault-bounded and hence have been interpreted as tectonic origin.

The join between western Bastar and the eastern Dharwar craton is mainly manifested by the Pranhita-Godavari basin (PG basin) (Saha and Patranabis-Deb, 2014) as a fossil rift. There are numerous deep-seated faults present within the fossil rift, especially the border faults which define the basin configuration. Das et al. (2003) categorized these faults and lineaments into minor, intermediate and major classes depending upon their distance of continuity (<100km: minor, 100 to 200 km: intermediate and >200 km: major). The PG basin witnessed many cycles of sedimentation influenced by the temporal reactivations of the marginal faults and volcanism (Dora and Randive, 2015), influenced by climatic fluctuation. As a result, a thick pile of sediment deposited in the sag basin separated by numerous unconformity surfaces, which records the tectonic and climatic scenario during and after the deposition.

Rift-related volcanism formed few economic mineral deposits such as barite, fluoride and copper along the basin boundary in both basement and sedimentary domains as hydrothermal deposit. Such hydrothermal activity is also well recorded in the present study area along the basin-boundary fault zone by intense silicification, and formation of colloform and comb structures in the iron-ore bed. Fracture and fault systems in the study area indicate the evidences of extensional regime during the intercontinental rifts within the Archaean basement.

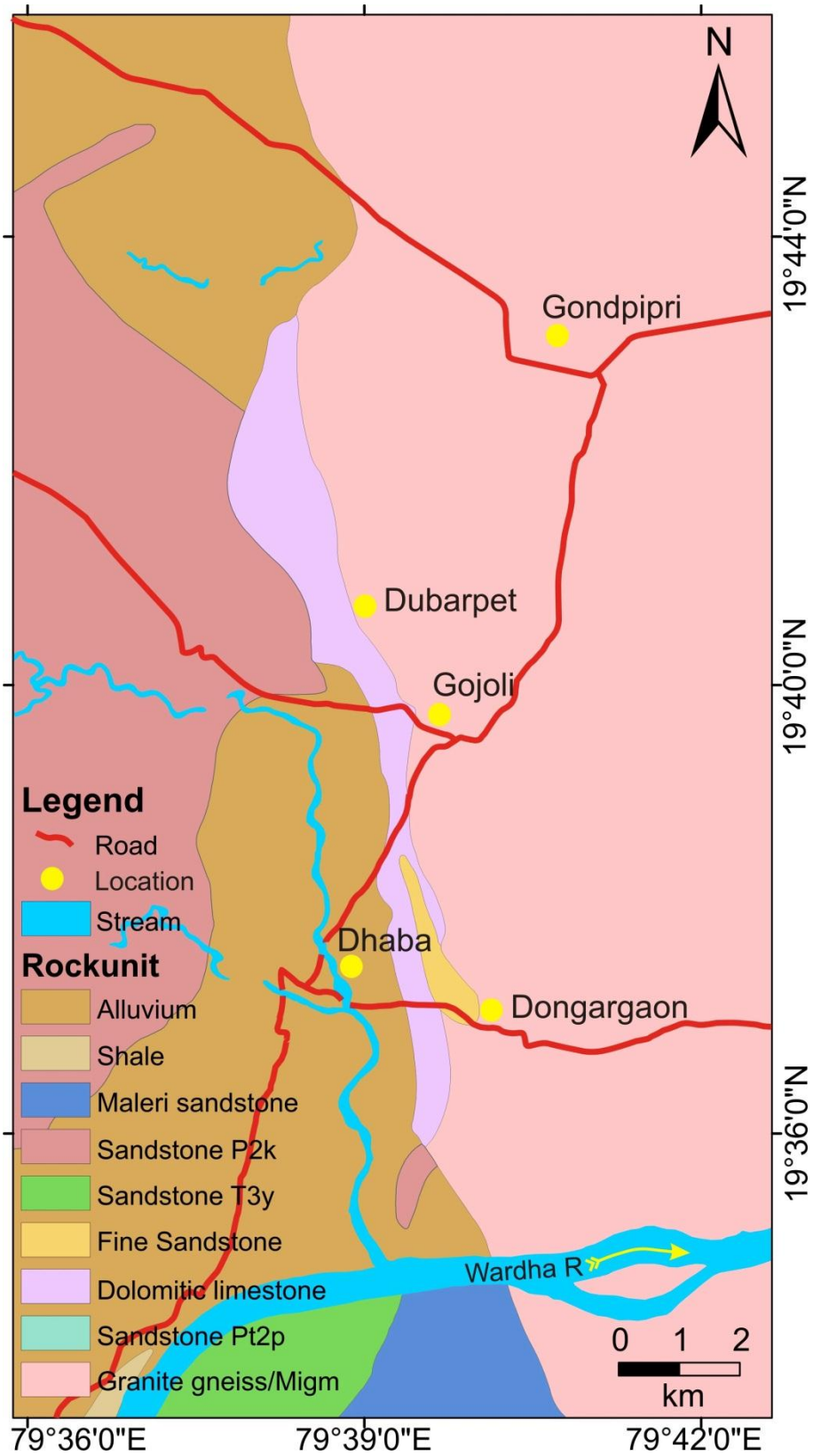


Figure 1.2: Major localities in the study area and their road linking as well as the various lithounit distributions in the study area.

The present study presents some of the evidences of those extensional tectonic episodes and their effect on the sedimentation along the basin-margin. The post depositional tectonic effect on the basin-margin geomorphology has also been discussed. Different lithological variations along the basin-margin were influenced by the temporal and spatial change in the basin level governed by tectonics and climate.

Climatic condition has been established using the palaeo-weathering pattern of the paleosol profile, the lithological assemblage has been well recorded along the boundary zone and their corresponding depositional systems have been established. The post deposition tectonic and weathering activities have been recorded by comparing the Proterozoic drainage system with the recent one in the study area. It is an integrated study carried out by addressing the sedimentology, geomorphology and tectonics of the area.

1.2 Location and Accessibility

The study area falls in parts of the Survey of India Toposheet No. 56M/9 and 56M/10 and geographically within the latitude 19°36'45"N to 19°40'38"N and longitude 79°37'04"E to 79°40'33"E. (Fig 1.2) in Chandrapur district, Maharashtra. Major localities in the area are Gojoli, Duberpeth, Dongargaon, Gondpipri are connected with all-weather roads with the district headquarter.

Politically the study area falls along the border of Maharashtra and Andhra Pradesh. Balharshah is the nearest railway station located about 40 km to the northwest of the area on Wardha-Kazipet section on the Central Railway.

1.3 Physiography and Drainage

The study area is characterized by moderately undulatory terrain with the present slope towards southeast (Fig.1.3). Highest and lowest topographic heights in this area from the mean sea-level are 330m and 140m, respectively. The Wardha River is the perennial river of the region, is a tributary of the Wainganga River. The Dhaba nala which runs straight through the central part of the region and connects to the Wardha River also contains water for few months of the year. All the rivers follow southerly and southwesterly directions and constitute the main drainage of this area.

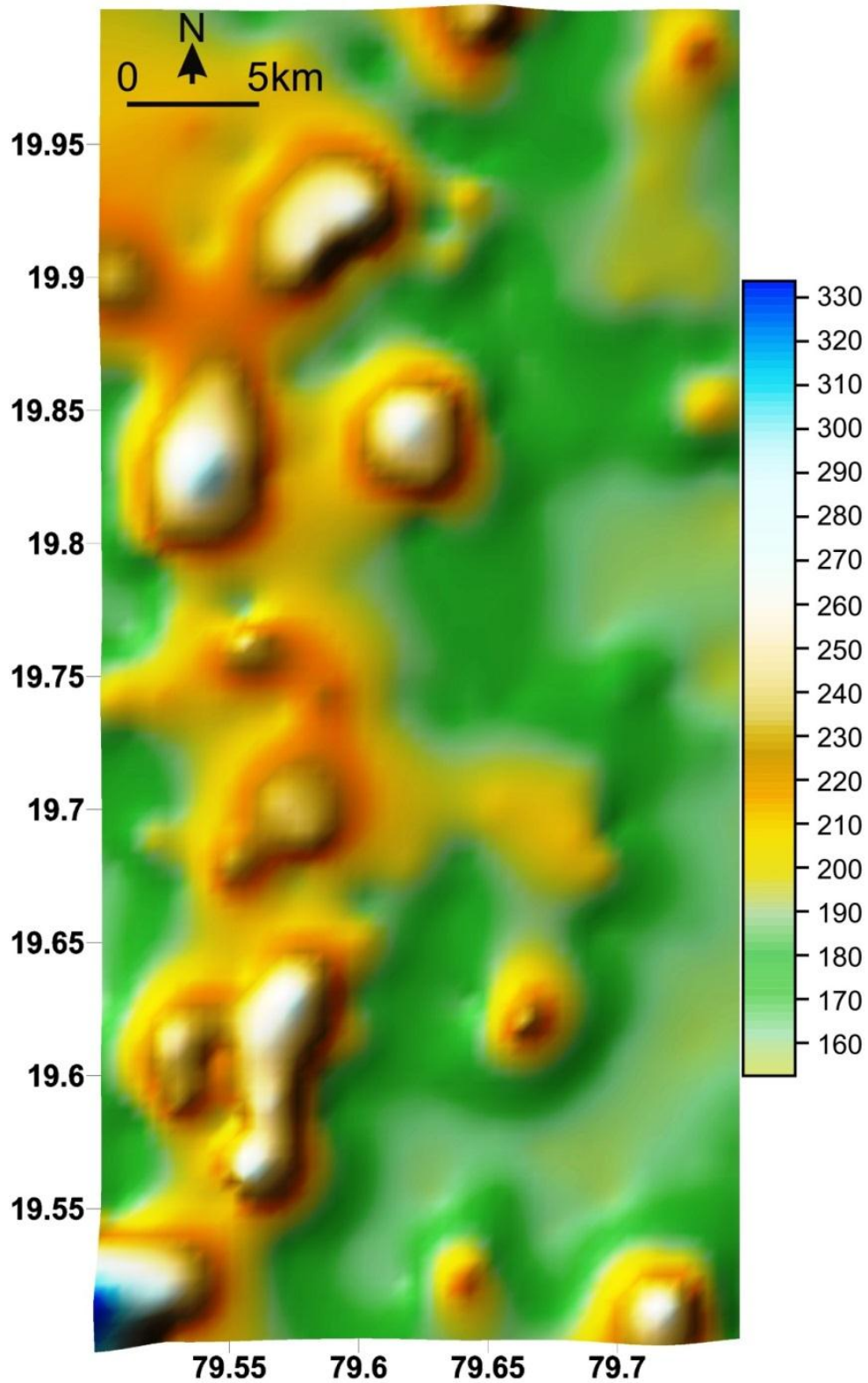


Figure 1.3: Type of undulations in the terrain shown in the Digital Elevation Model (DEM) as well as the slope towards the South-East direction.

Majority of the drainage system in the area is dendritic in nature with occasional parallel due to structural control (discussed in details in chapter-3). The sedimentary rock outcrops in the region are striking the basin margin running almost north-south to NNW-SSE.

1.4 Geomorphology

The area represents relict topography characterized by erosion in maximum parts. Deposition is only restricted along the river valleys. Therefore drainage geomorphology of the region is mainly lithologically and structurally controlled. The higher order streams are sub-parallel to the basin margin structures and lineaments (Fig.1.4). However, overall the drainage pattern of the study area is dendritic to sub-dendritic in nature.

The perennial N-S trending Andhari and Lahan River flowing towards South show prominent control by lineaments and faults along some segments of their courses by offsetting and straight channel characteristics. Different sets of lineaments of different generations show control of the fluvial geomorphology of the region.

1.5 Land use

Around 40% of the area is covered by the reserved forest, containing many types of vegetation from small shrubs to huge trees with major occupier “Sagwan tree (*Tectona Grandis*)”. Remaining 60% area is under the private habitat area or revenue land and crop fields. Some of the previous activities involve the mapping of the region and other prospects related to mineral prospecting and exploration for the Geological Survey of India (GSI). The region is almost flat with isolated hillocks at places which show good exposures of outcrops of lithology and structures.

1.6 Significance of the Research

Though a lot of geological activities have been carried out earlier related to mapping and exploration, in the area on a scale of 1:50,000 by the GSI, but there exist knowledge gaps regarding the basin development processes, sedimentation and role of tectonic and climate on spatial and temporal distribution of different sedimentary

lithounits.

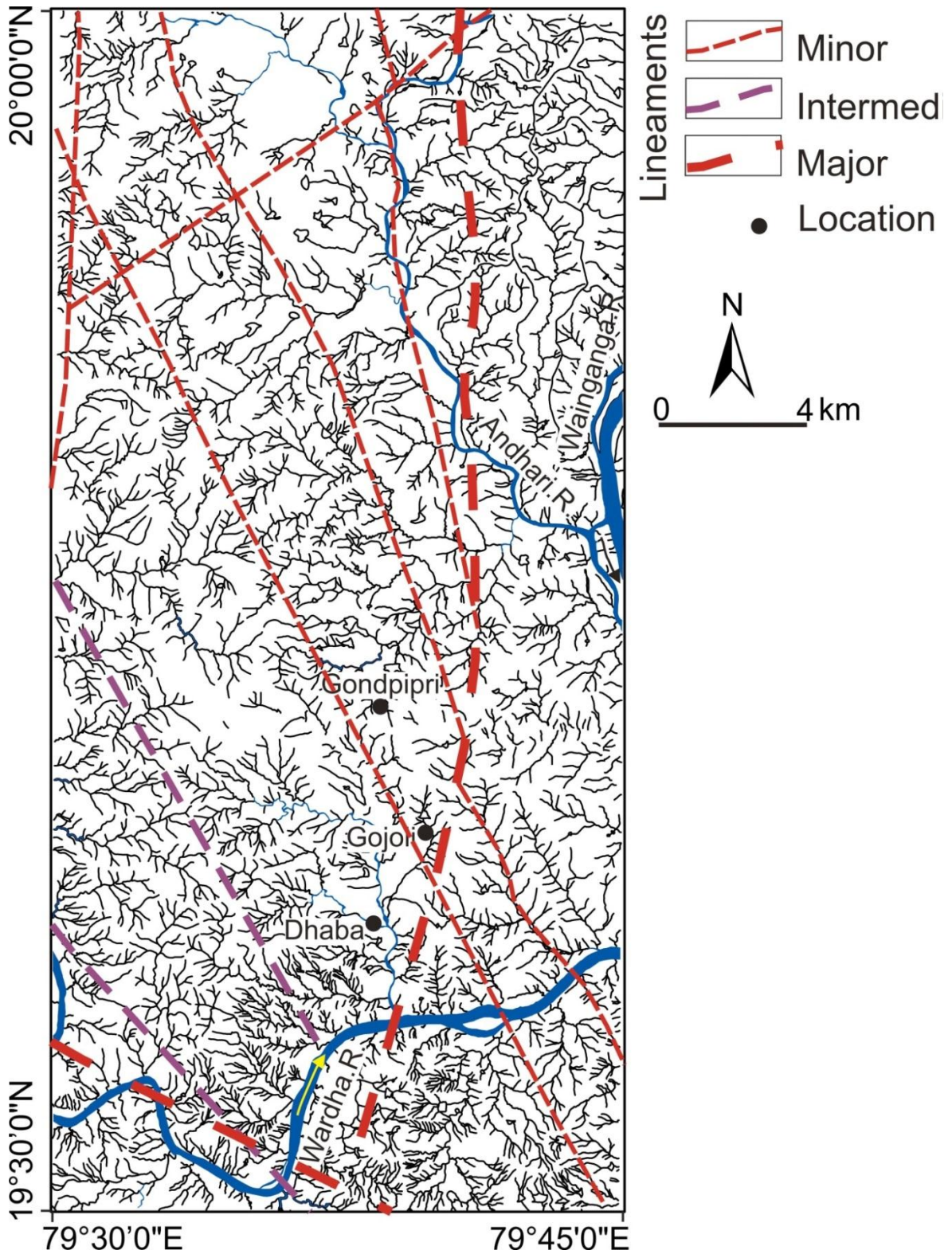


Figure 1.4: The concordant nature of higher order streams with the basin margin structures. (Lineaments after Das et al., 2003).

Hence, it was aimed to decipher the various constraints in the basin margin processes related to the evolutionary pattern and tectonics.

This study has brought out some logical results related to the facies distribution especially the mass flow type and patterns in and around Gojoli village, fan delta deposit and its facies near Dongargaon village and detailed paleosol analysis around Dubarpeth village, with large scale mapping on 1:1000 scale with special reference and mapping of the area on 1:5000 scales. This will help to understand and correlate the basin margin processes along both margins of the fossil rift.

1.7 Overview of previous works

The study area geologically constitutes the western part of the Bastar craton and eastern part of the Dharwar craton in the Pranhita-Godavari valley. Crookshank (1963) first gave the comprehensive account of the geology of the south Bastar craton where the study area lies. Based on the differences in geology, structure and metamorphism, the geological formations of this region have been categorized into following of which the various rocktypes are found and analyzed:

1.	Sullavai Group	Early Neoproterozoic	Sullavai sandstone (Sreenivasa Rao, 1987)
2.	Albaka Group	Neoproterozoic	Absent in study area, no outcrops seen
3.	Penganga Group (eastern margin)	Late Neoproterozoic	Established limestone sequence in study area (Present study)

Though the study area was first traversed by Hughes (1877), but the pioneering work by King (1881) divided the PG valley into three units, from bottom to top, the 'Pakhali subdivision', a mixed siliciclastic-carbonate succession; the 'Albaka subdivision', an assemblage essentially of siliciclastics; and the 'Sullvai Series', a 'red bed sequence'. Then the Proterozoic successions of Indian cratonic basins, traditionally known as the '*Puranas*', meaning 'old' in Sanskrit, were given by Holland 1906 and later it was carried forward by Hallows (1923). Further, Heron (1949) pointed

out the explanation about non-exclusiveness of the limestone deposits in conjunction with the Pakhal subdivision.

After independence, Karkare, carried out exploratory drilling during 1961-63. Kulkarni (1963-64) carried out systematic mapping on R.F. 1:63,360 followed by geochemical prospecting of the region. Gajbhiye (1965-66) further worked for the exploration of the area. King's three-fold classification was not enough from the point of view of basin evolution. Therefore, a number of pioneering works by Nageshwara Rao 1964; Basumallick 1967; Chaudhuri 1970; 1985; 2003; Chaudhuri et al., 2004; Subbaraju et al., 1978; Srinivasa Rao 1979a, b; Sreenivasa Rao 1985; 1987; 2001; Chaudhuri et al., 2002; 2012; 2015 have been credited and the present knowledge of the whole region is enlightened. The Purana rocks of the Pranhita-Godavari valley represent almost a complete succession between the Archaean granitic basement and the Paleozoic to Mesozoic Gondwana rocks. Several workers had studied the succession for more than a century ago. Present work near Gondpipri region along the basin margin will enhance the state of knowledge of geology of region.

1.8 Research aims and objectives

Facies assemblage along the western margin of the basin is well established and a thorough understanding has been made for their spatial and temporal variation relating to the tectonic and climate. However, the same along the eastern margin is missing due to the inaccessibility. As a result understanding the basin boundary processes along both the margins is not possible. Keeping this problem in view, the following objectives have been set:

1. To study the sedimentary facies along the eastern margin of the PG basin
2. To correlate the activity of the basin-margin faults on the facies variation
3. To study the changes of depositional environments along the boundary zone of the basin
4. To study the geomorphic evolution of the study area from Precambrian to Recent and the role of tectonism on geomorphic changes.

In order to address the above issues, it has been aimed to undertake detailed research work on the topic titled "TECTONIC EFFECTS ON GEOMORPHOLOGY

AND SEDIMENTATION IN PARTS OF WESTERN BASTAR CRATON” for the pursuance of this Ph.D. degree.

1.9 Methodology

The study presented in this work is mainly based on detailed facies analysis and bed-by-bed measurement of different sedimentary facies of different depositional environments. The outcrops in the study area are located within a narrow zone about 1.5 km wide and 5 km long. The outcrops are aligned along the regional NNW-SSE strike, exposed in a series of southwesterly gently-dipping units. Outcrops from more than twenty-five localities have been observed and the variation within a particular facies has been described in this study. Where the outcrops are well exposed, the complete vertical successions of different mass-flow events were observed and the subsequent study of their temporal and spatial relationships was established. The data used in this study consists of a set of field observations and photographs taken during fieldwork.

Apart from this, laboratory techniques include petrographic studies, XRD, XRF and CHNS were carried out.

The methodology adopted for the research work is given as under:

1. The first part of the research work was involved with the literature study and preliminary survey of the study area to find out the accessibility. Then research work involved was large scale mapping of the study area on 1:5000 and then sample collection for petrographic studies and other laboratory analysis. Here all the lithological contacts and exposed outcrops are delineated and all the structural features with other attitude details were recorded.
2. Detailed mapping of three areas i.e. around Gojoli, Dubarpet and Dongargaon villages has been done thoroughly on a scale of 1:1000. This was aimed to record details of the fan-delta setting and mass-flow in the various shelf environments and their study.
3. Preparation of geological maps and cross-sections of particular areas along the boundary zone.

4. Drainage study and other parameter based analysis of the area have been carried out to establish the effect of topography and structure on drainage geomorphology.
5. Preparation of a Digital Elevation Model (DEM) of the toposheets for topographic analysis with the lithology.
6. Hence the logical conclusions were compiled together to produce the comprehensive report of the study area.

1.10 Organization of the Thesis

This thesis contains seven chapters along with appendix, annexure, plates, figures, and tables.

Chapter 1-Introduction discusses about the general ideas, climate, vegetation, road network (accessibility), literature review etc. to provide some background knowledge about the study area.

Chapter 2-Regional geology and Stratigraphy describes the regional geological framework including Stratigraphy and tectonics of the region

Chapter 3-Geomorphological evolution of the region suggested the change in geomorphology from Precambrian to Recent. It provided the role of tectonism in changing the geomorphology by block tilting.

Chapter 4-Facies distribution and their environments discusses about the different lithological disposition and their properties both in field and laboratory with specific characters if any.

Chapter 5-GPR study suggests the shallow sub-surface stratigraphy along the boundary zone of the basin, structure and depositional patterns.

Chapter 6-Discussion describes the linkage of all the work carried out and the logic behind it. It links the observation with interpretation with satisfactory logics.

Chapter 7-Conclusion describes the outcome of the study and the utility of this work in case of understanding the tectonic processes and in the field of mineral exploration.

2.1 Introduction

Major Indian cratons namely the Bastar, Dharwar, Singhbhum, Aravalli and Bundelkhand comprise of the oldest nuclei of the continental crust of the Indian peninsula (Radhakrishna and Naqvi, 1986) and record 3.3 Ga old crusts in the form of Tonalite-Trondjemite-Granodiorite (TTG) (Ramachandra et al., 2001). The peninsular record of the Mesoproterozoic and Neoproterozoic successions is present in several mobile belts and cratonic basins, developed on the TTG gneiss.

The Bastar craton was evolved in space and time through the interaction of the Eastern Ghat Mobile Belt (EGMB) orogeny in the east and southeast; the Proterozoic younger orogens in the southwest and orogeny of Meso to Neoproterozoic Sausar mobile belt (SMB) in the north (Ramachandra et al., 1998). It is bounded three sides by three rifts i.e., Mahanadi, Godavari and Narmada rift in the NE, SW and NW direction, respectively. Whereas, the southeastern boundary is marked by the Eastern Ghats and western limit of the Eastern Ghats overlying the Bastar craton is marked by a shear zone (Bandopadhyay, 1996).

The Bastar craton in the Central India has various lithologic units showing age not older than 3.0 Ga as described by Sarkar et al. (1990). In the southern part it consists of deformed Tonalite-Trondjemite-Granodiorite above which mainly lie the Neoproterozoic sedimentary sequences (Sarkar et al., 1993). General crustal thickness of about 35 km for the Indian shield has been shown by teleseismic studies (Narain 1973; McCarthy et al., 1983). Thickness increases to about 50 km under the Eastern Ghats and thins to an uncertain amount under the Godavari rift valley. Bouguer and free air anomaly are generally low.

The marginal part of the Bastar craton is the region where junction between the eastern margin of the eastern Dharwar craton is coinciding with the western part of the Bastar craton forming a basin for the PG valley sediments. The basin is mainly filled with the Phanerozoic sediments in the middle and the Proterozoic sediments are outcropped along the margins (Chaudhuri, 2003). Along the North-Eastern margin, the Proterozoic belts are bounded by two sub-parallel faults; one separates the Proterozoics from Gondwanas and other from the crystalline rocks of basement

complex. Several outcrops of multiple dimensions occur in the Bastar cratonic block, towards the northeast of the Pranhita-Godavari valley.

2.2 The Pranhita-Godavari rift and the Basin margin overview

The Pranhita-Godavari rift valley is a graben that has shown several periods of reactivation (Subbaraju et al., 1978). The rift contains “Gondwana” sediments in the center of the valley and a sequence of older sediments (Pakhal Group) in linear outcrop belts along the northern and southern margins (Fig. 2.1). The Pakhal suite was presumably formed during Proterozoic rifting. Although no orogenic belt has been found along the Godavari rift, some differences between Dharwar and Bastar cratons indicate that the rift is a join between formerly separated blocks. The north-south zones of potassic granites in the Eastern Dharwar craton do not seem to extend into Bastar craton. Therefore, Godavari rift is regarded as a major structural join that delineates the northern border of the Dravidian shield.

The entire Indian crust was a single unit since middle Proterozoic (Rogers, 1986). The Pranhita-Godavari rift is located on a paleo-suture between the Dharwar and Bastar proto-cratons (Biswas, 2003). The master faults developed bordering the rift, and the intra-rift higher order faults followed by the pre-existing fabric. The transverse transfer zones manifested as basement ridges, and divide the rift into segments of tectono-sedimentary domains or various rocks groups. The major domains are the Chintalpudi, Godavari, and Chandrapur sub-basins, each of which has been subsided differently. The structural complexity of the various basins varies and accordingly the sediment accommodation took place.

Along these sub basins various sedimentary deposits or the covering sediment over the basement are formed which are described by various workers since a century. These successions are called the Proterozoic successions within the Bastar craton and in the Pranhita-Godavari valley. King (1881) initially founded the Purana stratigraphy of the valley and described the Proterozoic succession in two major unconformity bound units, the Upper Transition Series, and the overlying Sullavai Series. In this classification he divided former one into two i.e. lower, Pakhal subdivision, and the upper, Albaka subdivision. The mixed siliciclastic-carbonate successions occurring in the Western Belt, Eastern Belt as well as in the inliers were

all included in the Pakhal subdivision, however, the extensive siliciclastic successions

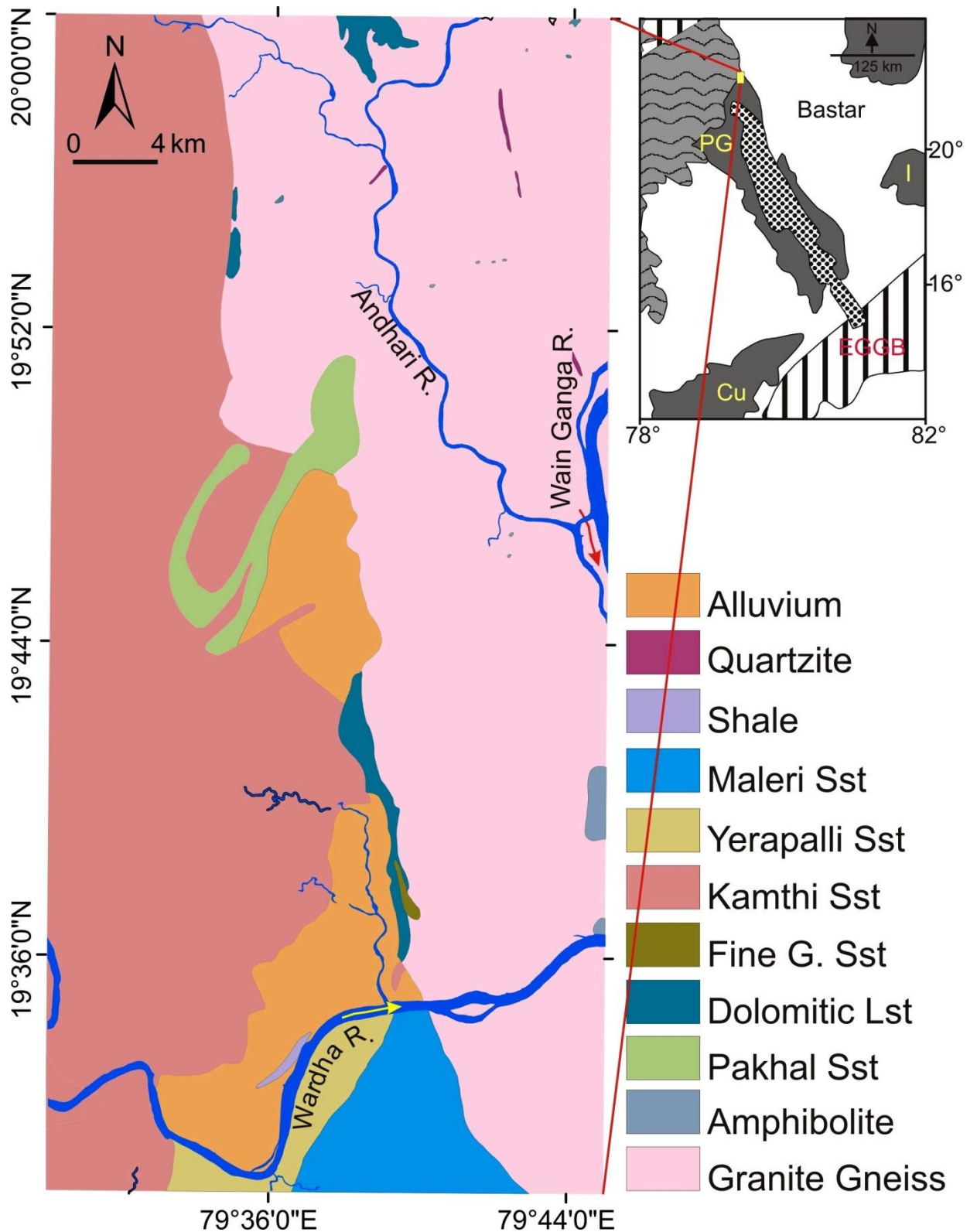


Figure 2.1: Geological map of the study area (after GSI) and the overall view of the Pranhita-Godavari valley in the inset (redrawn from Rao and Reddy, 2002).

of the Albaka plateau were classified as Albaka subdivision. He also classified the sandy and conglomeratic red beds straddling the western and eastern belt and the inliers as the Sullavai series.

Basumallick (1967) attempted a detailed stratigraphic classification of the Pakhal subdivision into lower Mallampalli Subgroup and upper, Mulug Subgroup. Srinivasa Rao et al. (1979, 1987) tried to correlate the Mulug orthoquartzite and Mulug Shale of Basumallick's classification with the basal divisions of the Albaka subdivision of Albaka plateau which implies that Mulug subgroup and Albaka Group forms a continuous succession. They separated the Sullavai group from Pakhal Supergroup in his classification of the region.

The Meso- to Neoproterozoic platformal cover facies of Pakhals (1686 ± 6 and 1620 ± 6 Ma) were deposited in linear half graben/ graben basins (Conrad et al., 2011). They are characterized by an unconformable contact along one side and faulted contact along the opposite side of the basin (Saha and Chaudhuri, 2003). The NNW-SSE to NW-SE intra continental extensional sedimentary basin was formed and lies parallel or sub-parallel with the Godavari trend. Chaudhuri (2003) inferred an unconformity at the base of the Mulug orthoquartzite while doing the reappraisal of Basumallick's geological map. Chaudhuri et al. (2012) reclassified the Mulug succession into four formations. They also reclassified the previously "subgroup" ranked entities into "Group" status to all the unconformity bound sequences.

The periphery of the Bastar craton in junction with Pranhita-Godavari valley is bounded by two NW-SE trending faults which separates the Purana outcrops from the Gondwana succession in the west, and from the Bhopalpatnam granulite belt on the east. Since this junction region was less studied therefore an attempt has been made in this study to resolve the basic gaps in research in this region. Chaudhuri et al. (2012) initiated mapping in the eastern part of the belt and found it different from the western part geology and requires to be classified as a new stratigraphic entity. Saha and Ghosh (1987, 1998) referred to the carbonate bearing assemblage around Somanpalli as Somanpalli Group and inferred its stratigraphic equivalence with the Pakhal rocks in the Western Belt.

For the carbonate bearing successions in the Pakhal subdivision, Heron (1949) contradicted the King's (1881) classification and introduced the Penganga Series from

the North of the Godavari River. Later, it was extensively worked out by Sarkar and Bose (1991) and Bose and Sarkar (1992) and they gave the complete lithological display in the western margin of the Godavari valley. Heron's view was supported by Sreenivasa Rao (1985, 1987) and Chaudhuri et al., (1989), who upgraded its status from "Series" to "Group". However, the correlation of the Sullavai and the Penganga Group has been done by Heron (1949) but it was rejected by the subsequent workers because there was an unconformable relation between the two (Chaudhuri et al., 2012). However, Sreenivasa Rao (1987) included the Penganga Group underlying Sullavai Group separated by the unconformities except the lower unit of Penganga was separated from the Sullvai by a Fault.

After extensive work in the Bastar craton or the Eastern margin of the Godavari valley Sreenivasa Rao (2001) hypothesized that Pakhal and Albaka rocks were deposited on the margins of Dharwar and Bastar cratons. These platforms were separated by an intervening ocean basin or an epeiric sea, and converged during post-Sullavai times along the present Gondwana-Albaka contact (Sreenivasa Rao, 1994). Thereafter, he classified all of the formations of the Albaka Plateau into two Groups, the Venkatapuram and the Usur Group and combined them into Albaka Supergroup (Sreenivasa Rao, 2001). Although, on the eastern margin he excluded the Penganga Group of rocks which were worked out by the (Bose and Sarkar, 1991; Sarkar and Bose, 1992) on the Western margin.

Further, Chaudhuri (2003) described some ambiguity about the presence or absence of Penganga/ Albaka Group over the eastern margin of the Pranhita-Godavari valley or the Western margin of the Bastar craton but similar lithological evidences in the eastern margin were encountered by them (Chaudhuri, 1985). Chaudhuri and Deb (2004) included the Penganga Group of rocks underlying the Albaka Group where he explained about the shale and limestone sequence with conglomerate in the Western margin of the Pranhita-Godavari valley. Therefore, after numerous explanations from various workers and inferences about the lithological and basin evolutionary trends, Penganga Group of rocks in the eastern margin needs to be described in a comprehensive manner and some sedimentary sequences in the already established part of Sullavai Group which has been attempted in this study.

The Penganga and Sullavai groups come under III and IVth cycle of deposition of the whole Proterozoic sedimentary cover sediments in the pocketed form. Penganga consists of four lithostratigraphic units of formation with an upward fining sequence as observed and reported by Bose and Sarkar (1991); Chaudhuri, (2015), Amarasinghe et al. (2015). The stable basin condition and depositional systems are reflected by homogeneous deposits of Chanda limestone and Satnala shale with a number of coarsening upward and fining upward sequences or stacked cyclothems of different orders. The Penganga has been affected by the fluvial-tidal to deep marine environments which caused the deposition of fan-delta, limestone and shale, shows uniformly deepening of the sea (Chaudhuri et al., 2015; Mitchum et al., 1977). Also, complex interplay of bar and interbar succession in the Pranhita sandstone marks the sea-level curve in a higher order scale (Mitchum et al., 1977).

The Albaka sequence consists of siliciclastics and most extensive sand depositing system in the Pranhita-Godavari basin. Chaudhuri et al. (2015) attempted to correlate the thick sand dominated coastal, tidal unit of Albaka with the deep-water limestone succession of the Penganga group and found it brimful of uncertainties without any age data. However, they indicated the possibility of coastal tidal sequence of Albaka Group can be correlated with the Penganga Group.

The Sullavai and Usur completely represent the IVth depositional cycle with very widespread siliciclastic depositing environments with sub-arkose and quartz-arenites at various levels of the succession. Sullavai sandstones with braid fluvial arkoses and quartz arenites and upper aeolian deposits are strikingly similar due to the red coloration in the different parts of the valley. It has high maturity of sediments and rapid transition from alluvial fan to braid-fluvial to erg depositional systems (Chakraborty 1991a, b, 1999; Chakraborty and Chaudhuri, 1993; Chaudhuri et al., 2015) indicates towards subdued topography and high tectonic stability with steady-state climatic condition. Albaka and Sullavai groups has achieved rapid maturity level in the sediments by virtue of absence of vegetation during Proterozoics and that had played aeolian abrasion of the sediments faster (Chaudhuri, 1977).

2.3 Tectonic setup of the region and the study area

The Proterozoic successions from of the join between the Dharwar and the Bastar along the Pranhita-Godavari valley had recorded multiple rifting events since

late Neoarchaean suturing of the two cratons (Saha and Deb, 2014). Major sea level fluctuations in the basin coupled with regional and local tectonic events shaped the lithology and geomorphology of the region. There were some tectonic cease events in between or the fossilization events which caused the strata to be bounded with unconformities (Chaudhuri et al., 2002). The oldest Paleoproterozoic intracratonic sedimentation is preserved in the Cudappah and the Pranhita-Godavari basin, while the sedimentation in the Bastar-Dharwar join is mainly Mesoproterozoic. There were fluvio-deltaic to shallow marine Neoproterozoic sedimentation which is followed by the igneous activity and emplacement of end-Mesoproterozoic kimberlites and lamproites indicating thermal activation of the continental crust beneath (Pati (Unpub.), 2010; Dora et al., 2011).

The development of the carbonate bearing sequences in the various rock groups of the region during Mesoproterozoic to Neoproterozoic indicates towards the peneplanation of the cratons and sedimentation over the stable platforms. The Neoproterozoic sedimentation was ended following the docking of the Eastern Ghat belt to the eastern margin of the Dharwar-Bastar ensemble and possible final tectonic activities in the central Indian Tectonic Zone (CITZ) bordering the Bastar craton (Saha and Deb., 2014).

In the present study area; mega, intermediate and short lineaments are present controlling the geometry and geomorphology of the basin. The main lineaments in the study area lie in the NW-SE direction and few of intermediate categories were in the NE-SW direction. However, the controls in the post-Proterozoic times were more dominant because the Pranhita-Godavari rift appears to have continued in the Indo-Antarctic plate before the Cretaceous break-up (Biswas, 2003).

2.4 Stratigraphic Overview

Based on the positions of the Purana rock sequences within both margins of the valley and current studies done by Chaudhuri et al. (2015), raise a basic question about Albaka problem which needs to be addressed. Therefore, present work done is an attempt to illuminate the same which is exclusive of the other attempts about tectonic addressal of the basin and extensive appraisal of the surrounding area. The Mallampalli Group is the oldest sequence having 1700 Ma old sediments, whereas, Sullavai Group is of Neoproterozoic age as given by the Amarasinghe et al. (2015).

The Devalmari Group represents the equivalent of Mallampalli Group in the eastern belt. According to Chaudhuri et al. (2015), Somanpalli and Mulug are the major rift sequences in the valley and highly correlatable and coeval in contrast to stable platform type successions of the Devalmari and Mallampalli Groups.

The Penganga Group and the Albaka Group lack the geochronological data till date which has compounded the problem and apparently their similar stratigraphic position was ambiguous. The Penganga Group lacks the thick siliciclastic lithology and an attempt has been made to relate it to the Albaka and the Sullavai. Therefore, geochronological evidence is needed or a good appraisal related to the geology and its correct position. A similar attempt has been made to bring enrichment in the status of knowledge of the region better.

Table 2.1: Lithostratigraphic classification of the Purana rocks in the Pranhita-Godavari valley (Chaudhuri et al., 2015).

Lithostratigraphic classification of the Purana rocks in the PG valley (Chaudhuri et al., 2015)			
Gondwana Supergroup (Permo-Triassic)			
Sullavai Group	Venkatpur sandstone (300) Encharani sandstone (290) = Kapra sandstone (200) = Mancheral quartzite (190)	Usur Group	Delam sandstone (200) Doli sandstone (975) Nambi conglomerate (200)*
c. 1000 Ma	?	Albaka Group	Chalmala sandstone (1500) Tippapuram shale (1340) Somandevara quartzite (915)
Penganga Group	Sat Nala shale (>1000) Chanda limestone (640) Pranhita sandstone (160) Nala Gutta Formation (515)	?	
c. 1400 Ma	Fold-thrust deformation and unconformity		
Pakhal Supergroup	Mulug Group	Somanpalli Group	An assemblage of conglomerate, subarkose, quartz arenite Limestone, Dolomitic limestone greywacke, black shale and pyroclastics (c. 3430)
1565 Ma	Jakaram conglomerate (30)	1620 Ma	
Mallampalli Group	Karlai shale (300) Pandikuntala limestone (1115) = Gunjeda dolomite (300) Bolapalli Formation = Bayyaram quartzite (192)	Cherla Formation (150)	
1685 Ma			
	Basement granites and gneisses		Basement granites and gneisses
Figures in parentheses stands in metres. Symbol '=' stands for facies equivalent			

Basically, the Purana rocks in the Pranhita-Godavari valley consists of mainly eight unconformity-bound sequences from eastern to western belts, which are to be ranked as 'groups'. There is a possibility of naming it as megasequence of first order cycle instead of supergroup as suggested by Chaudhuri et al. (2015) and they suggested the two first order cycle for the Pranhita-Godavari succession taking regional and global-scale orogenic events. They also inferred that the Somanpalli orogeny coinciding with the sub-Albaka/sub-Penganga unconformity divides the Purana basin history in the valley into two distinct cycles of basin opening and closure. The Mallampalli, Devalmari, Somanpalli and Mulug groups deposited within the lower first order basin cycle have been combined into a supergroup, the Pakhal Supergroup. Also, the Albaka-Penganga ambiguous relationship is the reason which is stopping the workers to give the supergroup designation to Penganga Group.

2.5 Geochronology

Some of the lithounits were dated by various workers in order to define the correlation between the stratigraphic sequence and other scientific purposes. They are as follows:

Table 2.2: Geochronological order of the Pakhal sediments worked out by various workers.

Geochronology of the Pakhal sediments				
Rock type	Locality	Method	Age (In Ma)	Reference
Dolomitic limestone	Mallampalli Subgroup,	K-Ar	1330±53 Ma	Vinogradov et al., (1964)
Glauconite	Low. Sullavai group	-	870 Ma	Chaudhuri et al., (1989)
Pundikunta limestone	Pakhal western belt	⁴⁰ Ar/ ³⁹ Ar	1686±6	Conrad et al., 2011
Glauconitic Chanda Limestone	Somanpalli Group	Ar/ Ar	1566±6 Ma	Conrad et al., 2011

3.1 Introduction

Geomorphology of any area is mainly manifested by the substrate nature, climate, structure and few more internal and external parameters. The drainage network at the earth's surface exerts a first order control on relief dynamics and the erosion of mountain belts. Beyond its role in shaping the topography, the drainage network is mainly controlled by the coupling between surface and deep crustal processes such as tectonic and climatic variations (Viaplana-Muzas et al., 2015). Drainage system is governed by the topographic gradients, lithology and structural attributes of a region.

Drainage patterns may reflect original slope and structure or the successive episodes by which the surface has been modified, including uplift, depression, tilting, warping, folding, faulting, and jointing, as well as deposition by the sea, glaciers, volcanoes, wind, and rivers. Impervious or moderately impervious lithology, flat or gently sloping plains generally exhibit dendritic drainage pattern where most streams follow the slope of the terrain and meet the major stream forming over a flat terrain.

Information regarding the palaeodrainage can be deduced from the characteristics of the palaeochannels and the associated facies and sedimentary structures. Therefore, as streams persist in a landscape they show the effects of a long geologic history as well as information on structure and surface conditions (Schumm et al., 1987). In such terrains, faulting and their reactivations due to tectonism lead alluvial and colluvial fan formation and landscape configuration (Thakkar et al., 1999).

Rivers contain fingerprints of past tectonic events is debated. Lithology influences drainage density by affecting the erosion process. The rate at which erosion proceeds depends on the susceptibility of the surface to erode and the runoff intensity (Strahler, 1956). The drainage density exhibited by a region is the balance between climate, geomorphology and hydrology, which in turn shows the degree of fluvial dissection of a region (Lin and Oguchi, 2004).

The present study area has been segmented into numerous blocks with bounding faults and lineaments. Also, the drainage of the area shows dendritic to sub-dendritic in most and feebly parallel to sub-parallel type of patterns along the basin-margin faults. Convergence and offsetting patterns of streams are common in faulted terrains

(Pati et al., 2011; Bhosle et al., 2009; Singh et al., 2006), which are very much prominent along the boundary faults in the study area.

The NW-SE trending lineaments are characterized by convergence and straight channels and regional drainage divides. Slope influences rates of runoff, soil creep, and soil flowage (Strahler, 1956) and it changes due to faulting and differential erosion changes the local geography and hence the drainage geomorphology.

In this study we are trying to compare the orientation of the past drainage system of Gojoli block with the present and to decipher how tectonic-controlled block tilting and differential erosion promotes topographic changes in the area. Apart from that, solution induced pore-filling has played a major role in the infiltration process which in turn defines the drainage characteristics.

Associated sedimentary structures suggest west-flowing Proterozoic channels were debouching along the eastern margin of the PG basin around Gojoli, Dubarpeth and Dongargaon. However, the present drainage around this area is completely different. Major structures (faults and lineaments) along the basin boundary are characterized by parallel to sub-parallel drainage pattern flowing to south. Surface of the fault-bounded blocks shows dendritic to sub-dendritic drainage.

This indicates that even if the area is peneplained to great extent from the Proterozoic to Recent, but the effects of structural features still persists on them and change of slope around the area is due to tectonism and erosion. Drainage parameters such as drainage pattern, drainage density, stream frequency, channel sinuosity and infiltration number of the present drainage have been used to study the present drainage characteristics.

The foundations of the modern drainage systems, cratonic boundaries, and the inland terrains were laid around the late Proterozoic times. Various depositional cycles and associated sea oscillations and the climatic factors have brought down indelible impressions in the form of sedimentary cover and structures in the region.

Erosional processes slowly stripped the surface cover and large scale sediment redistribution over the period of time. The present scenery is the net effect of all those constraints (Fig. 3.1).

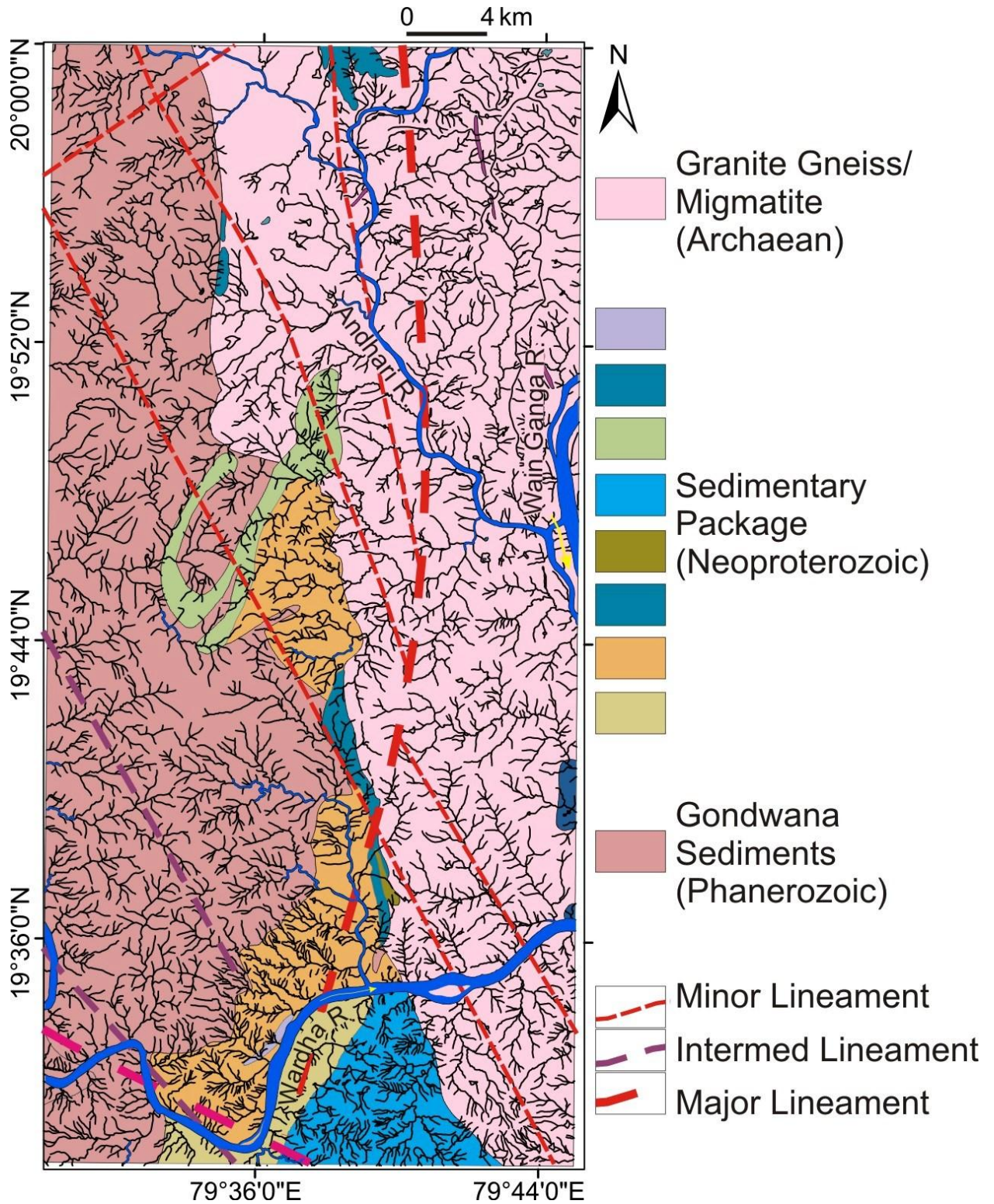


Figure 3.1: Diagram showing modern drainage system, cratonic boundaries and inland terranes along with various faults and lineaments of Das et al., (2003) and seismotectonic atlas of India.

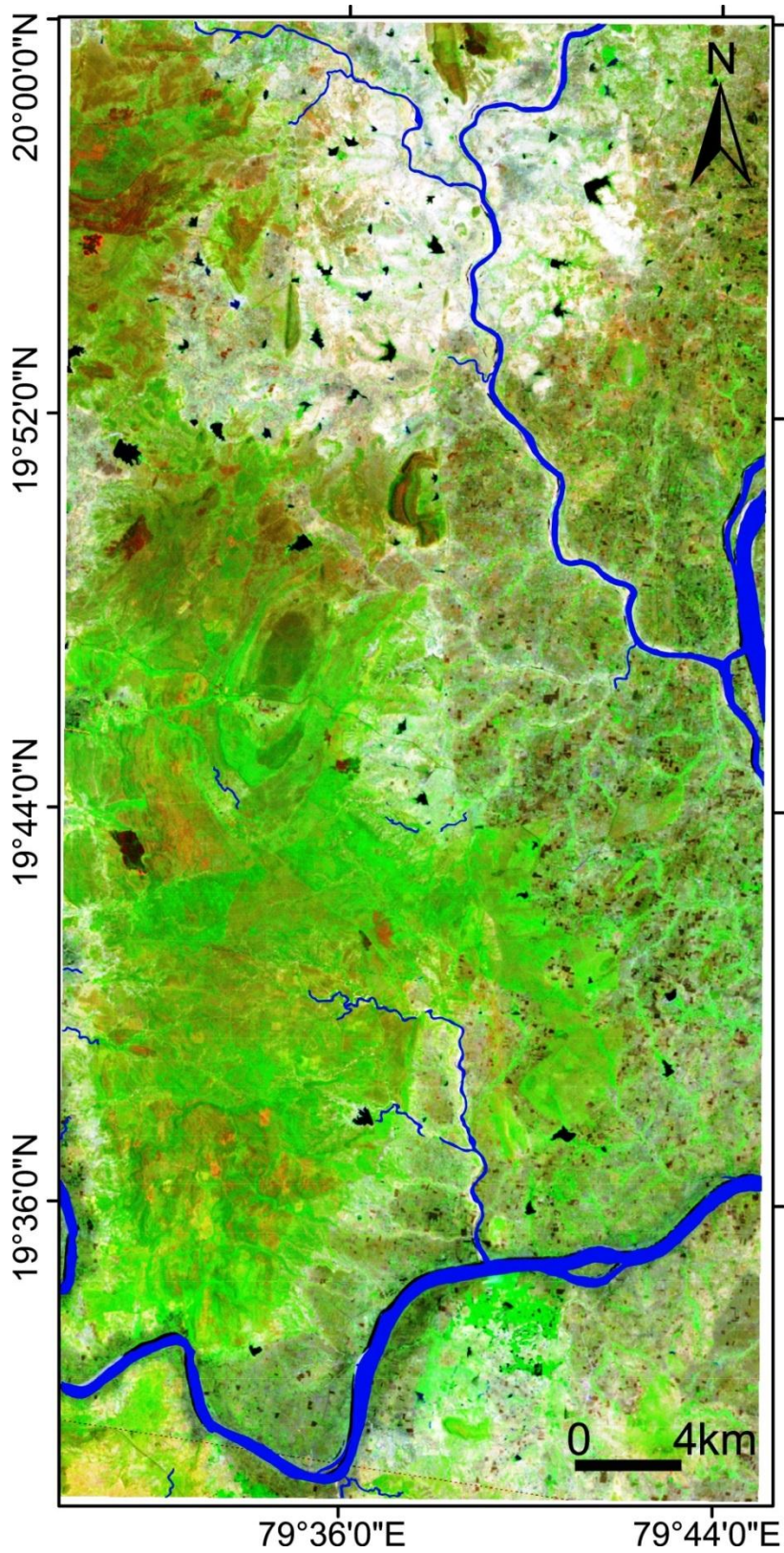


Figure 3.2 Landsat-TM image derived by stacking of the band 7-4-2 (P-143, R-047; 03/05/2011) prepared using software ArcGIS 10.2.2.

3.2 Study based on remote sensing

During this study, Landsat-TM image (P-143, R-047, acquired on 03/05/2011 at 11:08 am, (freely downloaded from www.earthexplorer.usgs.gov) processed by ArcGIS 10.2.2 software was used to identify various structures and major outcrops in the field (Figure 3.2). Remote sensing helps to define the areal continuity of Proterozoic and Gondwana sediments in the basin. Apart from that, major, intermediate, minor lineaments (>200 km, 100–200 km and <100 km, Das et al., 2003) which control the drainage geomorphology of the region were also identified by remote sensing and geomorphological studies.

Major lineaments has been defined as a linear topographic feature of some regional extent and supposed to reflect the basic structure of terrain (Hobbs, 1904; Das et al., 2003). The morphological and tectonic components give rise to lineaments of composite nature. The band combination of 7-4-2 as red, green and blue, respectively, provide good viewing and interpreting results. Various tones and textural elements also allowed identifying the lithounits which were checked during the field work. The contact between the basement rocks and the Proterozoic sedimentary cover of the region can be clearly demarcated in the NNW-SSE linear strip in the imagery. Its fault controlled nature brings it down to basin margin status in the region (Dora et al., 2011, 2015; Pati, 2010) whereas, the western zone from top to bottom is covered fully with the Gondwana sediments with few inliers of Proterozoic.

The clear distinction between the contrasting litho-units in Gojoli, Dhaba and Dongargaon is visible in the area. More than three parallel lineaments trending in NNW-SSE could clearly be identified from the imagery. Apart from that, other two sets of lineaments trending NW-SE and NE-SW are also demarcated on the satellite image (Fig. 3.3).

3.3 Digital Elevation Model

Digital Elevation Model (DEM) was defined by O'Callaghan and Mark (1984) on the basis of any numeric or digital representation of the elevations of all parts of the planetary surface. They restrict themselves to regular square grid which is the most common data structure. In such grid, elevations are present as matrix of points equally

spaced in two orthogonal directions. Also, a DEM resolution finer than the typical 30m by 30 m or up to this grid size is required to accurately resolve the hillslope/valley transition.

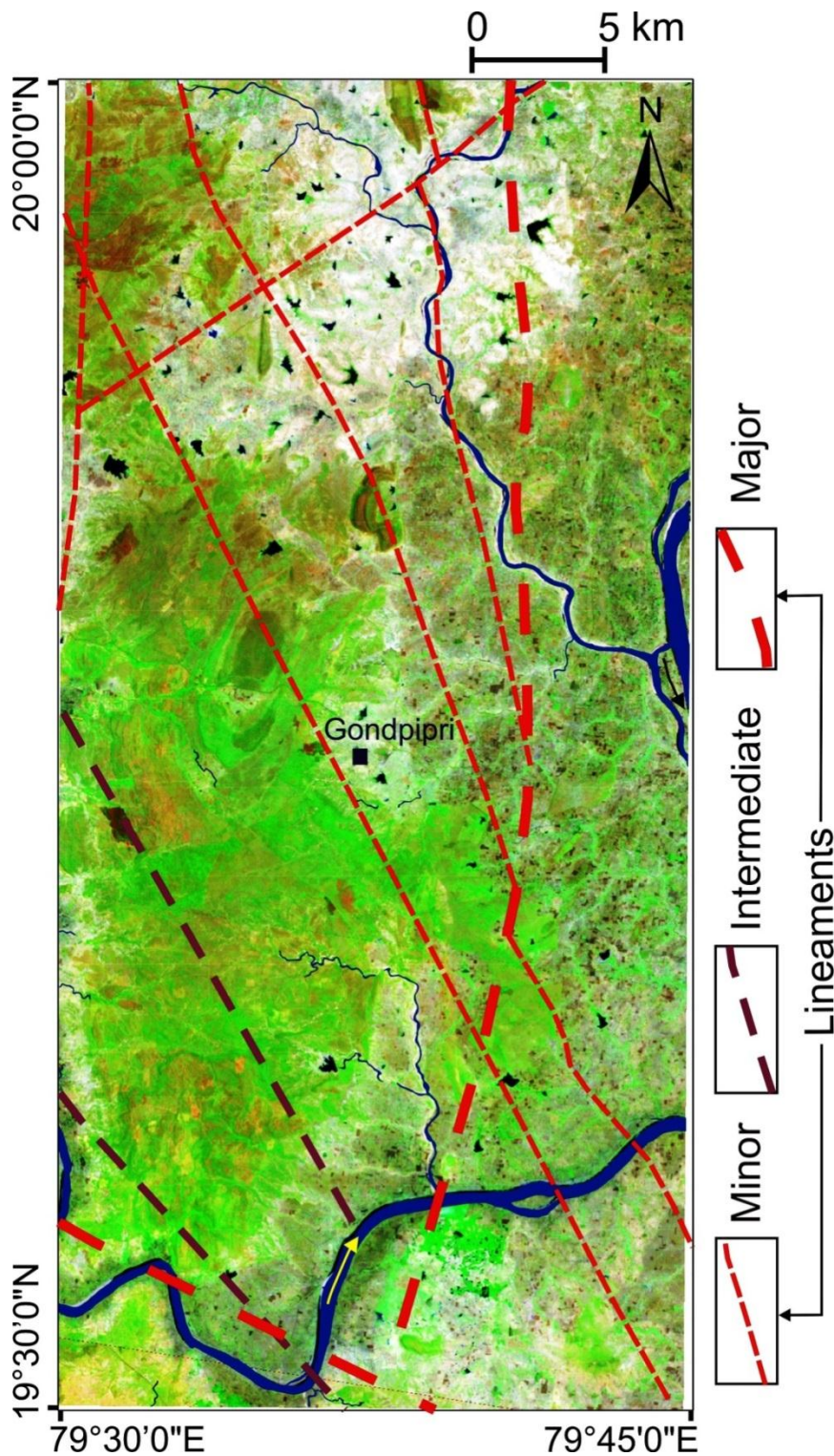


Figure 3.3: Various sets of lineaments of Das et al., (2003) of minor, medium and major range and structures are marked over Landsat-TM image for interpretation.

For many soil-mantled landscapes, a slope-dependent critical support area is both theoretically and empirically more appropriate for defining the extent of channel networks (Montgomery and Foufoula-Georgiou, 1993). Therefore, in this study, Point heights and contour map are digitized from the Survey of India toposheets using ArcGIS 10.2.2 platform to create a raster format of the region. Using kriging interpolation method Digital Elevation Model (DEM) was generated to get an accuracy of around 2m to study the regional topography of the study area (Fig. 3.4).

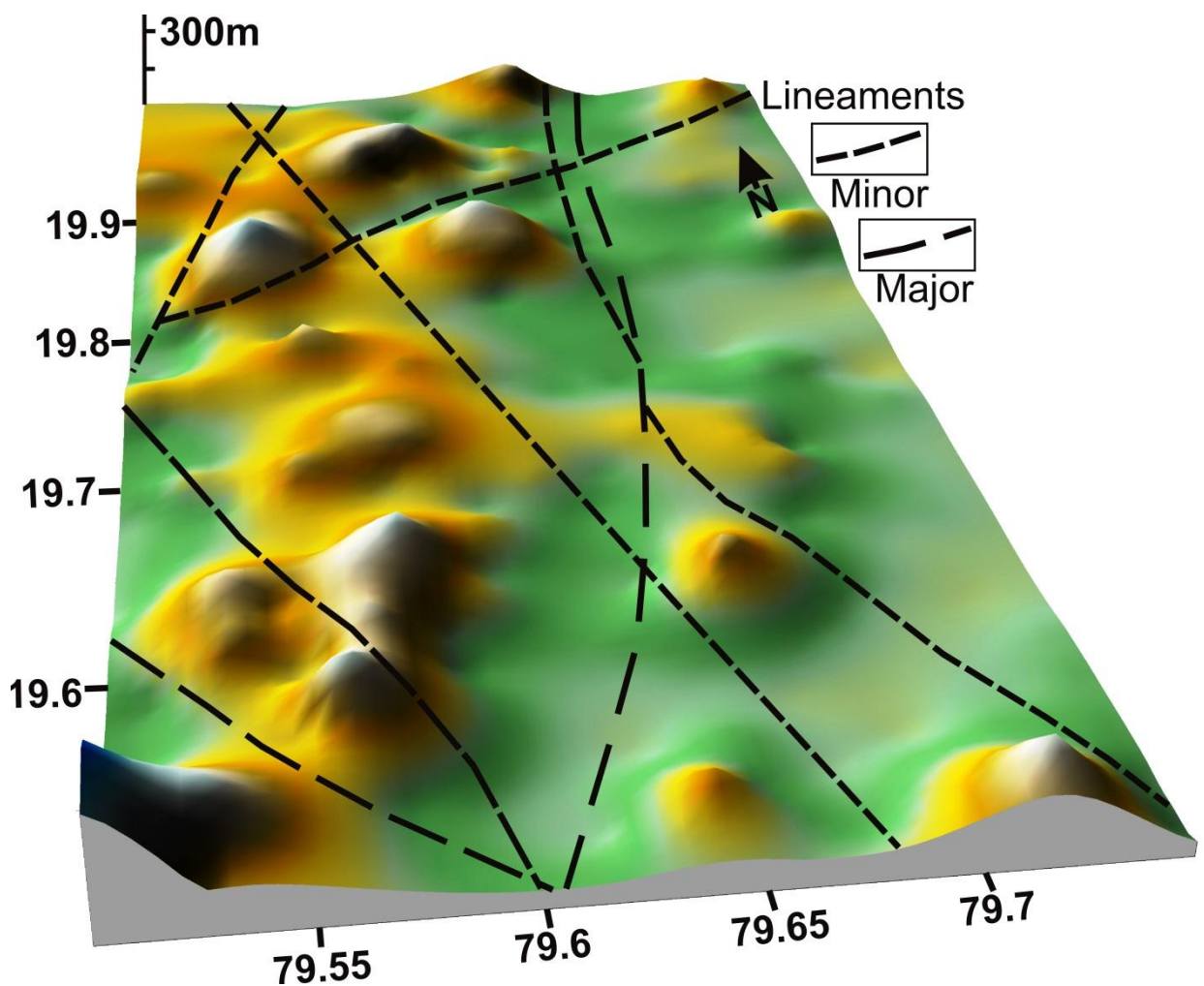


Figure 3.4: Digital Elevation Model (DEM) showing terrain and slope with lineaments prepared using softwares ArcGIS 10.2.2 and SURFER 8.0

3.4 Hydrological parameters

3.4.1 Bifurcation Ratio

Bifurcation ratio is the ratio between the number of streams of a given order (Nu) to the number of segments of the next higher order (Nu+1).

$$R_b = Nu / Nu+1$$

In the study area R_b varies from 0.82 to 2.54; the mean R_b of the entire basin is 1.88 as shown in the Table-3.1. High bifurcation ratio in any particular area indicates high drainage density (Chopra et al., 2005). In the present area, bifurcation ratio varies from 1.92 (Archaean gneiss) to 2.18 (Proterozoic sequence) which indicate a rolling or flat region without any structural control implying that it has suffered a lot of denudational activities in the past (Kalaivanan et al., 2014). However, the area has a low to moderate drainage density of 2.31 also supports to the low to moderate bifurcation ratio of 1.88 overall. Therefore, bifurcation ratio also infers low structural control over the drainage. Usually these values are common in the areas where geologic structure and tectonics of that region does not exercise a dominant influence on the drainage pattern.

3.4.2 Drainage pattern, drainage density and slope

Drainage pattern observed through the SOI toposheets show dendritic to sub-dendritic and more or less sub-parallel in few parts like the southeastern region. The drainage density varies according to the lithology, slope and structural control over the area. Ample variation in lithology assisted with slope has played principal role in drainage density variation (Fig. 3.1). But, overall drainage density value of 2.30 shows a low to moderate infiltration of the region besides similar channel spacing.

Slope is such important parameter that needs to be correlated with drainage density to analyse the processes. The environmental factors like rainfall, relief and erosion affect the slope and govern the hillslope processes like run-off generation and erosion rate (Tucker and Bras, 1998). Hence, relation between the slope and drainage density can be observed which predominates in this region due to more or less low topography. Yet, the drainage density and gradient also indicates medium to high infiltration and less active structures regionally. However, generation of slope is a manifestation of tectonics and erosion in any particular area.

3.4.3 Drainage Texture

Drainage texture (Dt) explains the relative spacing of drainage lines given by;
 $Dt = Nu/P$

Where, it is total number of stream segments of all orders per perimeter of that area (Horton, 1945). Dt is a measure of closeness of the channel spacing, depending on climate, rainfall, vegetation, lithology, infiltration capacity and relief aspect of the terrain. Smith (1950) classified drainage texture into five different classes. In the present case, the drainage texture of the region is 18.65 indicates “very fine” category drainage texture and moderately permeable lithology which matches with overall drainage density of 2.30 (Table 3.1).

3.4.4 Stream frequency

The term stream frequency was introduced by Horton (1932). It means the number of stream segments (Nu) per unit area (A).

$$Fs = Nu/A$$

In the present study, the stream frequency of the basin is 2.01/km² indicates low F_s . The stream frequency of the study area shows a positive correlation with the drainage density indicating that the stream population increases with the increase of drainage density. The development of the stream segments in the basin area is more or less affected by rainfall, temperature and permeability of the substrate.

3.4.5 Infiltration number

Faniran, (1968) explained infiltration number of a drainage basin is the product of drainage density (Dd) and stream frequency (F_s) given by relation;

$$If = F_s \times Dd$$

It is a parameter which gives an idea of the infiltration characteristics of the basin. The infiltration number is 4.70 and this value indicates moderate infiltration and medium to low runoff, the lithology of basin is not considerably hard but moderately permeable. The higher values of infiltration number indicate the lower infiltration and the higher runoff (Das and Mukherjee, 2005). Also, in the present study area, the middle zone (Proterozoic sediments affected by hydrothermal activities) show high infiltration number as compared to the granite gneiss (east) and the Gondwana sandstone (west). This clearly indicates the hydrothermal activity in the middle zone

has reduced the porosity and permeability by impregnation of hydrothermal fluid in the rock pores (Fig. 3.5).

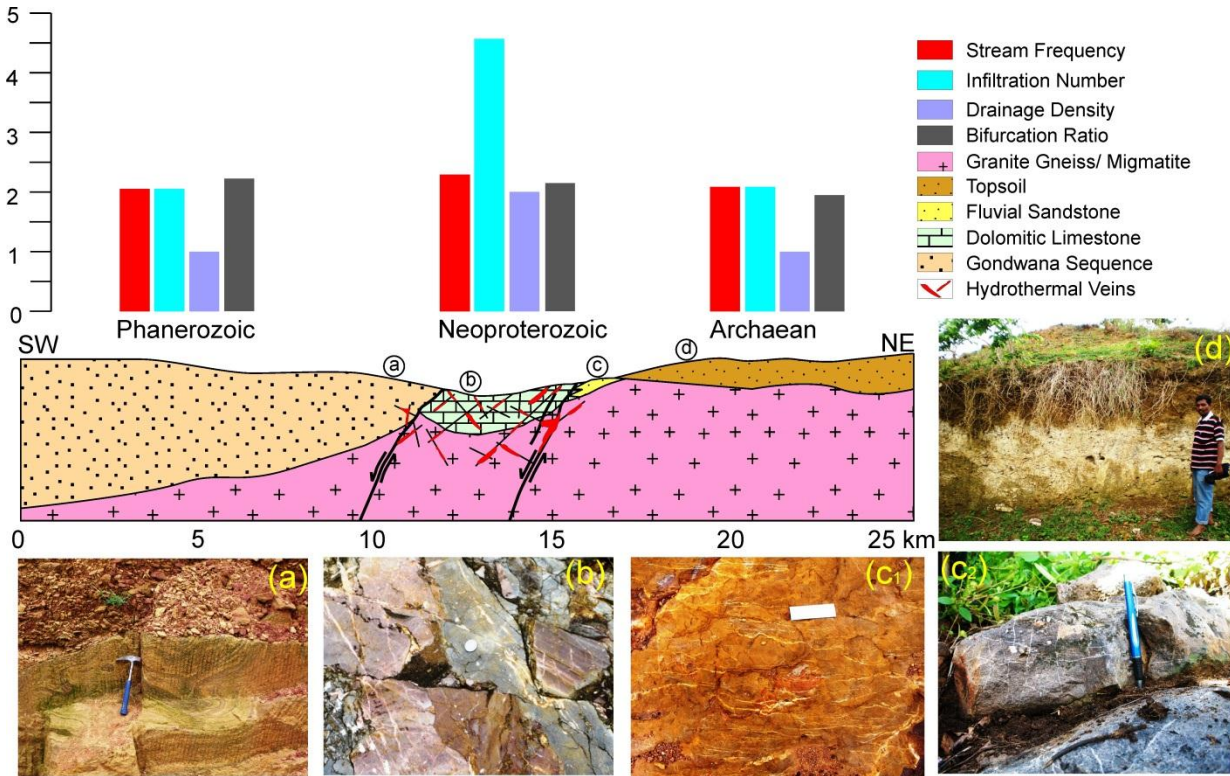


Figure 3.5: Diagrammatic representation of the lithological and structural disposition of the area with variation of drainage parameters. Circles represent the position of photographs shown below the figure. (a) Gondwana sandstone at Kirmiri (b) Hydrothermal injections in the form of veins within the basin boundary limestone near Gojoli (c¹) Hydrothermal veins within basin boundary sandstone surface at Dongargaon hill (c²) at Dubarpet (below the surface) (d) Development of thick weathering profile on Archaean gneiss terrain near Dongargaon.

3.4.6 Channel sinuosity

The deviation from straight line towards a curve gives the amount of sinuosity. Sinuosity (S) is a measure used to quantify the difference between meandering and straight channels. Sinuosity of a channel is defined as the channel length (L) measured along the center of the channel divided by the valley length (L_v) measured along the valley axis (Schumm, 1963):

$$S = L/L_v$$

Sinuosity of natural rivers generally varies between 1.0 (straight channels) and 3.0 (highly sinuous, or “tortuous” meanders). A completely straight channel will have a

sinuosity of 1. Channels with ratios ~1.5 are called sinuous channels channel with higher ratios are called meandering channels (Wolman and Miller, 1964). The major streams in the study area show an average sinuosity of 1.25 to 1.35 which determines the area to be low to moderately active.

Drainage analysis is useful in structural interpretation, particularly in areas of low relief. Analysis includes consideration of drainage patterns, drainage texture, individual stream patterns, and drainage anomalies. But, in this area anomalies are not found within the study scope and since the relief was medium, showing a 140 m and 241 m of minimum and maximum elevations, and various parameters also shows low to moderate values all of which are corresponding to each other.

This indicates that convergence of drainage, if any, lies mainly along the fault zones or basin margin and not much of it is due to the tectonics in other parts of the region. However, drainage anomalies are local deviations from drainage and stream patterns which elsewhere accord with the known regional geology or topography (Howard, 1967). Hence, such anomalies bring convergences in the drainage in the areas having different lithologies. Here, convergence of many streams in the southeastern and eastern part of the study area is seen whereas smaller convergences of first and second order streams in the upstream areas verifies the main dominances of slope in these areas and previously active zones of tectonism.

Fault controlled areas along the basin margin shows offsetting of the drainage in Andhari River and in Dhaba River which can be observed through the surface impressions in aerial view or traced on ground surface. This can assist in interpretation of various lineaments or faults in the region which are concordant to the major fault or the basin margin.

Table 3.1: Showing various parameters and their inferences based on actual values.

Parameters	Formula	Actual value	Standard value and its Inference	Actual value and its Inference
Bifurcation ratio (Rb)	$Rb = \frac{Nu}{Nu+1}$	1.88	<3, Flat region (Horton, 1945)	Low to moderate value show less

				structural control.
Drainage density (Dd)	$Dd = \sum Lu/A$	2.30	2-3, High (Dd) (Horton, 1932)	Low to moderate value show less tectonic disturbances.
Drainage texture (Dt)	$Dt = \sum Nu/P$	18.65	>10, Very fine texture (Smith, 1950)	Very fine drainage texture shows more infiltration and less structural control.
Stream Frequency (Fs)	$Fs = \sum Nu/A$	2.01	0-5, Low (Fs), (Horton, 1932)	Moderate (Dd) and low structural control.
Infiltration number (If)	$If = Fs \times Dd$	4.70	Medium infiltration and medium run-off (Faniran, 1968; Das and Mukherjee, 2005)	Medium infiltration and medium runoff and less hard lithology.
Channel Sinuosity (s)	$s = L/Lv$	1.35	1.5, Sinuos, >1.5, Meandering (Wolman and Miller, 1964)	Low to moderate shows feeble tectonism.

3.5 Impact of tectonics on drainage and geomorphology

To study the tectonic impact on geomorphology of the study area it is imperative to study about the drainage and structural discontinuities because the drainage network at the Earth's surface exerts a first order control on the relief dynamics and the erosion of mountain belts. Beyond its role in shaping the topography, the drainage network is a main controlling factor of the coupling between surface processes and deep crustal deformation, as well as of the relations between tectonics and climate variations, and the sedimentary record in basins (Viaplana-Muzas et al., 2015). Since, drainage system of the study area is defined by the natural flow of surface or sub-surface water towards the slopes and weak zones or along the lineaments. It is totally governed by the topographic gradients and structural attributes of the region. For example, impervious or moderately impervious lithology generally exhibits dendritic type of drainage system where most streams follows the slope of the terrain and comes to join the major stream forming over a flat terrain or the parallel one which is ruled by parallel faulting and steep slopes or elongated resistant rock bands etc. Therefore, structural and lithological variation information can be drawn from drainage patterns. Zernitz (1932) stated, "Patterns which streams form are determined by inequalities of surface slope and rock resistance. This being true, it is evident that drainage patterns may reflect original slope and original structure or the successive episodes by which the surface has been modified, including uplift, depression, tilting, warping, folding, faulting, and jointing, as well as deposition by the sea, glaciers, volcanoes, wind, and rivers." Therefore, as streams persist in a landscape they show the effects of a long geologic history as well as information on structure and surface conditions (Schumm et al., 1987).

River drainage patterns sculpt terrestrial landscapes. Whether these patterns contain fingerprints of past tectonic events is debated. On the one hand, elaborate dendritic river networks always retain an invariant structure, implying that rivers will simply reorganize in response to tectonic perturbations, without long-term trace of the tectonic event (Castelltort et al., 2012). However, lithology influences drainage density by affecting the erosion process. The rate at which erosion proceeds depends on the susceptibility of the surface to erosion and the runoff intensity (Strahler, 1956). The drainage density exhibited by a basin is at the heart of the balance between climate,

geomorphology, and hydrology. It shows the degree of fluvial dissection (Lin and Oguchi, 2004).

In the present study, drainage of the study area shows dendritic to sub dendritic in most and then feebly sub-parallel type of pattern in few areas. There are streams showing convergence at places and some exhibits offsetting patterns where fault activity due to slip movement might have taken place. Therefore, structural influence with respect to lithology over drainage can be interpreted up to some extent. Also, the Proterozoic channels were west-flowing evidenced by the sedimentary structures and facies assemblage as seen in the field (Fig. 3.6). However, the present channels are flowing towards south and east showing inversion of drainage in the block.

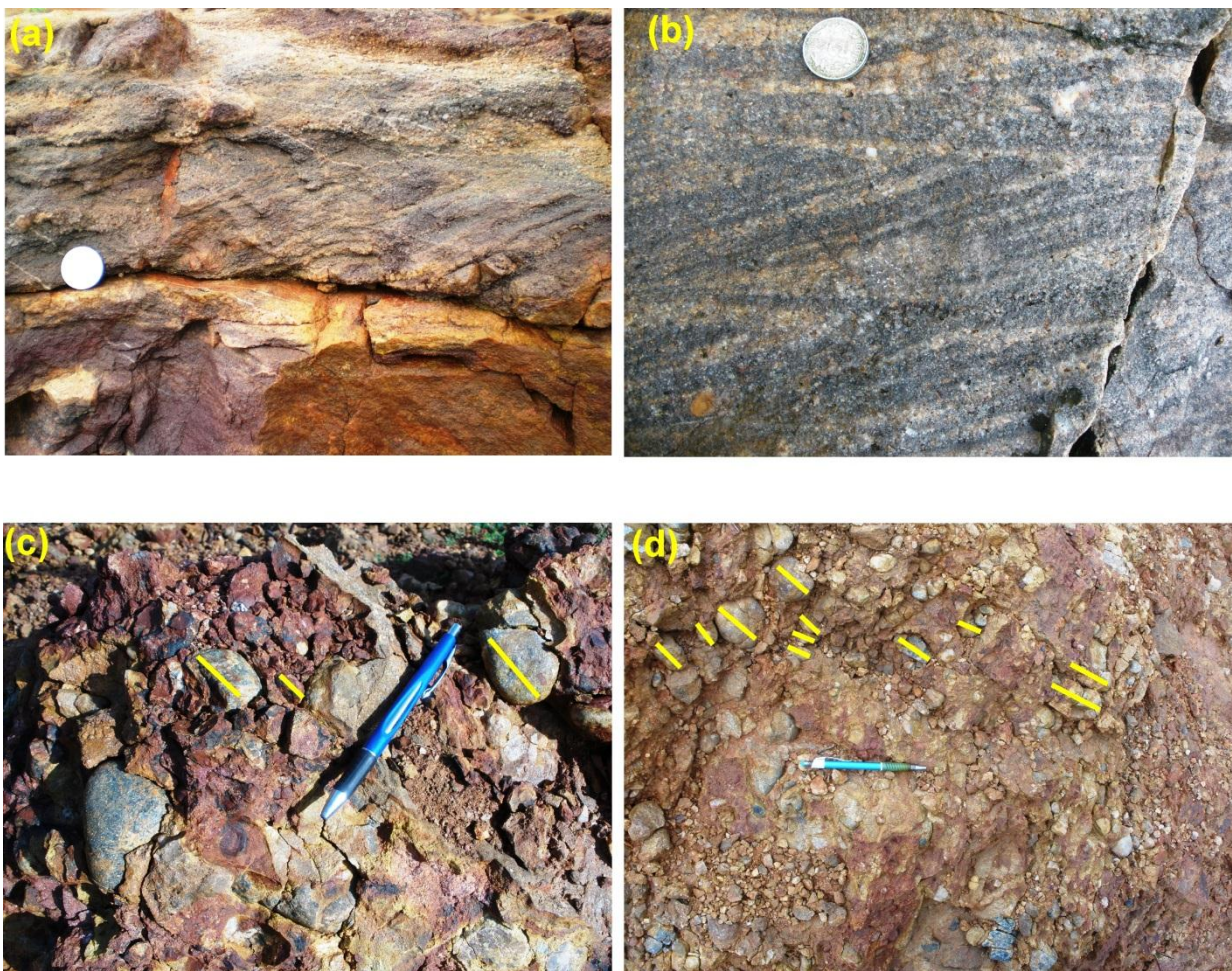


Figure 3.6: Proterozoic channels were west flowing evidenced by (a) Cross-bedding of sandstone showing westward flowing channels near Dubarpet (b) near Dongargaon (c) & (d) imbricated pebbles (yellow lines) in the conglomerate beds at Dongargaon hill showing flow direction.

In this study, effect of lithology and gradient over drainage patterns and control by the structural elements, if any, to elaborate the geomorphology of the study area have been explained. Major structures (faults) along the basin boundary are characterized by parallel to sub-parallel drainage pattern. However, the surface of the fault-bounded block shows dendritic to sub-dendritic drainage. This shows that even if the area is peneplained to great extent from the Proterozoic to Recent, but the effect of structural features still persists on them. Meanwhile, the region is juxtaposed by igneous terrain, therefore, due to filling of the rock-pores by hydrothermal veins in the fault zone, the Proterozoic sequence which also show different drainage characteristics (Figure 3.5).

3.6 Lithology and relief interaction

The chemical, physical and biological properties of sedimentary rocks are strongly inclined by nature of sediment source areas (Provenance) and the conditions of the depositional environment. Hence, the source area characteristics and depositional environments are, in turn, the result of geologic and tectonic history of the region in which accumulation of sediment takes place. So, drainage is the one of the primary agency for such crustal manifestations and sediment transportation. The study area has Lower Gondwana sandstones on the western part of the region which shows moderate to the semi-sparse number of streams evidencing dendritic to sub dendritic type of drainage pattern.

Lithologically, Granite gneiss/migmatite on the eastern margin covers the maximum area of the region showing purely dendritic to parallel and subparallel type of drainage patterns with gentle slopes in the range of 5°-10°. Sandstones of Kamthi Formation, Yerrapalli Formation and Kota Formation are present in small patches from south to north along with Maleri friable sandstone in the southeast which also shows the parallel and dendritic-type of drainage patterns with gentle to high slope values between 5°-25° degrees. Slope decreases from 25° in southern part to a gentler of 5°-6° towards northern corresponding to the topography and proximity to the basin margin which manifested it temporally to the Upper Neoproterozoic. However, no major tectonic activity or crustal perturbations, afterward, came into existence otherwise, it might have reflected from the pattern and texture of the drainage. Thus,

drainage has been acted according to the gradient of various lithologies in different areas and permeable to semi-permeable nature of lithology while considering the factors of erosion rate and precipitation.

High relief and steep slopes impart higher runoff bringing higher drainage density into picture and such area also show increased surface runoff compared to low drainage density area (Shahid et al., 2000). There are some hard and resistant lithologies like dolomitic limestone or fine grained sandstone in some areas along the basin margin show very low drainage density due to gentle gradient of 6°-12° and high resistance of erosion and infiltration. This can be explained as resistant lithounits with low runoff intensity require more drainage area to accumulate runoff of sufficient erosive power to initiate a channel.

Also, slope and drainage density correlate positively if overland flow promotes erosion but negative if shallow mass wasting is dominant (Lin and Aguchi, 2004). Hence, current drainage and slope relationship can be explained on these factors with respect to lithology and slope. Now, the drainage since not much changed due to tectonics and the structural aspects also not very much affected the strata since Upper Neoproterozoic. Because, most of the changes took place in the drainage are between Pliocene to Recent (Brookfield, 1998).

3.7 Structural orientation and tectonics

The study area falls under the eastern part of the Pranhita-Godavari basin which overall came across a series of episodes of tectonic activity since Proterozoic. Denudation activities brought the current topography into existence which is evidenced by feeble structural control over the region as represented by moderate bifurcation ratio. However, few segments of the region show dendritic to subdendritic and somewhat sub-parallel drainage pattern, whereas, the boundary zone shows straight drainage controlled by faults.

Primitive structural control in relict form can be clearly seen in some of the straight and fault guided streams in the central parts near to Dhaba Nala and Andhari River which represents the basin margin and its proximity. Even the Wainganga River and the Wardha River can be seen running major part of their courses along the associated faults. Regional continuity and straight orientation of the structure like a

fault cannot be ruled out in the light of sub-parallel drainage pattern present along areas proximal to basin margin present in the central region.

Regional compressional activities along the Pranhita-Godavari valley caused folding and later due to intra basinal tectonic activities caused the strata to refold which also has altered the drainage but to a very less extent during Upper Neoproterozoic and further up to Mesozoics. Because, similar activities were almost abandoned due to the passive nature in the Quaternary except active denudational activities up to Recent which were strong enough to erode the area to an extent that topography and structures do not affect much. However, the geomorphology of the landscape represents the balance between process creating and destroying topographic relief.

Initially, ample upliftment and subsidence took place followed by the extensional activity in the passive basin margin creating numerous listric faults in the region resulting in horst and graben kind of structures. Inactiveness of these structures at present is also the manifestation of proper settlements on account of accommodation of sediments in the roll-overs or gaps during Upper-Proterozoic and further. However, there were substantial episodes of fossilization of rift caused the readjustment and redevelopment of the geomorphology of the region due to various geological agencies. Thereafter, these all sequences of events had developed and readjusted the drainage patterns partially and many times identification of which may not be possible to define in the field due to denudation effect.

The drainage patterns which developed in the present scenario are moderately controlled by structural affinities and mostly by lithological assemblage of the region. Presence of moderate relief features in the region does not bring changes in the behavior of the drainage pattern and its density. Therefore, drainage behavior and its pattern is a consequence of convergence of common variables like lithology and of the area, structural control, relief, climate and temperature. However, lithology, relief, slope and structural control are the intrinsic factors which directly affect the drainage pattern and its density.

3.8 Interpretations

Relict of the basin boundary faults still has certain influence on the present day drainage system as evidenced by the convergence, offsetting and straightness of few

channel courses. Different parameters suggest the present-day drainage characteristics are mainly controlled by lithology and slope. Lithological contrast can be seen through the drainage density contrast in the blocks. Present-day drainage is flowing southerly following the basin boundary faults instead of west. However, the Proterozoic channels in the block were west flowing as evidenced by the facies and sedimentary structure which shows a change in the topography from Proterozoic to Recent due to tectonism and erosion.

4.1 Introduction

Facies is a term which denotes the particular set of conditions for sedimentation and different kind of environments in which they are accumulated due to the work of geological agencies (Pettijohn, 1984). Distribution of different facies depends on the climatic and tectonic conditions along with the provenance of any area where local tectonism is responsible for their spread or confinement in particular region and the dew, frost or aridity may decide the climatic conditions to work upon the same.

The Pranhita-Godavari basin comprises several unconformity-bound sequences of group status, and exhibits strong regional variations in the distribution of different groups deposited in widely variable conditions, ranging from alluvial-fan setting to deep-water slope, base-of-slope and basinal environments. The lithologic assemblages indicate that the basin experienced multiple rifting, and tectonic environment varied from an unstable rift setting to a stable shelf regime (Chaudhuri, 2003).

Individual rock groups were deposited at different stages of the rift evolution during Meso-Neoproterozoic and Mesozoic (Biswas, 2003; Deb, 2003). Thus the stratigraphic framework of the PG basin was collectively shaped by various factors like tectonics, climate, sea level changes and different degree of fluvial inputs along the basin margin (Chaudhuri and Deb, 2004). The outbursts of felsic volcanism during the rifting caused addition in repeated rifting of the craton within the basin (Sarhani P Deb, 2003). Episodic rifting, activity of the basin-margin faults and rift fossilization events are well preserved in the lithostratigraphic successions in space and time (Chaudhuri et al., 2002; Chaudhuri and Deb, 2004).

At present, these unconformity bounded Proterozoic rocks are exposed as two linear belts along the basin margin, flanked by the Archaean gneiss and granulites as basement (>2500 Ma, Rajesham et al., 1993) towards the outer margin (Fig. 4.1) and separated by the Paleozoic Gondwana formation in the center (Robinson, 1971). The Proterozoic sedimentary rock groups along the western margin of the basin named as Penganga or Sullvai and Albaka were studied in fair detail (Bose and Sarkar, 1991; Chaudhuri et al., 2002; Biswas, 2003; Deb, 2003; Chaudhuri and Deb, 2004) and with

a special emphasis on the carbonate sequences by Bose and Sarkar (1991).

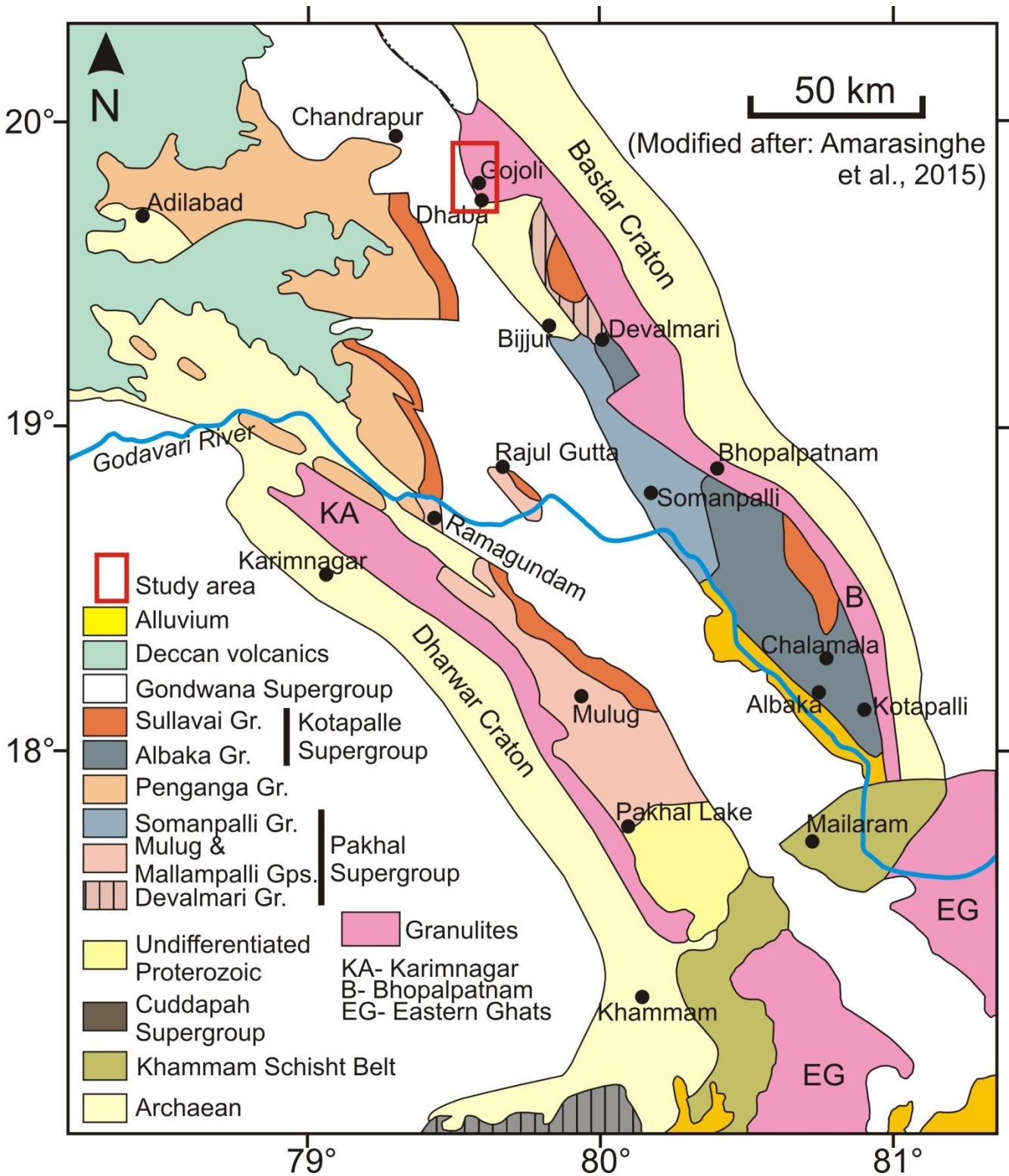


Figure 4.1: Regional map of the Pranhita-Godavari basin and its adjacent blocks showing convergence of Bastar and Dharwar craton and the study area near Chandrapur near eastern margin of Pranhita-Godavari basin.

Limestone facies (ca. 773±30 Ma, Chaudhury et al., 1989) in the western margin of the basin was classified according to their depositional characteristics (Bose and Sarkar, 1991) and was correlated with the basin boundary tectonic processes.

Presently, three different localities in the area of study are showing various kinds of environmental conditions responsible for the accumulation of sediments. Each lithounit has its own depositional history and environment of deposition which indicates towards the variation in paleogeomorphological and paleotectonic conditions of that particular region. Large variation in facies within a small region definitely points towards isolated nature of depositional environments, and small sub-basins at the basin boundary. Occurrence of faults along the basin margin may suggest the fault-bounded block-walled sub-basins along the basin margin were responsible for such variation. The detailed geological and tectonic related works carried out by various authors and lithological advancements are given in the previous chapters therefore straightway an attempt is required to bring forth the facies description related to the mapped area for the detailed analysis.

The upper part of the region (see Fig. 4.2) consists of thick sandstone and conglomerate beds which accommodates a paleosol horizon within the sandstone. This paleosol horizon has been examined for paleoweathering and paleoclimatic reconstructions in the region.

The central part of the basin margin represents massive cherty limestone with autoclastic limestone conglomerates which covers almost complete basin margin of the study area. Variation in clasts-size, clast proportions and characteristics of flows in the autoclastic mass flow conglomerates suggests sediment gravity flow due to basin-margin failure. This failure is attributed to the reactivation of basin-margin faults at different intervals. These reactivations of the basin-margin faults have been correlated with the rifting processes during the basin development. Intermittent tectonically stable periods are represented by formation of stromatolites fringing the basin margin.

Therefore, analysis is required to decipher carbonate facies assemblages represented by massive limestone at the basin margin followed by the stromatolitic limestone with numerous autoclastic mass flow conglomerate carbonate sequences interventions. The limestone development is of considerable general interest for its Precambrian age, deposition amply under wave base and entirely being a sequence of

autoclastic mass flow deposits, as expected in the Precambrian sea, and being developed in the Late Proterozoic, where life signatures also initiated to become visible.

The carbonate sequences were enveloped by shallow marine waters and feeble carbonate mud turbidites, which is visible in their depositional patterns of texture and structural variation. Uniformity of clasts and the enclosing matrix in terms of its lithology along with internal structure describes it as autoclastic mass flow deposit (Cook, 1979). These are supposed to be syn-depositional extensional tectonic origin as described by Bose and Sarkar (1991) along the western margin of the basin. The conglomerates are essentially identical in many ways to the autochthonous carbonate mass movement as described by Bose and Sarkar (1991) along the western margin of the PG basin and Cook et al. (1972); Mountjoy et al. (1972); Hobson et al. (1985); Eberli (1987).

The lowermost region of the study area along the basin margin represents a fan-delta sequence in and around Dongargaon village, was mapped on 1:1000 scale for detailed variation of lithology and sea-level fluctuation. Therefore, the sequences deposited are the manifestations of the interplay between sea level fluctuation, subsidence, climate, energy etc. The Dongargaon fan-delta is a good example of clastic wedge prograded into an isolated marine basin. The major controlling factors shaping the fan delta were firstly, the tectonic instability of the basin due to the rift margin (Biswas, 2003; Galloway, 1976). Secondly, the irregular supply of enough volume of comparatively coarse grained sediments. Third, the energy level of the basin to which the fan-delta was prograding. Since, the study area is a basin margin fault-controlled system; the fault geometry controls the location, scale and gradient of the drainage system, as well as the dimension of the depositional systems in the hanging wall depocentre.

The coarse alluvial fan and stream flow deposits were derived from a surrounding Igneous and sedimentary provenance (McLaughlin and Nilsen, 1982; Pati, 2010). The fan-delta contains valuable information related to environment, climate and tectonic movements of their hinterland because they are much more sensitive to fluctuations in the climate-driven sediment and water supply (Hornung and Hinderer, 2011). Therefore, a slight variation in base level induced either by tectonic movements

or climatic changes can give rise to significant differentiation in sedimentary facies and architecture (e.g. Postma and Cruickshank, 1988).

In this region large scale mapping has been carried out for the first time which helps to decipher the various facies and environments. Also, the lithostratigraphy suffered deformations due to tectonics can be clearly visualized by the field based evidences which will be explained further in the detailed facies explanations. Hence, the basin margin area was assessed keenly to deduce the overall evolutionary pattern of the region within the tectonic, sedimentological and geomorphological frameworks.

4.2 Different facies observed along the basin margin

As discussed earlier, the different facies are restricted in three different localities along the basin-margin. The details have been discussed here.

❖ Dubarpet region

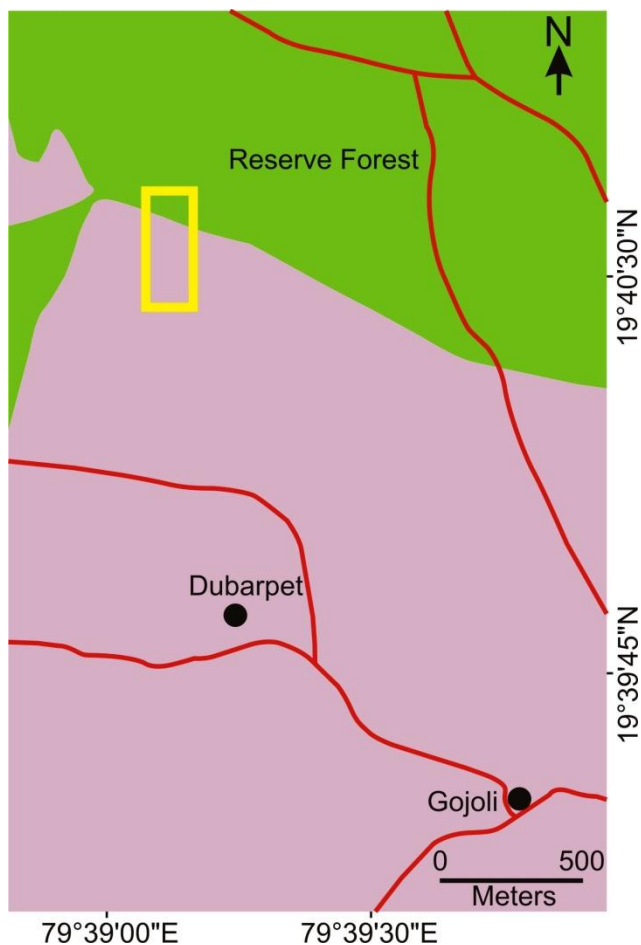


Figure 4.2: Dubarpet region in the toposheet clip showing elongated sandstone ridge in the NNW part (shown in yellow box)

Towards the NNW of Dubarpet village (Fig. 4.2) lays a thick elongated ridge of sandstone dipping in the westward direction. This region consists of two main facies one is the conglomerate facies and the other is sandstone facies. These facies are explained as follows.

4.2.1 Conglomerate facies

The conglomerate facies which are developed in the Dubarpet region consists of gravel-sized clast and the coarse grained matrix (Fig 4.3a). The intraformational character explains deposition of material from the basin itself derived by eroding and transporting of the rock material. They are widespread in geological record and show the shallow marine deposits. Such conglomerates may accumulate as depositional aprons that flank the scarps (steeper slopes) bounding the shallow water platformal areas. But, in present case shows the deposition of sandstone immediately after the conglomerate indicates towards the cyclicity of the complete depositional process (Fig. 4.3b&c).

The rift fossilization or presence of some tectonically quiescent period (Chaudhuri et al., 2002), after the deposition of conglomerate and before the initiation of the marine transgression which was responsible for the deposition of the fine-mud sequences which later on completely disintegrated and carried away by the flows. The conglomerate also shows angular fragments due to fault-related crushing which can misguide the observer to take it as angular breccia. The thickness of the conglomerate bed is about 12-13 m (true thickness) but horizontally it has a good areal extent of about 25 m (exposed). The denudation effect has covered the area effectively which completely covers the outcrop from the naked eye and not identifiable on the first observation. Since, due to absence of life or just due to the initiation of the life at that time, no fossils were present in this member.

Presence of rounded gravels in the peripheries of the contact between the sandstone and the conglomerates probably indicate the shore-face at which the gravels were experiencing forward and backward motion by the waves and hence became texturally matured. Thin (~10-15 cm) mud beds intervene the sandstone and conglomerate may indicate decreasing energy sequence.



Figure 4.3: Photographs shows (a) Gravel sized clast and coarse grained matrix (b) Thick elongated bodies of sandstone, conglomerate and their cyclicity (c) Loose clasts of conglomerate in the weathered matrix and soil.

These facies assemblage (conglomerate-sandstone-mudstone) occur as isolated patches without lateral coalescence may suggest feeble fluvial activity along the basin margin and no redistribution of sediments by the long-shore current. This may suggest an arid (dry/cold) climate was prevailing during the deposition. However, the intervening paleosol clearly indicates about the prevailing cold climate during the deposition. Presence of this kind of intermittent shallow basins also indicates sagging within the graben which causes partitioning of a separate environment albeit different surrounding environmental parameters.

4.2.2 Sandstone facies:

The sandstone facies developed around Dubarpet was the host rock for the paleosol horizons. Sandstone formed along the basin margin by the smaller incoming streams for certain period of time. There are small lensoidal patches of chloritised

zones within the basin marginal contact between the sandstone and conglomerate which possesses the later deformation and fluid passage events. The thickness of the sandstone is almost 20-25m and this type of thick elongated bodies of sandstone (Fig 4.3b) are present throughout the basin margin intermittently (Dora et al., 2011; Pati, 2010).

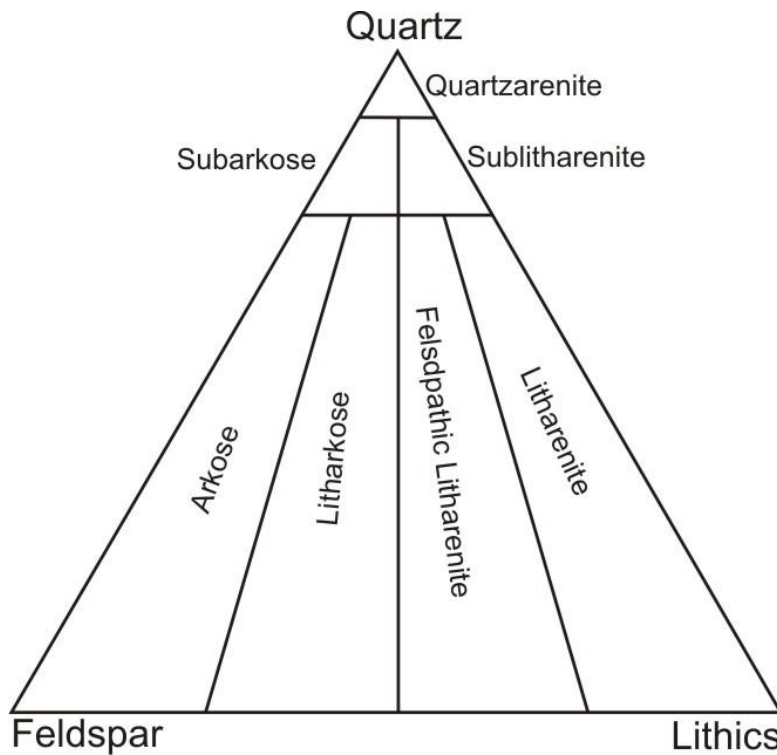


Figure 4.4: Folk (1974) classification showing position of quartz arenite.

This facies was developed due to the influence of minor fan deltaic setting on small shallow marine basin where incoming streams debouching their sediments (Pati, 2010). This sandstone shows textural and mineralogical maturity and falls in the quartz arenite category in Folk's classification (Fig. 4.4). Presence of glauconite in the sandstone suggests it to be a shallow marine deposit at the basin margin and was reworked at the shore-fane to gain textural maturity.

4.2.3 Paleosol

The paleosol is associated with the Sullavai Group yields the K-Ar age of 871 ± 14 Ma (Chaudhuri and Howard, 1985). The westward dipping litho-package of the

region represents a fan-delta deposit at the basin boundary, consisting of fluviially deposited conglomerate, sandstone (hosting paleosol) and shale (Fig 4.5a).

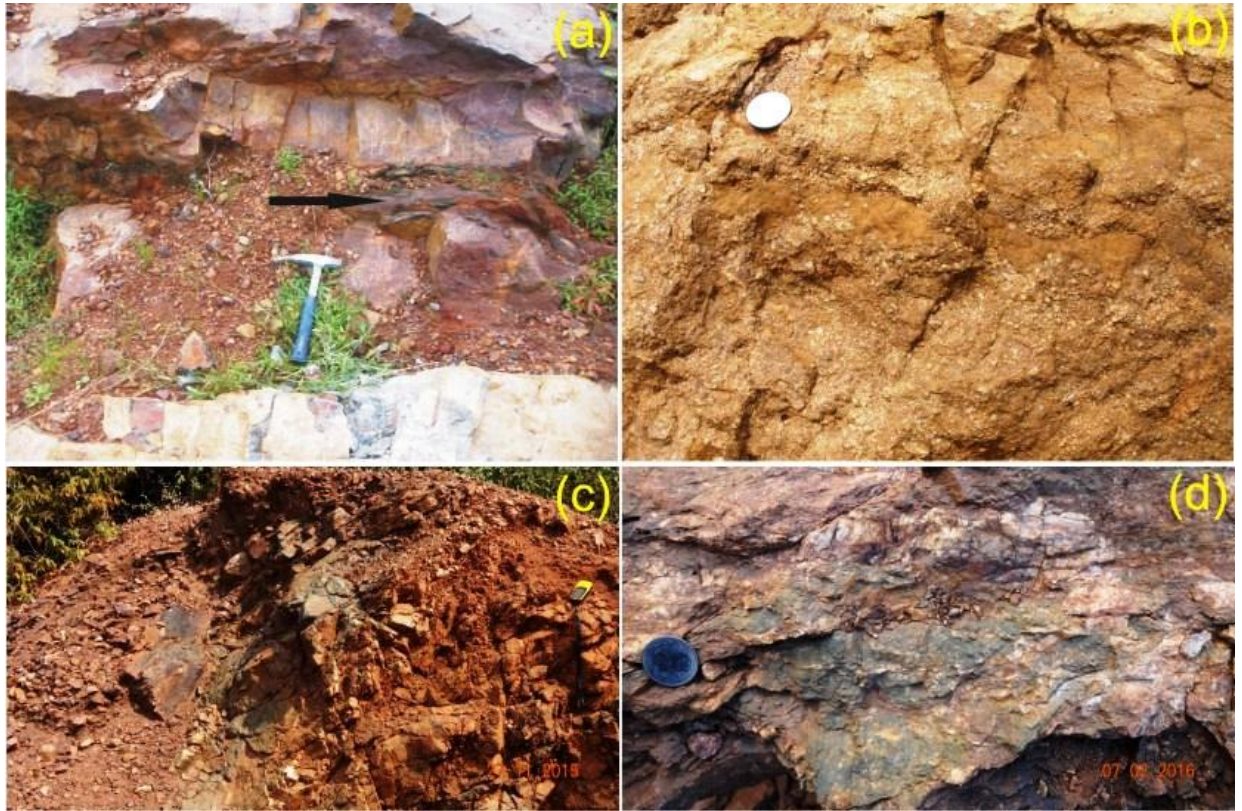


Figure 4.5: Field photographs showing (a) sandstone hosting paleosol (b) Alternating sandstone conglomerate sequence (c) Weathered chloritized zone in the sandstone and (d) Close view of chloritized sandstone.

This lithopackage is overlain by a transgressive sequence consisting of sandstone and conglomerate at the basin margin and limestone in the shelf environment. Faulting induced block tilting has modified the primary depositional attitude of the litho package (Deb, 2003; Pati, 2010). Influence of faulting is well represented by intense silicification and chloritization of the rocks along the fault zone (Fig 4.5c,d) and autoclastic conglomerate in the basin-margin limestone sequence. Hence, detailed analysis of the sandstone and the paleosol has been done to deduce the paleoweathering and paleoclimatic implications in the region. The paleosol horizon is found in Dubarpet region which was sampled for detailed analysis.

Precambrian paleosols have been discovered and documented in large numbers, in recent years by various workers from different geological environments i.e. continental depositional settings including palustrine (Tandon et al., 1995; Wright and Platt, 1995; Tandon and Gibling, 1997), deltaic sequences (Fastovsky and McSweeney, 1987; Arndorff, 1993) and in marginal marine strata (Lander et al., 1991; Wright, 1994). Driese et al. (1994) and Webb (1994) reported the presence of paleosol on the marine sediments and argued the formation of soil on the marine strata on exposure, by sea-level fall.

Presence of paleosol represents a hiatus in the stratigraphy and has regional significance in the geological history of any area. In addition to their stratigraphic applications, paleosols can be used to interpret landscapes of the past by analyzing paleosol–landscape associations at different spatial scales, ranging from local to basin-wide in scope. At the local scale, lateral changes in paleosol properties are largely the result of variations in grain size and topography. At the scale of the sedimentary basin, paleosols in different locations differ because of basinal variations in topography, grain size, climate, and subsidence rate.

Paleosols can be used to determine the oxygen content of the Precambrian atmosphere (Holland, 1984; Retallack et al., 1984) and thus provide valuable information on early atmospheric evolution, because they formed at the Earth's surface in direct contact with the atmosphere (Holland, 1994). Paleosols serve as one of the powerful tools for studying the paleogeography, paleoenvironmental and paleoclimatic conditions on the earth at the time of their formation (Sheldon and Tabor, 2009; Holland, 1994), hence help in better understanding of the ancient atmosphere and atmospheric changes over geologic time (Krauss, 1999).

Quantitative paleosol geochemistry is widely being used in reconstructing the atmospheric composition at the time of their formation, differentiating between metasomatic alteration of sedimentary rocks and pedogenesis (Retallack, 1986; Zbinden et al., 1988; Holland et al., 1989; Maynard., 1992; Sheldon, 2006b) and determining paleotemperature and paleoweathering patterns. Study of paleosol is a field science (Retallack, 1988) and hence its recognition and properties like soil-horizons and structures are best studied in the field itself (Retallack, 1992). But, in the areas of deformation and metamorphism subsequent to the formation of weathering

profile such as those found in many Precambrian terrains, field recognition and study of field properties are not so simple.

This study is the first report of occurrence of a paleosol horizon (20-25 cm thick) along the basin margin in the eastern margin of the Pranhita-Godavari basin, in Central India (see fig. 4.1). Field study of facies association and petrography of the paleosol and parent sandstone has been used to interpret the depositional environment. Detailed field study of the pedogenic features and geochemical composition of the paleosol provides valuable information on paleoenvironmental parameters.

❖ **Methodology adopted for paleosol analysis:**

An integrated methodology was adopted in the present study such as field mapping of facies association and recognition of paleosol, petrography of paleosol and host sandstone, magnetic susceptibility study of paleosol horizon, XRD analysis and major element geochemistry of the paleosol and its application. The details of the methodology adopted are shown in the flowchart (Fig. 4.6).

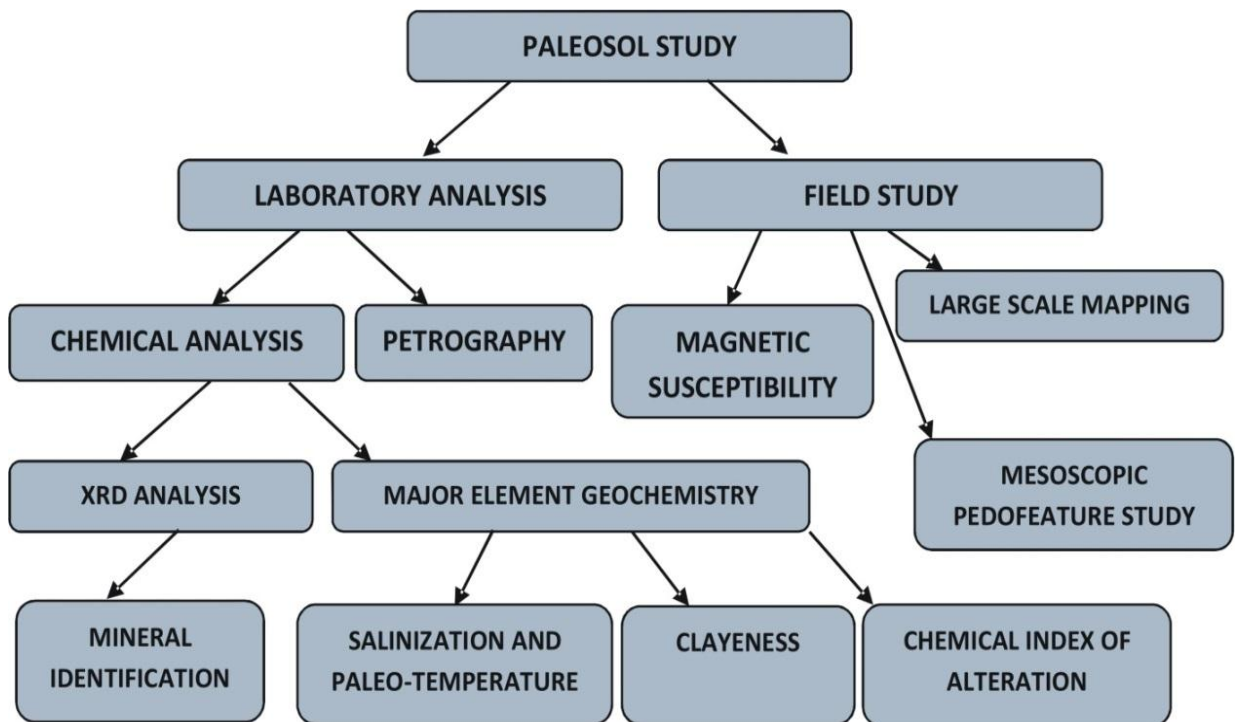


Figure 4.6: The methodology adopted for paleosol analysis is shown in the given flowchart.

4.2.3.1 Field mapping and recognition of paleosol

Large scale field mapping (1:1000 scales) was carried out (Fig. 4.7) to map the

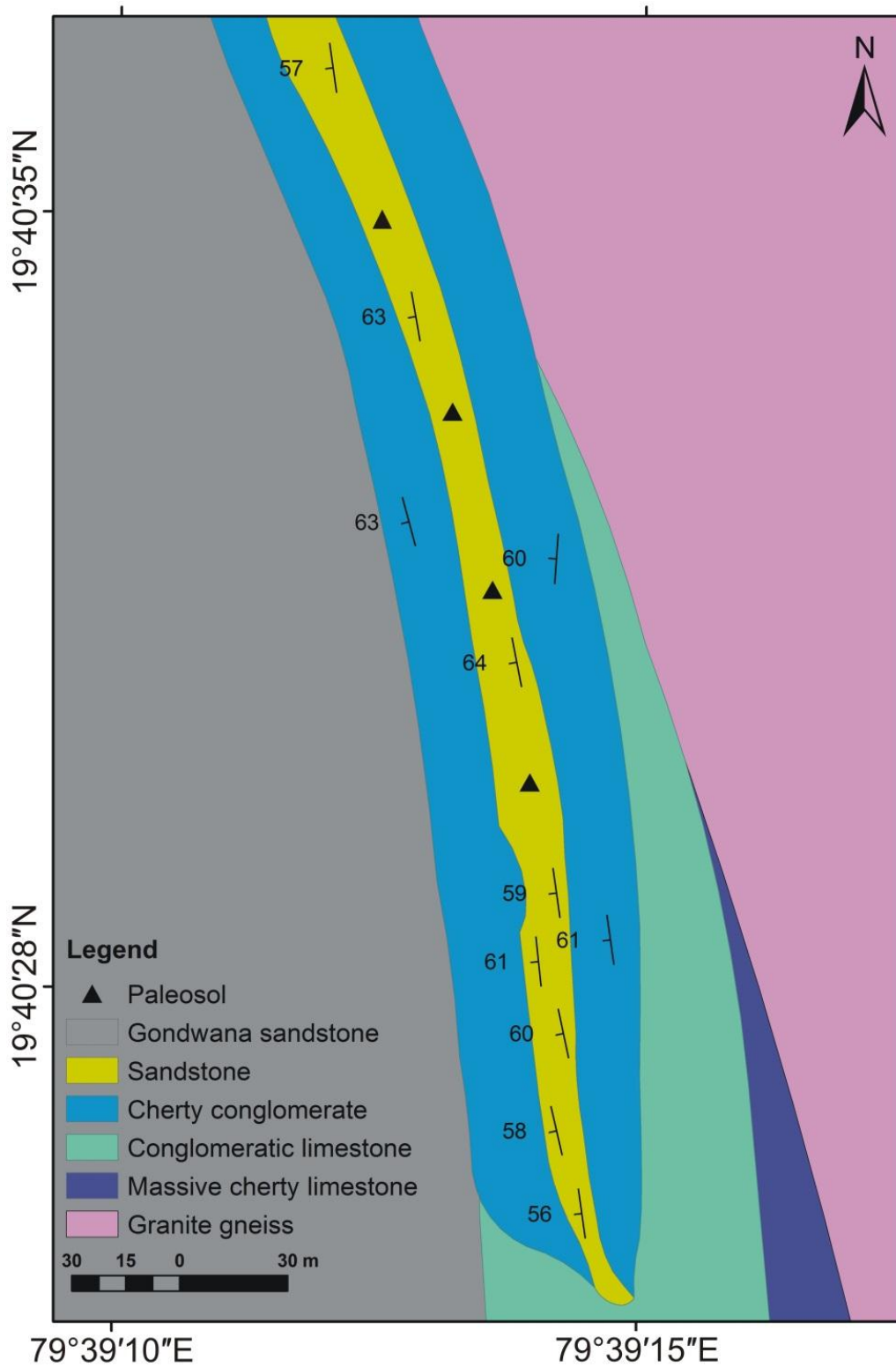


Figure 4.7: Geological map of the Dubarpet region on large scale of 1:1000

facies association and the paleosol horizon. Most parts of the litho-package along the basin margin are buried under recent sediments and soil cover, however, in sandstone queries the vertical sections are exposed (Fig. 4.3b). Facies mapping along the basin margin reveals the presence of transgressive and regressive sequences and the paleosol development defines a time break in the deposition at the marginal zone and a corresponding unconformity surface to certain extent into the basin interior (Fig. 4.8).

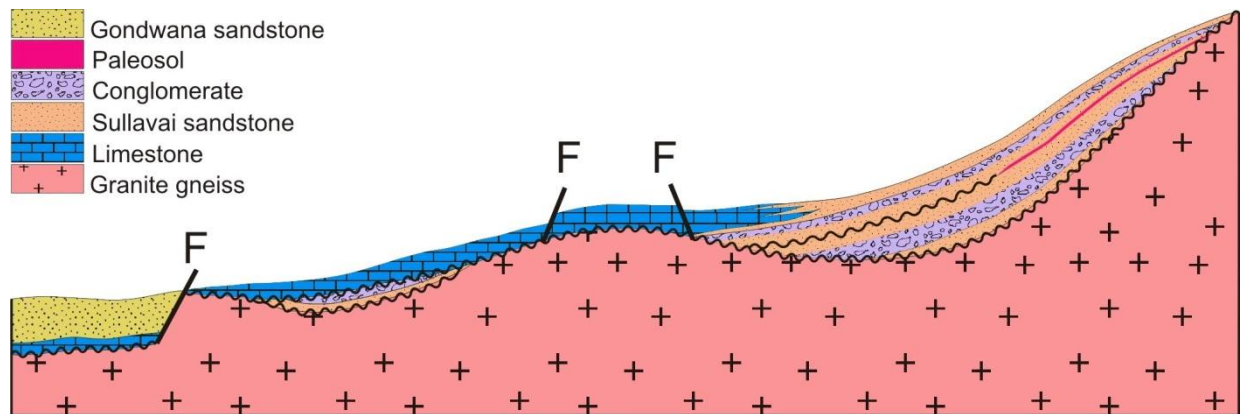


Figure 4.8: Model (schematic) showing development of paleosol and unconformity in the basin, prepared based on field evidences and literature reviews.

The paleosol horizon is developed on the top of a regressive sequence of quartz arenite (Fig. 4.5 a) and is overlain by a transgressive sequence represented by sandstone and conglomerate at the basin boundary and limestone in the shelf environment (Fig. 4.8). Cyclic sedimentation at the basin boundary is represented by the intercalation between conglomerate and sandstone (see Fig. 4.5b). Ghosh and Saha (2003) correlated this cyclicity with the extensional tectonic episodes during the basin development.

Paleosols are difficult to recognize in early Paleozoic and Precambrian alluvial sedimentary rocks because they lack the large root traces of vascular plants that characterize late Paleozoic and geologically younger paleosols (Retallack, 2001). Therefore, other macroscopic characteristics (Retallack, 1988) such as colour, soil structure have been adopted for field recognition. As thickness of the paleosol horizon

is about 15 cm, no distinct soil sub-horizons were precisely marked. However, the upper 6-8 cm of the soil horizon shows moderately developed soil structure (blocky structure) developed in the intensely weathered (grain-size sufficiently reduced) parent material as compared to the rest of the profile, which is almost friable character and crude lamination is preserved. Soil-colour was documented to be varying from 5Y 7/4, 5Y7/3 and 7.5YR 5/8 using the Munsell Soil Colour chart (Munsell, 2005).

Generally, palaeosols are described based on the presence (or absence) of well- developed horizons preserved within strata, which can be connected to soil process (Birkeland, 1999; Buol et al., 1997). In this manner, readily preserved paleosols and their horizon characteristics associated with various processes elucidates the environment of deposition. Identification of paleosol was also confirmed by the field magnetic susceptibility study of the profile and added by laboratory geochemical analysis.

Sampling of paleosol was carried out using the established methods suggested by Kraus, (1999); Krauss and Aslan, (1993) and Retallack, (1998). As the paleosol horizon was extremely friable, samples were collected carefully in tin boxes for the preparation of thin sections. Along with petrography, X-ray diffraction techniques (XRD) was used to find out the elemental geochemistry of the three powdered samples of paleosol with the help of identification of peaks and XRF was also used for the same. For such purpose, fresh paleosol samples were collected by removing the upper surface from the exposure for geochemical study.

4.2.3.2 Petrography

As the paleosol was very much friable, its samples were soaked and hardened using a mixture of toluene and canada balsam and then cutting and polishing was carried out using slab saw and grinder for thin section preparation.

Photomicrographs of the upper part (1-5 cm) of the paleosol horizon shows development of pedo features (Fig. 4.9a, b) where as in the lower part shows hardly any such features. Fractures in the soil horizon are filled with silica veins as seen in the photomicrograph (Fig. 4.9a).

In the lower part of the profile, crude laminations are preserved (Fig. 4.9c). Grain size variation from bottom to top can also be observed from the photomicrographs. The upper part shows intense weathering characteristics with

grain-size reduction and well developed pedo-features. However, in the lower part, crude lamination is well preserved. Silica and iron encrustations on the grain boundary are also seen in the lower part of the soil profile (Fig. 4.9d).

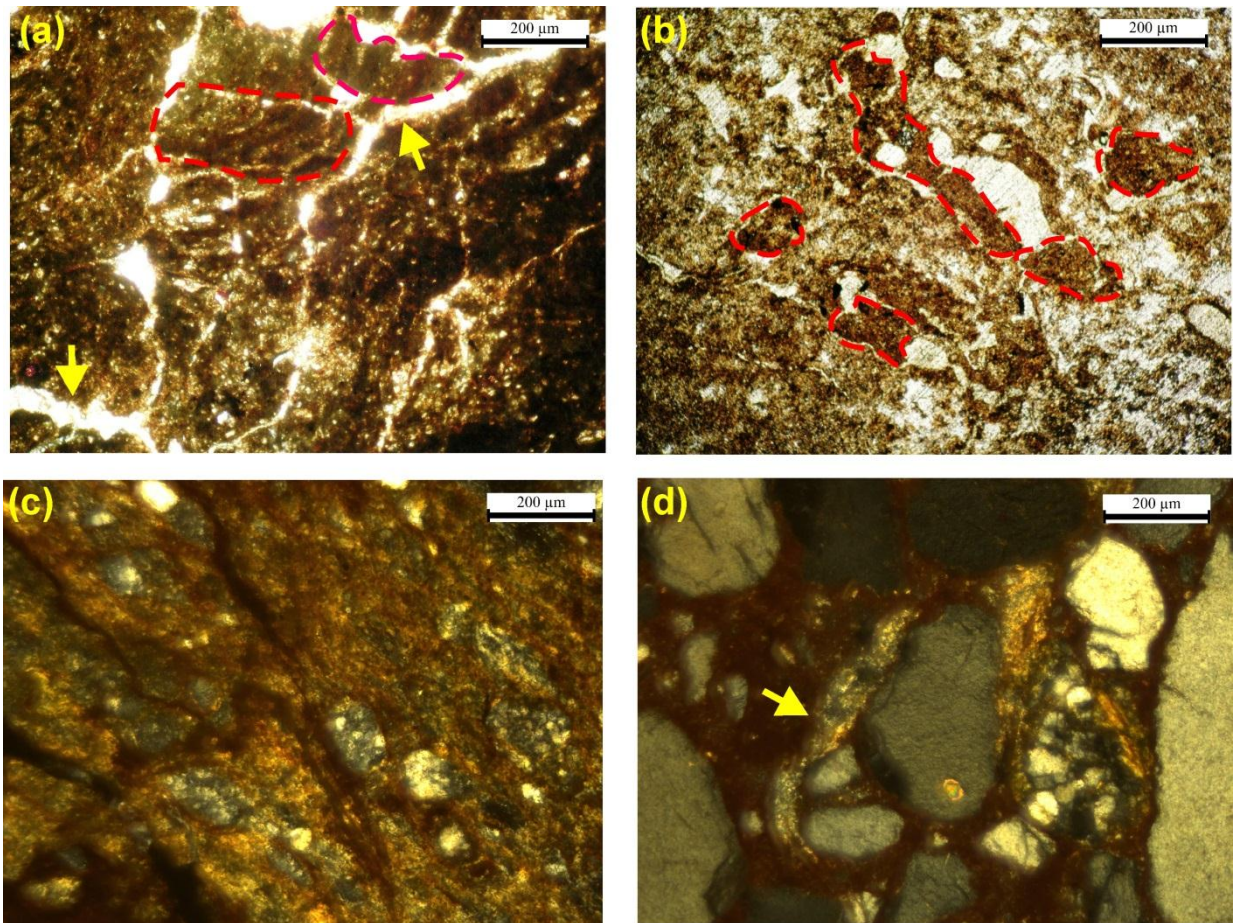


Figure 4.9: Photomicrograph of paleosol (a and b) show development of pedo features (marked as red dotted lines) and fractures are filled with silica veins in the upper part of the soil horizon, (c) shows crude lamination in the lower part of the soil horizon, (d) encrustation around the quartz grain and rock fragments as diagenetic changes.

Also, the petrography of sandstone is also done and small sized rounded grains of quartz were found in the thin sections. The absence of feldspar content in sandstone shows its high maturity. Meeting point of more than four or five grains are also found (Fig. 4.10).

This indicates the occurrence of low grade metamorphism of the rocks which may be due to the nearby igneous activities or other processes.



Figure 4.10: Photomicrographs (a&b) shows the rounded and multiple grains containing grains of quartz with their outcrop images of sandstone below in (c&d).

4.2.3.3 Magnetic Susceptibility

Surficial enhancement of magnetic susceptibility can be a useful confirmation that some Precambrian and early Paleozoic rocks were paleosols (Retallack et al., 2003; Grimley and Vepraskas, 2000). However, magnetic susceptibility enhancement of some paleosol profiles is compromised by burial gleization, which reduces overall susceptibility values, but especially susceptibility at the surface of the profile, and produces a marked covariance of magnetic susceptibility with total iron content. Groundwater and surface water gleization during soil formation also depletes susceptibility over a wide range of iron content to give relatively flat depth functions of susceptibility (Retallack, et al., 2003). Perhaps recrystallization or metamorphism can explain the low magnetic susceptibility of Precambrian and Paleozoic paleosols (Retallack, 1991).

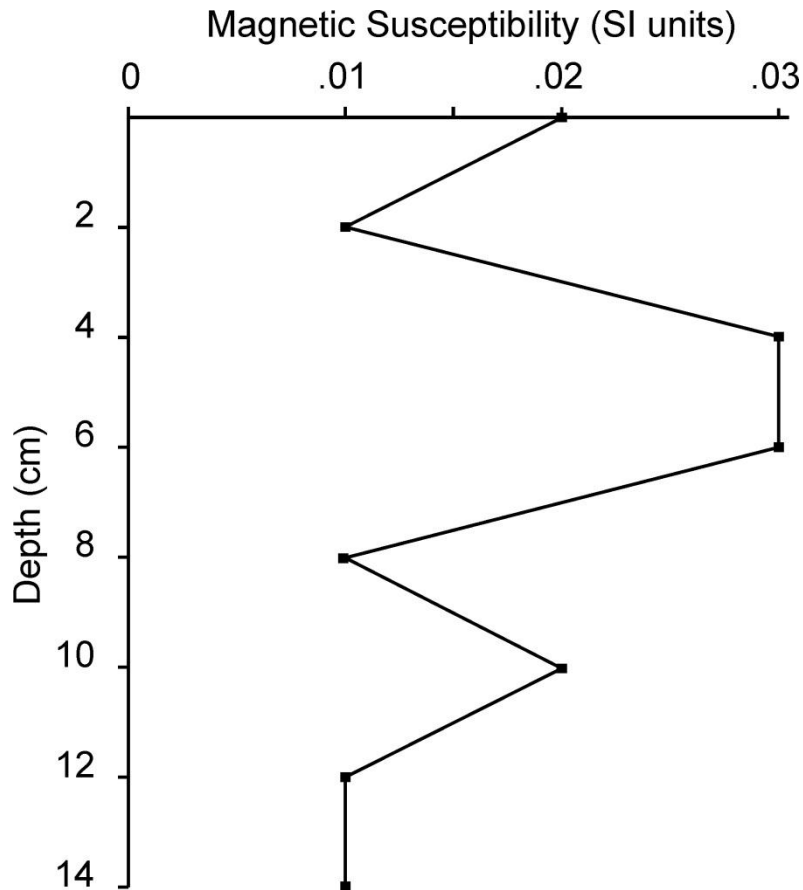


Figure 4.11: Magnetic susceptibility of the paleosol profile shows bottom-ward decrease of susceptibility.

Field study of magnetic susceptibility of the paleosol shows a decreasing trend with depth (Fig. 4.11). K-2 magnetic susceptibility meter was used in field to study the susceptibility of the profile at 2 cm interval. The highest susceptibility value has been observed in the upper-middle part of the profile. Top surface of the paleosol horizon shows less susceptibility which may suggest gleization on the surface due to poor drainage. Development of some clay in the profile and detrital quartz influx from the parent rock as well as feeble iron enrichment may illuminate the low magnetic susceptibility at the lower part horizon.

4.2.3.4 XRD analysis

X-ray diffraction (XRD) is an analytical technique primarily used for the crystal structure of a crystalline material which should be finely ground and homogenized. The paleosol samples were ground to a fine powder of ~200 mesh size. Powdered sample

was spread uniformly over glass surface when monochromatic X-ray strikes the mount and diffracted in all possible directions as suggested by Klein and Dutrow, (2008). The particles are oriented in such a way that they make a proper angle with incident beam to satisfy Bragg's Law. For each sample, one gram powder of paleosol was analyzed in single crystal X-ray diffractometer (SC-XRD) using K780 X-ray generator with Cu ($K\alpha$) as target.

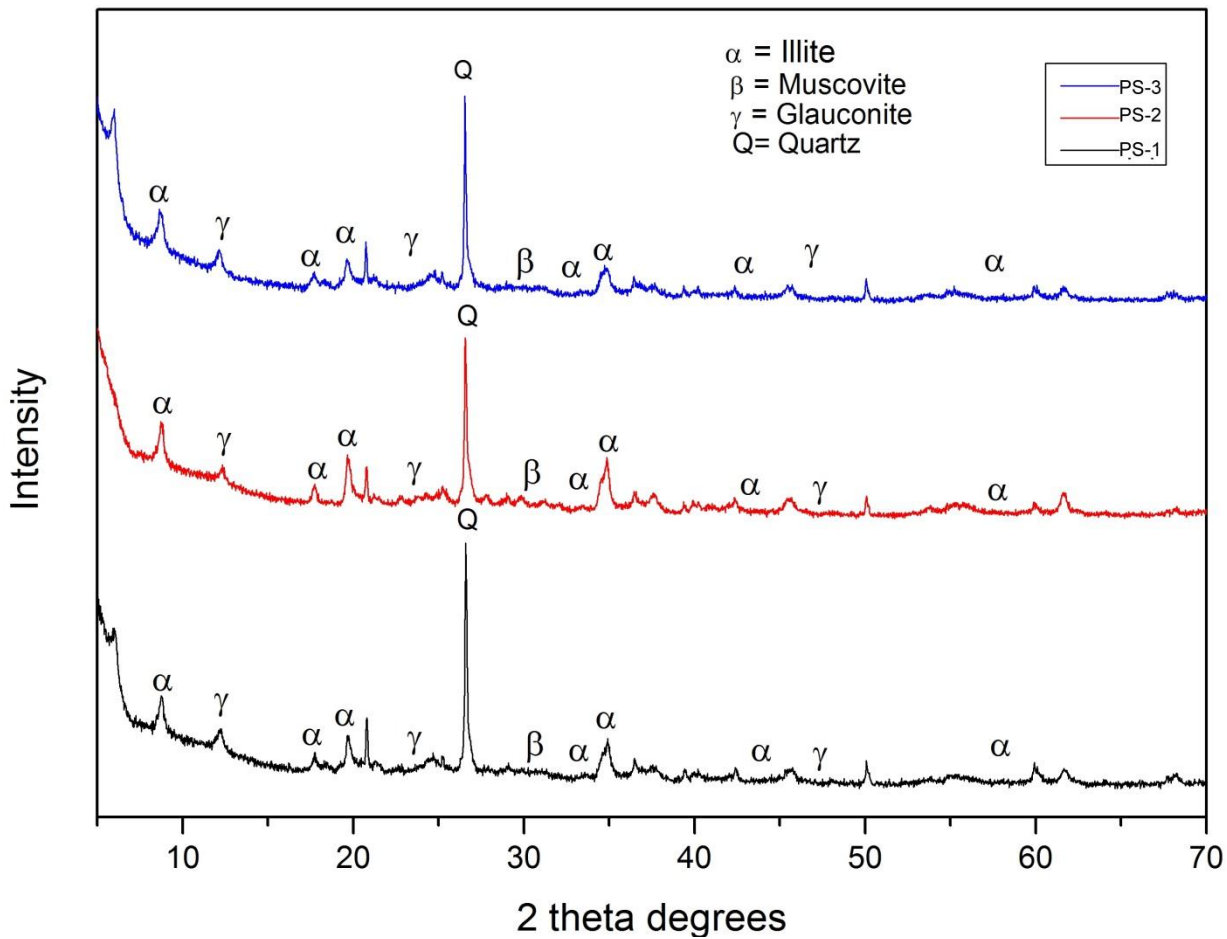


Figure 4.12: XRD analysis of paleosol samples named as PS-1, PS-2 and PS-3

XRD analysis of three paleosol samples (Fig. 4.12) was carried out using Cu ($K\alpha$) as target and 2θ angle from 2 to 70 degree. The identified mineral from XRD peaks in the samples is dominantly quartz followed by illite and glauconite, respectively. The clay minerals formed by weathering of all kind of silicates shows

different climate and environment (Galan, 2006). Glauconite is a strong tool for reconstruction of palaeo-environment (Amorosi, 1997). It has dioctahedral (2:1) structure (Weaver, 1968) and its presence reveals the climate to be marine dominantly and within shallow water environment with slow and intermittent rates of deposition (Prothero and Schwab, 2004). It is one of the abundant mineral at unconformities; e.g., at the top of marine regressive sequences on which the paleosol was developed.

It is formed in reducing environment and normal shallow marine waters with depth ranging from 50 m to 500 m (Odin and Fullagar, 1988; McRae, 1972) as generally common in a fan-delta setting which fits to the present observation. To form, glauconite must reside at sediment-water interface for 1000 to 10,000 years (Odin and Matter, 1981).

4.2.3.5 Major element geochemistry of the paleosol and its application

“Major elements” refers to the primary rock-forming elements Ca, Fe, K, Mg, and Na, along with Al, O, and Si as building block elements for silicate minerals, and minor amount of Mn, P, and Ti (Li, 2000).

Table 4.1: Proxies used for chemical analysis and their outcome (Sheldon and Tabor, 2009)

S. No.	Method	Outcome
1.	Major element weathering indices:	These index values represent extent of weathering.
	1) Chemical Index of Alteration ($Al_2O_3 / Al_2O_3 + Na_2O + K_2O + CaO$)	Breakdown of Feldspars to clay.
	2) Salinization ($Na_2O + K_2O / Al_2O_3$)	More salts accumulate during weathering.
	3) Clayeness (Al_2O_3 / SiO_2)	More clay production as rock weathers.
2.	Clay Mineralogy: Identification of clay minerals using the value of d-spacing, (XRD).	The type of clay mineral present will itself indicate type of climate.
3.	Paleotemperature $T (^{\circ}C) = -18.5S + 17.3$, where S is Salinization	High salinization value indicates low mean annual temperature (MAT)

Different proxies (Table 4.1) derived from the major element geochemistry have successfully been used for paleo-environmental reconstruction (Liivamägi et al., 2015; Feakes and Retallack, 1988; Retallack, 1997; Sheldon, 2006; Sheldon and Tabor, 2009; Nordt and Driese, 2012). By convention, major element data are presented as weight percentages of oxides and trace elements as ppm.

Table 4.2: Oxide weight percentage obtained from XRF

Oxides	PS-1	PS-2	PS-3	PS-4
Na ₂ O	0%	0.06%	0.06%	0%
MgO	3.82 %	2.73 %	3.517 %	1.29%
Al ₂ O ₃	19.7 %	24.4 %	19.92 %	10.1%
SiO ₂	39.9 %	45.1 %	40.61 %	66.45%
P ₂ O ₅	854 PPM	527 PPM	0.106 %	0.083%
SO ₃	0 PPM	0 PPM	0 PPM	0.008%
Cl	0 PPM	0 PPM	0 PPM	0PPM
K ₂ O	5.23 %	7.15 %	4.924 %	1.94%
CaO	0.456 %	0.135 %	0.451 %	0.09%
Sc ₂ O ₃	0 PPM	0 PPM	0 PPM	0 PPM
TiO ₂	0.862 %	0.894 %	0.926 %	0.37%
V ₂ O ₅	216 PPM	224 PPM	180 PPM	0 PPM
Cr ₂ O ₃	516 PPM	309 PPM	529 PPM	0.0351%
MnO	801 PPM	666 PPM	970 PPM	0.0215%
Fe ₂ O ₃	9.91 %	7.54 %	10.6 %	4.468%
CoO	0 PPM	170 PPM	170 PPM	0.0131%
NiO	286 PPM	108 PPM	256 PPM	0.0064%
CuO	0.489 %	0.430 %	0.5389%	0.146%
ZnO	128 PPM	62 PPM	124 PPM	0 PPM
Rb ₂ O	180 PPM	252 PPM	169 PPM	0.0051%
SrO	0 PPM	0 PPM	48 PPM	0 PPM
Y ₂ O ₃	0 PPM	0 PPM	0 PPM	0 PPM
ZrO ₂	365 PPM	464 PPM	371 PPM	0.0287%

From there, the convention is to convert the raw abundances into moles by dividing the weight percentage (or ppm) by the molecular mass before the equations are solved.

Bulk geochemistry of paleosol was determined through X-ray fluorescence spectroscopy (XRF) for four samples collected from different locations of the soil profile (Table 4.2).

Chemical Index of Alteration (CIA)

The chemical index of alteration (CIA; Nesbitt and Young, 1982) was calculated to evaluate the degree of chemical weathering (Table 4.3).

Table 4.3: CIA value and representing mineral (Nesbitt and Young, 1982; Fedo et al., 1995)

CIA Value	Mineral present
100	Kaolinite
75-90	Illite
75	Muscovite
50	Feldspar
30-45	Fresh basalts
45-55	Fresh granites and Granodiorites

CIA is a dimensionless number between 0 and 100 and shows the weathering of feldspar minerals and their hydration to clay minerals. It is calculated using molecular proportions:

$$\text{CIA} = [\text{Al}_2\text{O}_3 / (\text{Al}_2\text{O}_3 + \text{CaO} + \text{Na}_2\text{O} + \text{K}_2\text{O})] \times 100$$

The resultant value is a measure of the proportion of Al_2O_3 versus the labile oxide in the analyzed sample (Table 4.4).

Table 4.4: Chemical Index of Alteration ($\text{Al}_2\text{O}_3 / (\text{Al}_2\text{O}_3 + \text{Na}_2\text{O} + \text{K}_2\text{O} + \text{CaO})$) for samples:

Sample	CIA
PS-1	77.60
PS-2	76.86
PS-3	78.56
PS-4	83.20

The CIA values are not considered to be changed during metamorphism (Nesbitt and Young, 1982). The general understanding of this index lies in the assumption that as clay content increases in the upper part of the paleosol profiles, Al should also increase and Ca, Na, K should decrease and this would lead to higher CIA values. Although CIA is widely used, it does not account for the post-burial addition of

K by metasomatism (Driese et al., 2007) or possible illitization of pedogenic clay minerals (e.g. smectite).

Clayeness

Clayeness is the measure of clay content in the soil/paleosol (Sheldon and Tabor, 2009; Ruxton, 1968). Cations such as Na⁺, K⁺, Ca²⁺, and Si⁴⁺ are lost during chemical weathering. Al/Si is thought to be a measure of “clayeness” because Al accumulates in clay minerals relative to a silicate mineral parent. The ratio was first proposed (though inverted from the present form) by Ruxton (1968) and has been widely applied (Sheldon and Tabor, 2009; Retallack, 2000; Prochnow et al., 2006; Sheldon, 2006; Hamer et al., 2007).

$$\text{Clayeness} = \text{Al}_2\text{O}_3/\text{SiO}_2$$

The clayeness values deduced from the above equation are given in (Table-4.5). The molar ratio of Al to Si is a function of the clayeyness of a paleosol (Retallack, 1997).

Table 4.5: Clayeness values (Al₂O₃/SiO₂)

Sample	Clayeness
PS-1	0.49
PS-2	0.54
PS-3	0.49
PS-4	0.15

Salinization and Paleo-temperature

Salinization is the process by which mobile cations such as K and Na (alkali elements) accumulate as soluble salts in soil or paleosol where older examples are much more rare because salts are often removed by diagenesis, leaving evaporite mineral pseudomorphs rather than the original minerals (Sheldon and Tabor, 2009). A relation between paleo-temperature and salinization was established by Sheldon et al. (2002) as:

$$T (\text{°C}) = -18.5S + 17.3, \text{ where } S \text{ is salinization and standard error } RE = \pm 4.4\text{°C}, R^2 = 0.37, \text{ the temperature range for the formula is } 2\text{°}-20\text{°C} \text{ (Sheldon et al., 2002).}$$

Salinization,

$$S = (\text{Na}_2\text{O} + \text{K}_2\text{O})/\text{Al}_2\text{O}_3$$

It helps in finding the paleotemperature estimates which is a good proxy for finding the paleoclimatic conditions. Values for salinization and paleotemperature are given in (Table 4.6).

Table 4.6: Paleotemperature calculated from salinization values.

Sample	Salinization	Paleotemperature(°C)
PS-1	0.27	12.39
PS-2	0.30	11.83
PS-3	0.25	12.67
PS-4	0.19	13.75

Interpretations

Outcomes obtained from various methods converge towards the development of the paleosol profile in the mid-northern latitude in a cold environment at the boundary of an isolated fault-bounded basin. The presence of glauconite and illite revealed through petrographic studies and XRD analysis suggests the presence of shallow marine environment at the basin boundary in isolation. Petrography of paleosol indicates moderately-developed pedo-features in the upper part of the horizon and the lower part preserves the crude lamination (primary depositional feature). Limited vertical and horizontal exposure may be attributed due to weathering.

Feeble presence of sedimentary structure (lamination) and less degree of development of pedo-features which is seen in the photomicrographs as well as magnetic susceptibility behaviour of paleosol do suggest relatively less time of exposure for pedogenesis. This time gap represents the interval between the regression and transgression of the sea in the rift basin. The CIA and presence of clay mineral like illite also attest to the colder climate of about 12°C. Abundance of cations indicates it as a poorly drained basin probably in a shallow shelf marine environment cut-off from the main water body.

❖ **Around Gojoli (middle part of the basin margin)**

The middle part along the basin-margin is represented by carbonate facies with



Figure 4.13: Photograph showing iron ore bed resting over the dolomitic limestone.

massive cherty limestone, limestone conglomerate and stromatolite along with a thin bed of iron ore resting over the limestone (Fig 4.13). The conglomeratic limestone represents different flows of autoclastic massflow sequence. This is the dominant lithology of the region.

The autoclastic mass flow conglomerates reported in the present study have been grouped under three flows and seven distinctive conglomerate facies based on their nature of contact, geometry, texture and clast imbrications as described below.

As some of the facies in the latter two flows are identical, facies-based description has been emphasized (across the flows) here rather than flow-based description. Apart from those, two other carbonate facies i.e. massive cherty limestone and stromatolitic limestone have also been discussed.

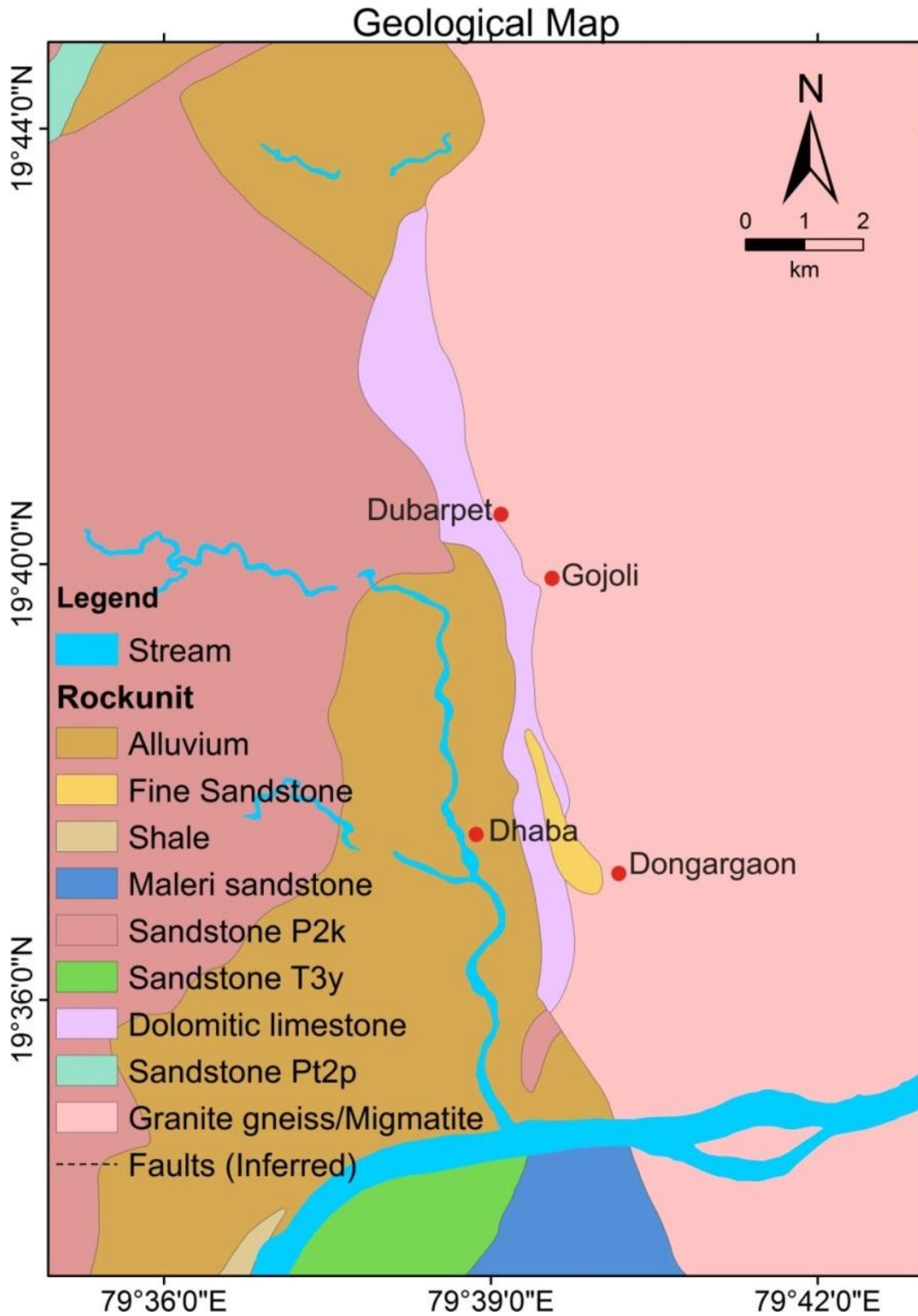


Figure 4.14: Study area showing various locations near Gojoli and the nearby region of mass flow.

4.2.4 Limestone Facies

The limestone sequence is exposed around Dhaba, Dubarpeth and Gojoli (Fig. 4.14), unconformably rests over the Archaean gneissic basement and the basin-boundary fan-delta sequences in the east, and is terminated by the Gondwana sandstone in the west. This is represented by about a 400m thick limestone sequence of micritic nature near to the basin margin dipping about 40° westerly followed by stromatolitic limestone with intervention of a series of autoclastic limestone conglomerate (flow-2) towards the basin interior. Autoclastic mass flow in the shallow marine carbonate sequence presumably triggered by the basin-margin faulting as it is striking along the basin-boundary fault (Fig 4.15). A series of mass flow is evident from the enclosure of clasts within the clasts of later generations.

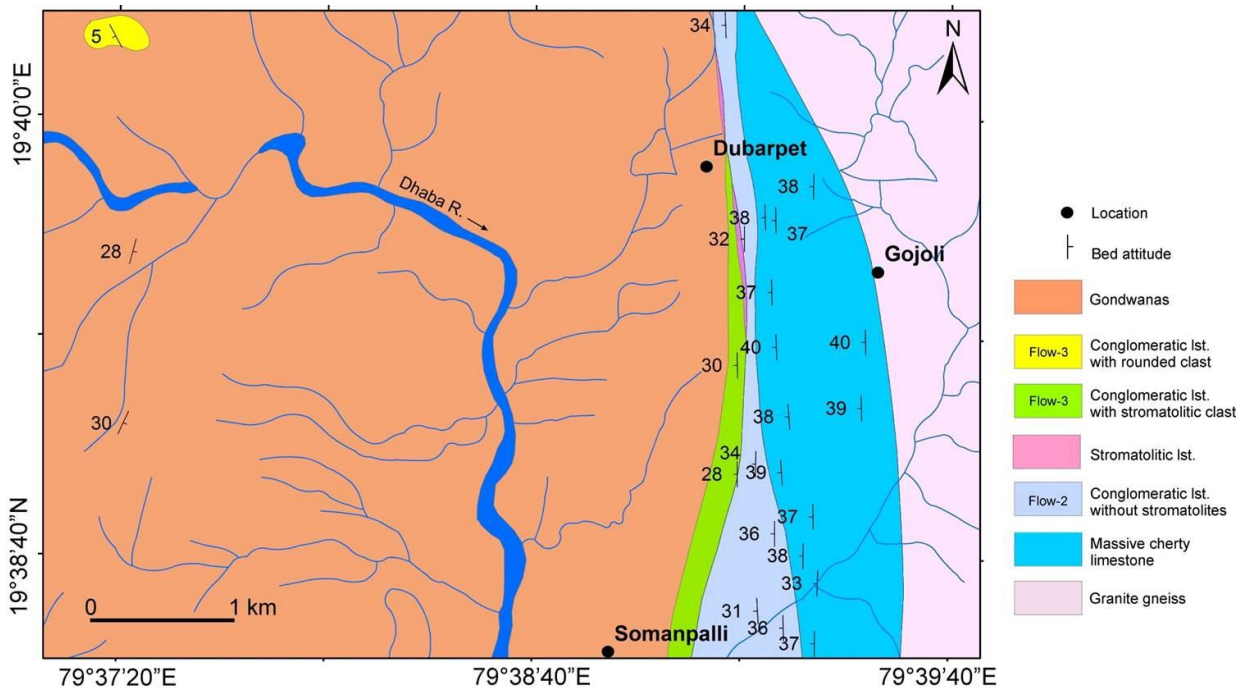


Figure 4.15: Large scale geological map of the region at 1:1000 where the autoclastic mass flow took place near village Gojoli and Dhaba.

4.2.5 Autoclastic massflow conglomerates

Autoclastic massflow conglomerate along the western margin of the PG basin was defined by Bose and Sarkar (1991) based on the lithological similarity among the

matrix and enclosing clasts and their internal structure. Autoclastic character of the conglomerate lithofacies in the western margin is logical due to the monotony of limestone sequence along the basin margin. Such basinal para-autochthonous

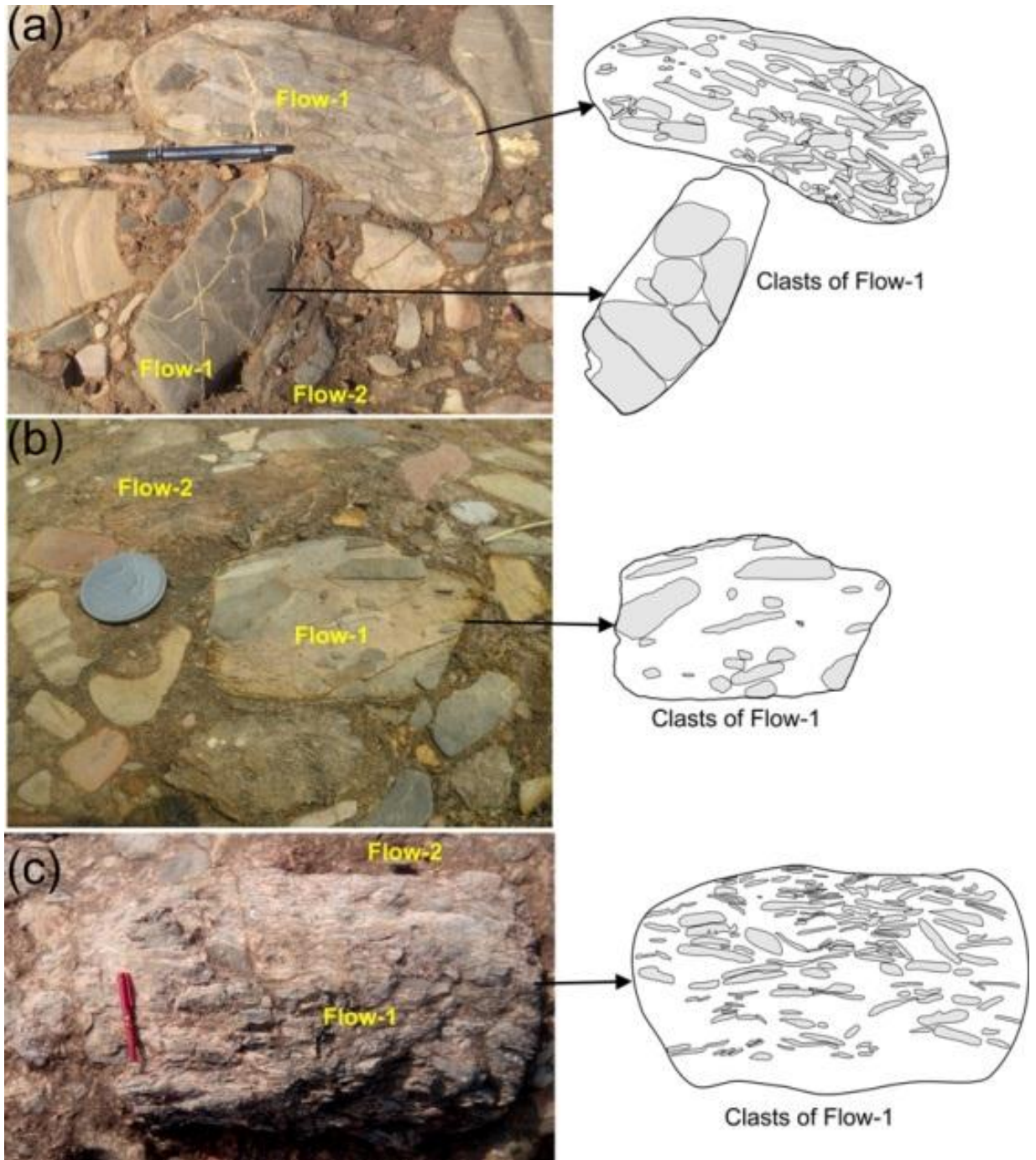


Figure 4.16: Distribution of limestone facies (facies-C) representing the flow-1 as clasts within the flow-2 along the basin boundary (a, b & c) shows the clast in clast of flow-1 within flow-2 with tabular and elongated clasts in (a) and (c).

carbonate deposits are explained by Ekdale and Broomley (1988) from Late Cretaceous European chalk. In the present study (part of the eastern margin of the PG basin), limestone conglomerate similar to the western margin has been found resting on a massive cherty limestone horizon fringing the basin margin. Two autoclastic conglomerate horizons representing two successive mass flows are consisting of pebble to boulder (up to 30 cm) size clasts and constitute major part of the carbonate sequence.

Autoclastic mass flow origin of these conglomerate facies are evident from: (1) same composition of clast and matrix; (2) Partial or feeble normal and reverse grading in many beds mostly chaotic; (3) non-uniform graded nature of the conglomerate bed packages; (4) non-uniform structural and textural variation tendency; (5) partially developed imbrication in certain facies at random locations; (6) improvement of roundness supplemented by reduction of clast-size in the successive beds in some packages; (7) coexistence of angular cemented clasts with deformed, unconsolidated, disparately bed parallel clasts specially stromatolites, perceptibly plucked or broken from the surface at the basal part of some subsequences; (8) enclosure of clast within the clast (Fig 4.16) reasonably explaining later phase flows after a freeze of mass movement within the basin margin in space and time.

Strike continuity of these conglomerate horizons coincides with the eastern basin-margin fault (Dora et al., 2011; 2015, Fig 4.17), which suggests the origin of the autoclastic conglomerate is due to the activity of this fault at different intervals during the rifting process. The conglomerate horizons are separated by a horizon of stromatolitic limestone indicating an intermittent tectonically stable period and shallowing of the basin.

Based on the facies assemblage, three mass flows have been identified in the study area. However, *in situ* facies corresponding to the earliest flow is nowhere found but these are presented as boulders in the second flow (see Fig 4.16c). Due to concealed nature and lack of exposure of vertical section, study of all facies variations corresponding to the second flow is not possible. Conglomerates corresponding to the third (youngest) flow are well distributed in the area and the facies variations in the flow have been studied in fair detail.

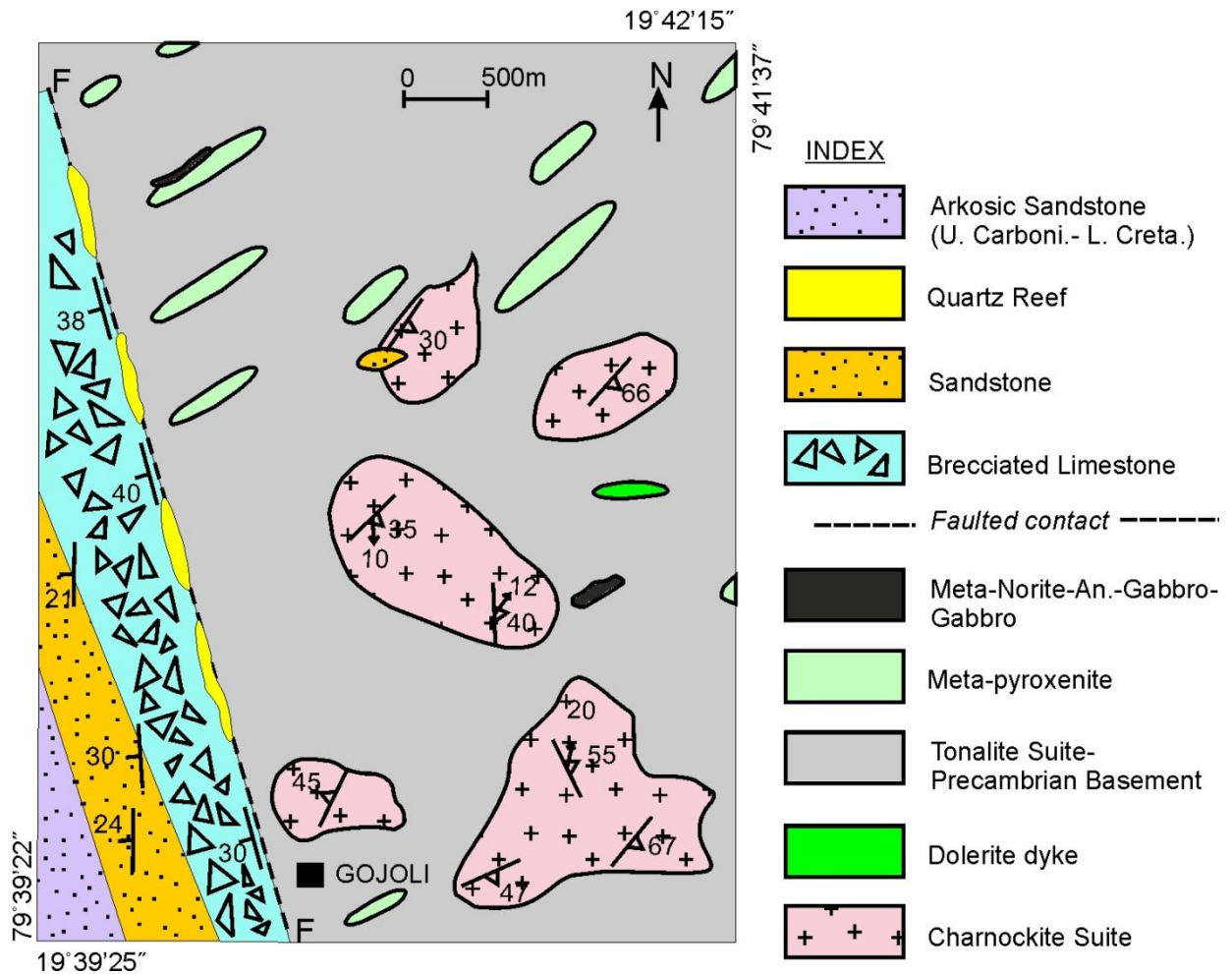


Figure 4.17: Map showing the fault originated activity in the region causing formation of autoclastic conglomerate (Dora et al., 2011; 2015).

Lateral transitions from one facies to another i.e. homogeneous, poorly imbricated and imbricated (Postma, 1984) has been observed in the conglomerates corresponding to the youngest flow. Most of the flow behaves plastically depending upon the flow thickness and steeper slope shows thinner mass flow deposits as described by Hiscott and Middleton (1979).

This is because of the faulted margin; steeper slope existed at the basin boundary which promoted mass flow and gradually thickens into the basin as described by Postma (1984). The clast-size shows inverse correlation i.e. close to the basin boundary, larger the clast size and vice versa.

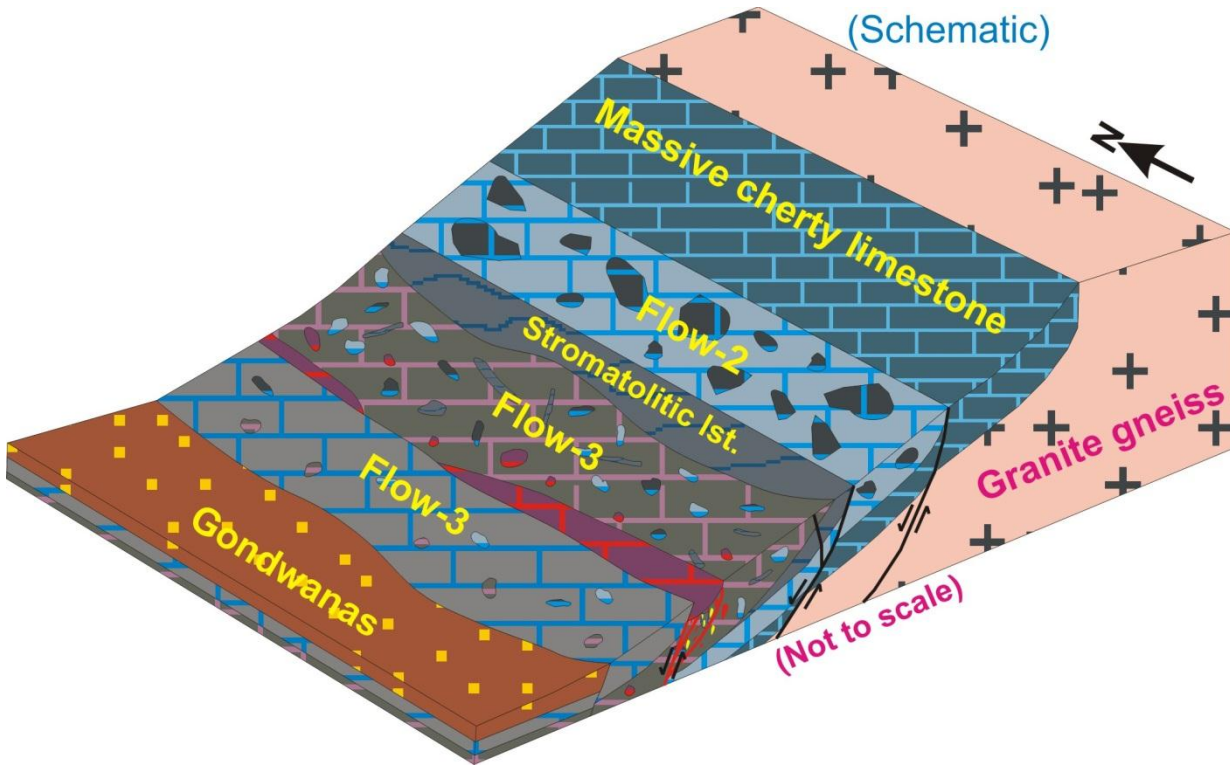


Figure 4.18: A schematic model showing various facies assemblages of the autoclastic mass flow over the slope with various faults.

Sudden release of energy due to faulting activities provided momentum to mass flow. However, quick freezing of flows due to a sharp hydraulic jump at the base of slopes, perhaps well account for the over-thickening of presumed traction deposits (Eyles et al., 1987; Bose and Sarkar, 1991). Higher slope (38° - 42°) at proximity of the basin boundary delivered most of the clast which collectively acted as plug or mass of various sized clast and got deposited on lower slope (28° - 32°) on the basin plain at a very short distance. A model showing massflow of the massive cherty limestone towards the interior of the basin and showing the types of flow has been prepared (Fig 4.18).

4.2.6 Massive cherty limestone (dolomitic)

Along the basin margin due to the warm and alkaline nature of the sea in the basin the deposition of massive cherty limestone took place initially which turned out to be of massive type. Due to the high initial dipping angle and falling out of broken rock

clasts and bigger chunks of rock it all was got collected over the bank in the form of plugs and linear bodies along the basin margin.

Most of the limestone represents massive cherty nature suggesting silica input through volcanism (hydrothermal) during precipitation. In the initial carbonate depositional region, it underwent localized penecontemporaneous dolomitization (Bose and Sarkar, 1991; Sarkar et al., 1993). Also, the replacement of calcium by magnesium due to the chemical reactions and changing sea chemistry in the interstitial spaces of the limestone caused it to turn into dolomitic limestone. Number of calcite veins in the limestone in addition to few silica veins indicates that the later tectonic activities in the margin were enough to create mineral authigenesis and pressure solution along with the mass flow events.

All those tectonic activities and sea chemistry in addition to the climate and absence of any vegetation caused the present dolomitic limestone to be massive and compact. It has somewhat dark grey colouration intermittent due to the high carbon content (Bose and Sarkar, 1991). The linear long belt of limestone clearly demarcates the margin which is observable.

4.2.6.1 Mass flow associated facies and flow

Facies-A: Massive cherty limestone

This limestone representing a transgressive facies (Ghosh and Saha, 2003) rests over the Archaean basement (granitic gneiss and granulite) and the basin-margin fan-delta package, juxtaposed to the east (see Fig 4.17). It shows peculiar change in colour from pink to grey and dark grey (Fig 4.19a, b).

This unit shows no indication of soft- sediment deformation continentward which testifying to its stability during the mass flow. However, it shows fragmented characteristics basinward (close to the basin-boundary fault). Intense venation and K-alteration by hydrothermal activities at places has been reported in this facies (Fig 4.19c, d) by Dora and Randive (2015).

This westerly dipping (36°- 40°) limestone facies (see Fig 4.18) provides the base and ingredient for the mass flow towards the west.

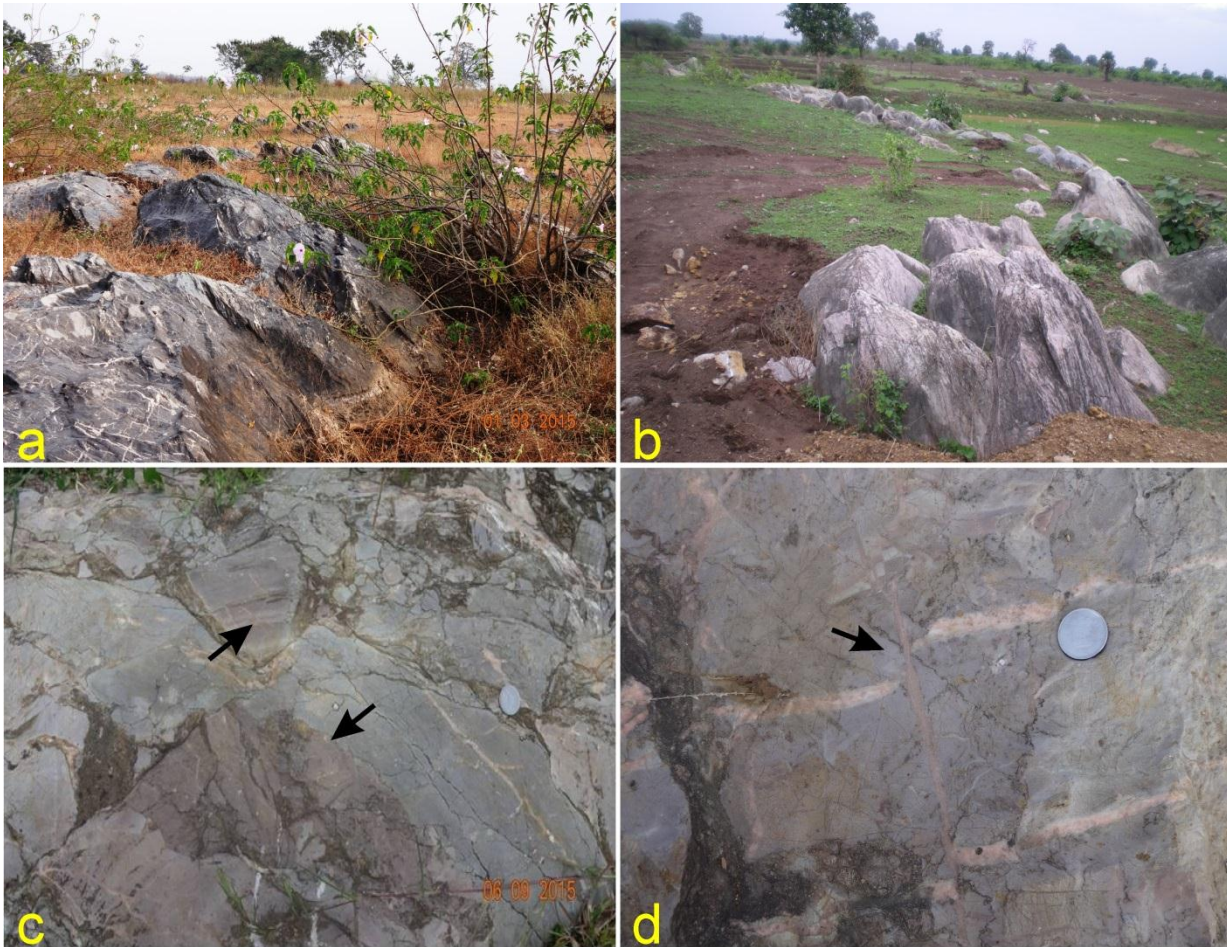


Figure 4.19: Diagram showing massive cherty limestone where (a&b) change in colour can be observed from pink to grey and dark grey (c&d) K-alteration due to hydrothermal activities in limestone facies due to volcanic activities juxtaposed.

Facies-B: Stromatolitic limestone

Stromatolites are found widely in late Archaean and Paleoproterozoic carbonates (Martindale et al., 2015) and several important contributions have been made for their paleogeographic and paleoecological reconstructions (Logan et al., 1964; Walter et al., 1980; Beukes and Lowe, 1989; Planavsky et al., 2009; Van Loon et al., 2013). Stromatolites show diversification of life through 3 billion years and are widespread in shallow marine seas in the form laminated carbonate build-ups (Walter et al., 1980; Reid et al., 2000). Due to the organic film of blue green algae (Rezak, 1957) diverse forms of stromatolites are produced on interaction with detrital sediment and physical environments by binding fine particulate sediment (Logan et al., 1964).

They show periods of rapid accretion and forming a thin crust of microcrystalline carbonate (Reid et al., 2000) in low energy settings (Sarkar and Bose, 1992).

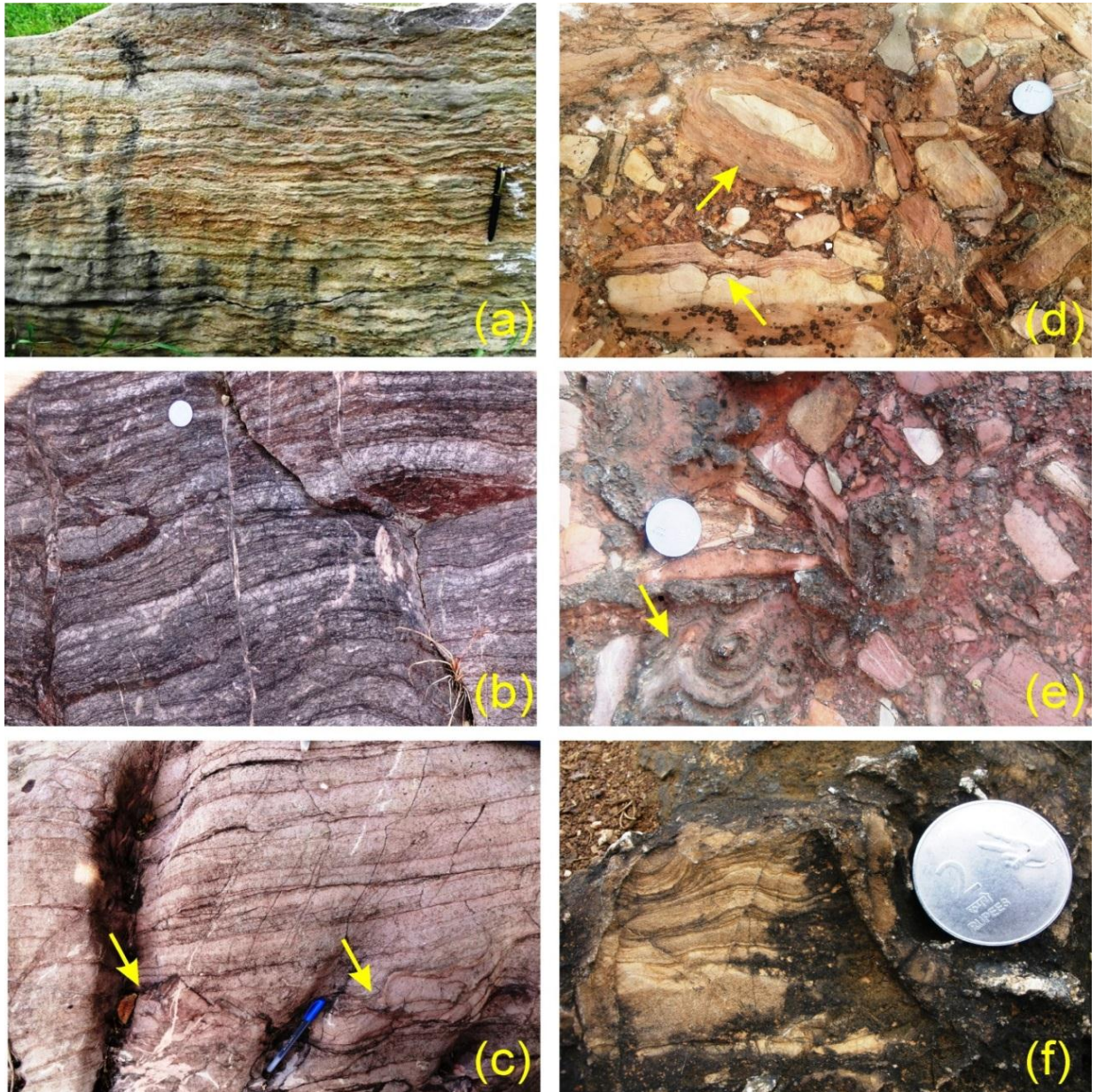


Figure 4.20: Stromatolitic limestone (Facies-B) exposed in the study area. (a) Stratiform stromatolites (b) Stratiform stromatolites showing calcilutite and dolosiltite (c) micro-faults (arrow) in the stromatolitic bands developed due to lack of cohesion and increasing intergranular friction (d, e, f) biohermal stromatolites are found as clasts within the mass flow.

In the present study, stromatolitic limestone horizons have been recorded resting over the mass flow sequence (flow-2) along the basin boundary (see Fig 4.18)

Stromatolites of this facies are present with two broad geometry viz. stratiform and biohermal (Fig 4.20); the former is, by far, the more common type and found *in situ*. However, the later type found as clasts within the second flow (see Fig 4.20 d, e, and f). The stromatolitic sequence in this area is patchy lensoidal striking almost NW-SE and occasionally shows thick bedding of algal mats.

Towards the shelf, bands variation in stromatolites was noted in the form of even laminated dark and light colored bands (see Fig 4.20b) of calcilutite and dolosiltite as explained by Sarkar and Bose (1992) in the western margin of the basin. Since, steepness of the depositional substrate increases fluidity of the stromatolitic facies increases too. Therefore, micro-faults in the stromatolitic bands (see Fig 4.20c) are visible developed due to increasing slope with lack of cohesion and increasing intergranular friction in the massive plug. Stromatolites are the signs of a quiescent period within the mass flow events. After a considerable gap recorded by the development of stromatolite, another phase of rifting is witnessed by the reactivation of the basin margin fault. This triggered another mass flow event, which is characterized by brecciation of the earlier deposits, found as clasts in the later flow.

Autoclastic mass flow-1

The earliest flow along the basin-margin is characterized by the tabular and rounded clast- supported conglomerates (see Fig 4.16a, c). *In-situ* facies representing this flow is not present in the area. However, boulders representing this flow are floating as clasts in the later flows. It is believed that, due to repeated faulting, other components of this flow have probably been reworked and mixed or buried under the successive flow facies. In the basin, continuous mass movement and subsequent deposition of carbonate sequences advanced with intermittent activations of the fossil rift (Chaudhuri et al., 2002)

Facies-C: Tabular and rounded clast-supported conglomerate ungraded

Tabular and rod-like clasts with high degree of roundness representing this facies (see Fig 4.16a, c), suggests their sliding and prior rolling before cementation. Rolling and spinning of the clasts must have dampened the dispersive pressure

(Bagnold, 1954), and the flow had earlier been turbulent (Middleton, 1967). This facies can thus be identified as a traction carpet (Dzulynski and Sanders, 1962) deposited at the base of the slope.

Autoclastic mass flow-2

Autoclastic conglomeratic limestone representing this flow is juxtaposed to the west of the basin-boundary fault (see Fig 4.17) represented by a curved base with the massive cherty limestone (Facies-A). Second event of mass flow occurred due to the reactivation of the basin-margin fault, fractured the cherty limestone and the earlier flow deposits into various size clasts, which are distributed along the margin as diverse facies within the flow as discussed below. As this flow in most part is concealed and due to lack of exposure of vertical section, detail study of facies variation along this flow is not possible. However, some of the facies exposed has been discussed here.

Flow-3 is lithologically similar to flow-2. However, it differs from the former on the basis of possession of stromatolite clasts. Thus it indicates the third phase of mass flow occurred after the proliferation of stromatolite along the basin boundary. Facies observed in flow-2 and 3 have been described below.

Facies-D: Matrix supported ungraded conglomerate

This facies is essentially a structure-less, matrix-supported conglomerate deposit comprising large limestone clasts (10-20 cm) dispersed relatively uniformly through carbonate matrix (see Fig. 4.21a, b). Beds of this facies can be very thick (in places > 7 m) but they are usually laterally impersistent. Boulders of several centimeters in diameter are common and in general this facies contains larger clasts than any other facies. These beds are interpreted as a product of turbulent debris flow in which the clasts were held suspended by matrix strength and dispersive forces.

Lack of grading accompanied by disordered arrangement of clasts implies lack of ability of grains to move with respect to each other within a high concentration debris flow. The overall fining- and thinning-up trend in short sequences indicate deposition from surge-type (Helmholtz wave, Middleton, 1967) overall waning flows. Sub-vertical broad based columns of small angular clasts cutting across the mass of assorted clasts (see Fig. 4.21d) possibly record of fluidization events. Similar facies is also found in the mass flow-3 (see Fig. 4.21c, d).

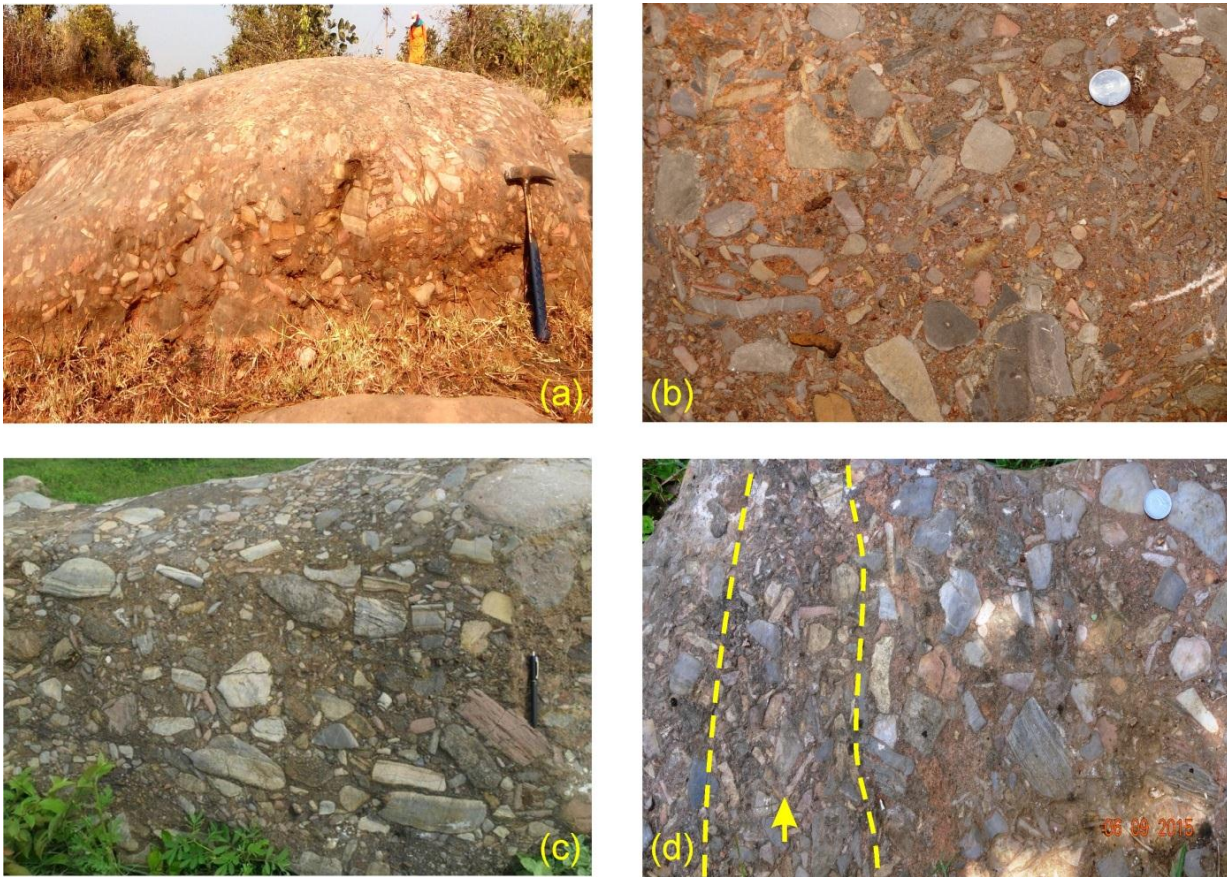


Figure 4.21: Structureless, matrix-supported conglomerate deposit (Facies-D) comprising large limestone clasts (10-20 cm) dispersed relatively uniformly through carbonate matrix (a, b for flow-2 & c, d for flow-3). (d) Sub-vertical broad based columns of small angular clasts cutting across the mass of assorted clasts possibly record of fluidization events

Facies-E: Clast-supported imbricated conglomerate

Well-developed long axis-parallel imbrication of the clasts (Fig. 4.22a, b) strongly suggests their settling from dispersion (Walker, 1975, 1978). Imbrication usually requires scouring at the up-current end of already settled clasts and foundering of the clasts within the scours gradually enlarged (Sengupta, 1966). This explanation is untenable here because deposition from grain flows commences from the top where the dispersive pressure recedes below the yield strength of the clasts. Imbrication may also arise for internal shear and traction.

Alternatively, this could have resulted from simultaneous operation of oppositely acting forces, viz., a frictional resistance at the bottom acting in an up-current direction, and a down-current acting shear exerted by the overriding faster moving turbidity

current. The resultant imbrication is, as usual, likely to be in an up-current direction. The flow was, interpretatively, westerly and that agrees well with the overall mass flow direction deduced from facies assemblages. This facies is common in two flows (flow-2 & 3)



Figure 4.22: (a) Clast-supported imbricated conglomerate (Facies-E) of flow-2 and (b) flow-3, respectively, is succeeded by bed-parallel and normally graded conglomerate (Facies-F). (c), (d) Massflow representing flow-2 and flow-3 respectively, shows reverse grading conglomerate (Facies-G).

Facies-F: Clast-supported conglomerate, normally graded

This facies occurs above the facies-E (imbricated conglomerate). Normal grading (Fig. 4.22a, b) in the conglomerate identifies turbulence as the principal mechanism for transport of sediment (Walker, 1975) in a non-cohesive flow and low mud content favored concentration of the clasts. It is most likely that fluidization and also possibly release of a considerable amount of water underneath by consolidation

(Bourrouilh, 1987) facilitated the flow to considerable distance. Down-current reduction of clast-size is well noticed in this facies (Fig. 4.22a, b). This facies is common in flow-2 and 3. However, flow-3 shows more abundance of clasts than flow -2 as shown in Fig. 4.22.

Facies-G: Clast-supported conglomerate, reverse graded

Facies deposited by grain flow show pronounced reverse grading in part of the flow (Fig. 4.22c, d). Dominant bed-parallel alignment of the clasts suggests a laminar nature of the flow (Fisher, 1971). Deposition, understandably, occurred when the strength of the basal dispersing exceeded the shear stress from the overriding turbidity current (Hein, 1982). This may indicate consolidation of the flow started from the bottom when the upper part of the flow was active. This facies representing the flow-2 contains more matrix percentage as compared to the flow-3 (see Fig. 4.22c, d).

Facies-H: Conglomeratic limestone with rounded clasts

This facies developed further basinward and shows contrasting clast size, sorting and structures among the flow-2 and flow-3. Clasts in this facies with high degree of roundness, in contrast to the tabular, angular and considerably larger clasts of other facies, suggest their prior rolling.

Rolling and spinning of the clasts must have dampened the dispersive pressure (Bagnold, 1954), and the flow had earlier been turbulent (Middleton, 1967). This facies shows rotational sliding (Buchbinder et al., 1988) at places. Due to more distance travelled by the clasts in form of rotational and sliding motion from their origin, it became more rounded and smaller in size. Rotational motion of the slide is well preserved in flow-2 (Fig. 4.23a, b).

Flow-3 shows more reduction of clast-size (Fig. 4.23c, d and e). As the mass flow advanced further basinward, the slide planes tend to be gentler in slope and cohesive flow nature of the plug initiated to form. The clast collected at the scree deposits kept on moving further westward and at places they are slowly get cemented due to intervention of freeze cycles causing rupturing and deforming of these bodies at places.

The random orientation of the clasts, suggests that freezing of the debris flow took place almost as soon as it had set in, owing presumably to abrupt loss in gradient

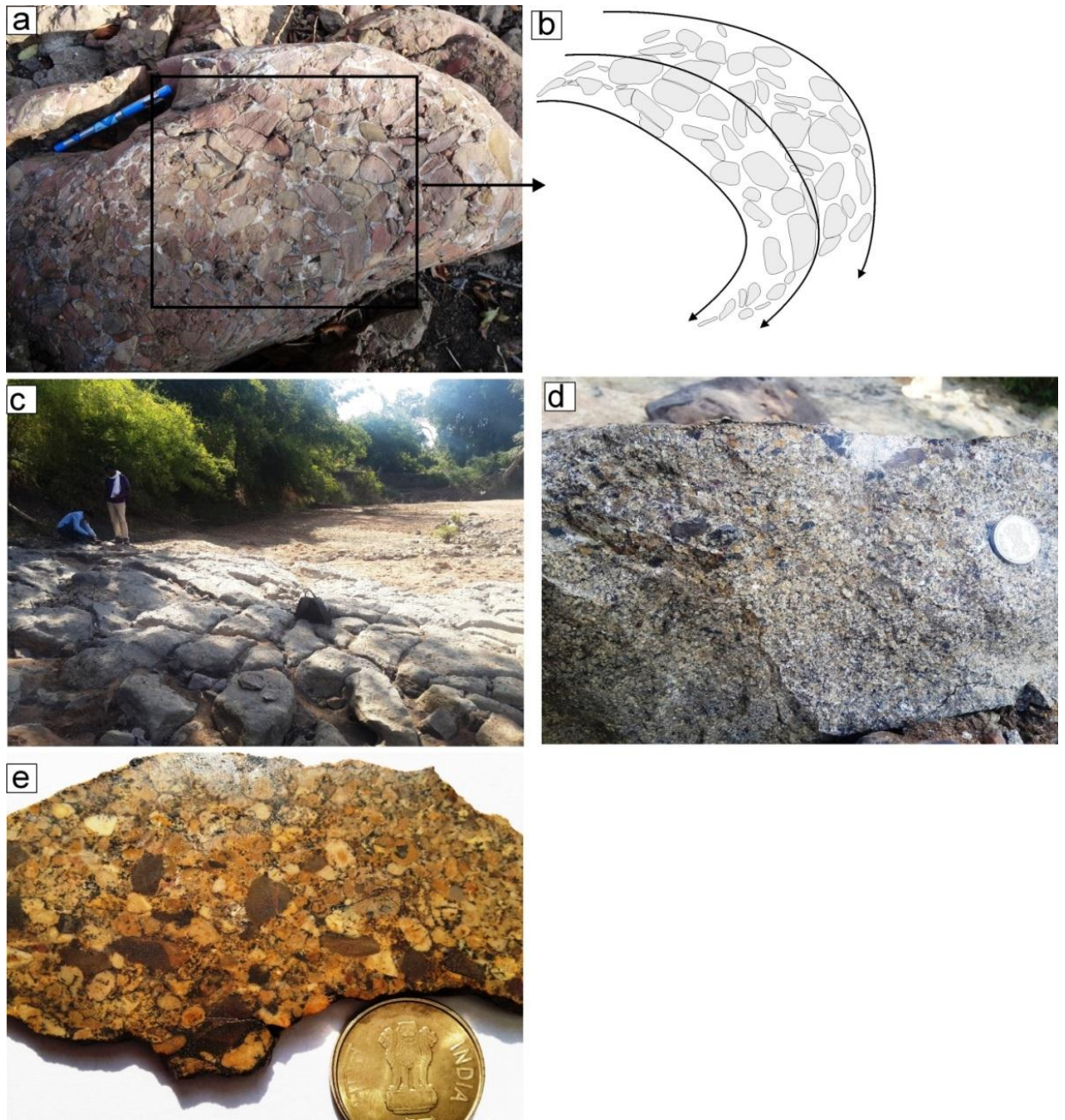


Figure 4.23: Rounded clast conglomerate of facies H. (a), (b) representing flow-2 and shows sense of rotation of the whole mass. (c), (d), (e) representing flow-3.

of the substrate. This facies is identified as a traction carpet (Dzulynski and Sanders, 1962) on the basin floor. Similar facies occurs along the western margin of the basin (facies D of Bose and Sarkar, 1991).

High degree of roundness and increased reduction of clast-size in flow-3 (Fig. 4.23) suggests its more distance of migration as compared to the flow-2.

Facies-I: Fine mud facies



Figure 4.24: Fine-grained limestone representing the turbidite resting over the mass flow deposit

Massive limestone caps the flow top (Fig. 4.24) indicates the end of the mass flow. Grading is not recognizable in the field except only when sand-sized clasts exist. The grading is, however, apparent under the microscope in the distribution of dispersed silt and clay sized grains. This has been interpreted deposited due to settling of the turbidite after the mass flow at the basin floor. This facies is noticed only in flow-3. Absence of this facies in flow-2 may suggest its complete burial or destruction by the flow-3 sediments.

A comparative model for the various facies on both the margins of the Pranhita-Godavari valley has been prepared (Fig 4.25). There are very less common features found along both the margins.

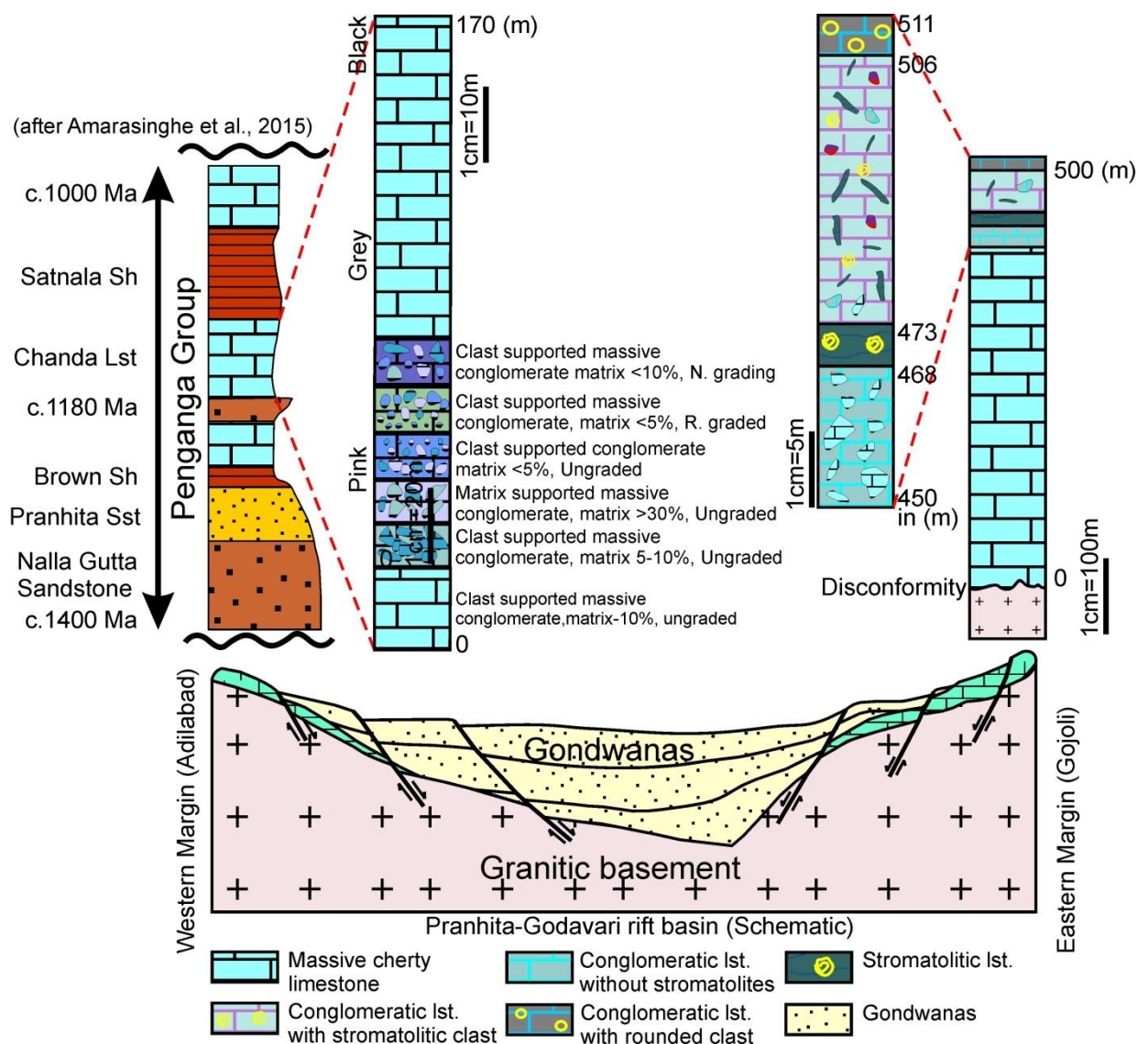


Figure 4.25: Comparison of facies assemblages among the western and eastern margin of the basin. The western margin stratigraphic sequence have been developed by compiling Bose and Sarkar, 1991; Amarasinghe et al., 2015).

Iron ore facies

There is a formation of lensoidal body of iron ore in between the limestone formation (Fig. 4.26) along the eastern margin periphery. Presence of massive iron ore in shallow water environment in such form indicates iron enrichment from the hydrothermal source. Since the Pranhita-Godavari valley is a rift basin (Sarma and

Rao, 2005) and juxtaposed to felsic volcanism at its periphery, which may be the main reason for ingress of hydrothermal fluids through the basin-margin faults.

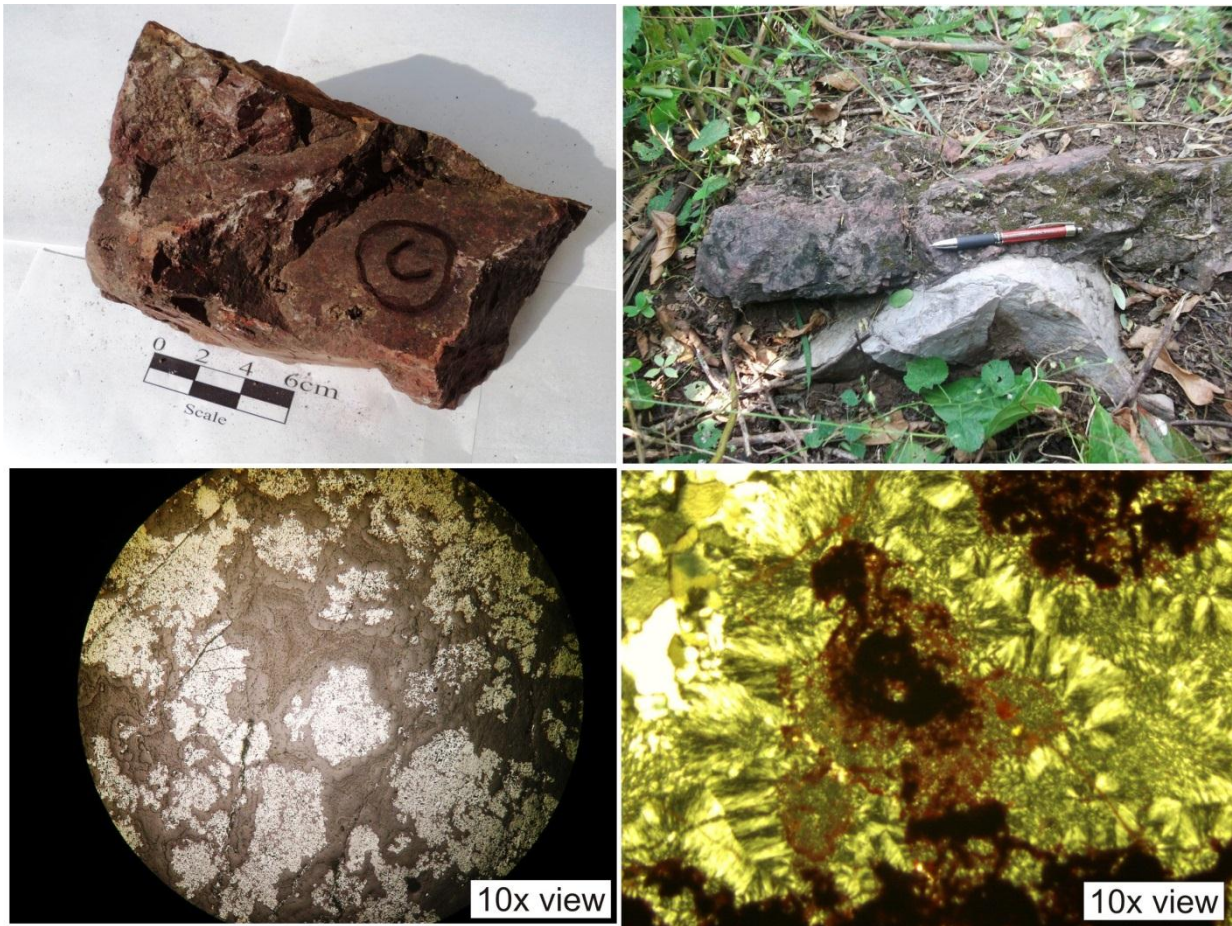


Figure 4.26: (a) Iron ore sample with dark reddish tint (b) Iron ore resting over dolomitic limestone (c&d) Presence of colloform texture as well as presence of haemetite with high reflectance in the 10X view of reflecting microscope.

Similar kinds of iron ores were previously described by Srinivas, (1987) from Ramagundam area.

Also, post depositional microscale fracturing and displacement present in the outcrop shows multistage deformation history and dark grey colouration indicates magnetite and other iron minerals. Lower two images in the figure (Fig. 4.26 c, d) show the reflectance and the presence of haemetite, while the both upper photos of iron ore shows the outcrop and the sample (Fig. 4.26 a, b).

❖ Dongargaon fan delta system

Modern depositional environments linked with drainage systems within the rift basins enlighten the relationship between sediment supply, drainage catchments and fan-delta geometries (Eliet and Gawthorpe, 1995; Muravchik et al., 2014).

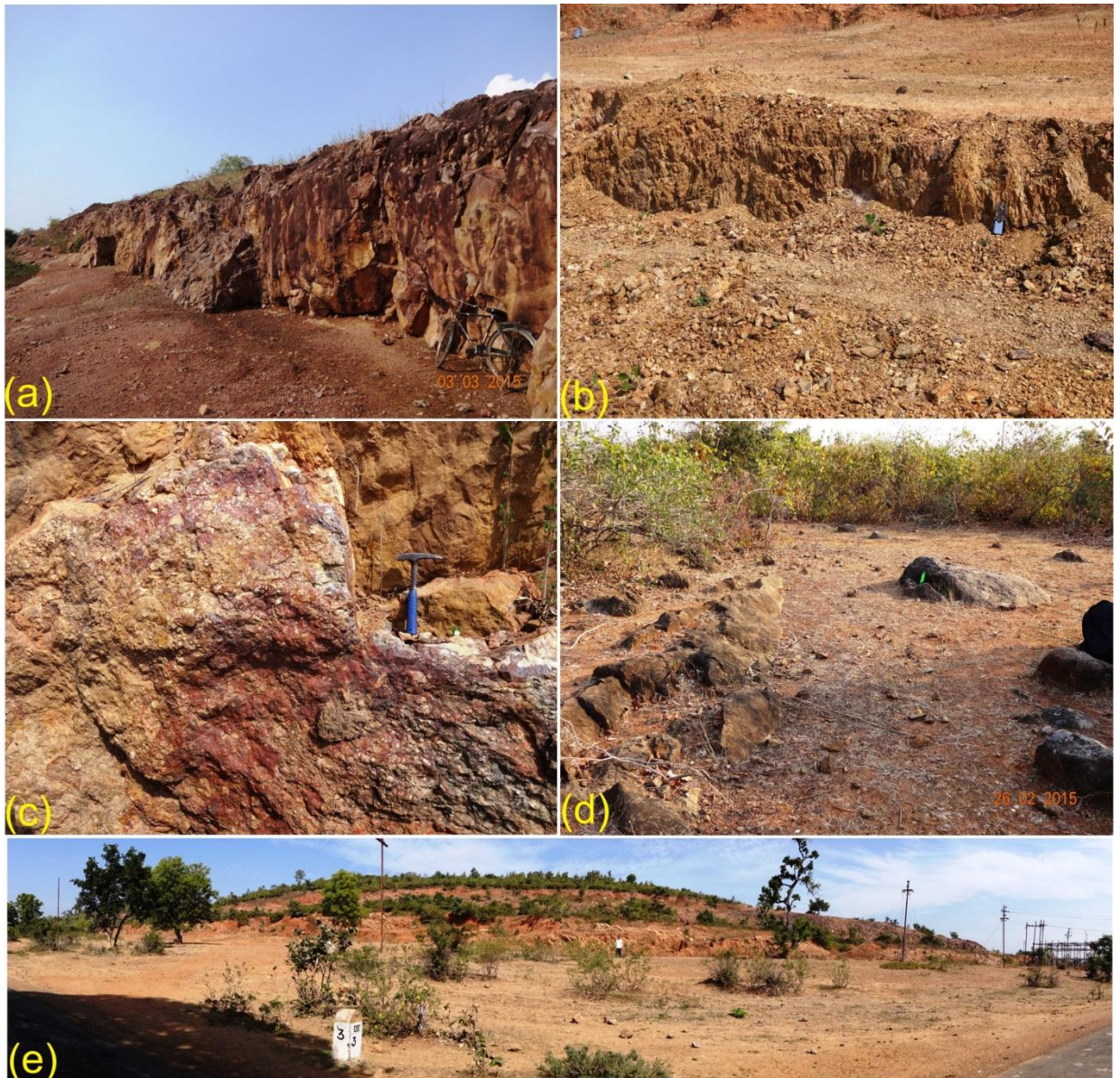


Figure 4.27: Various rocktypes of Dongargaon fan-delta (a&b) shows massive fine grained sandstone and shale facies (c&d) clast supported conglomerate and the limestone sequence in the prodeltaic part of the region (e) Panoramic view of the exposed southern part of the fan delta.

The Penganga Group comprises mainly fine grained sandstone, sandstone-conglomerate intercalatory sequence of shale and limestone sequence. The rocktypes of the Dongargaon are shown in the figure (Fig. 4.27) wherein, (a) and (b) shows the massive fine grained sandstone facies and shale facies. Also, (c) and (d) of figure 4.27 show the clast supported conglomerate and limestone sequence in the prodeltaic part of the fan delta.

Complete frontal view of the Dongargaon fan delta can be visualized in the figure 4.27(e).

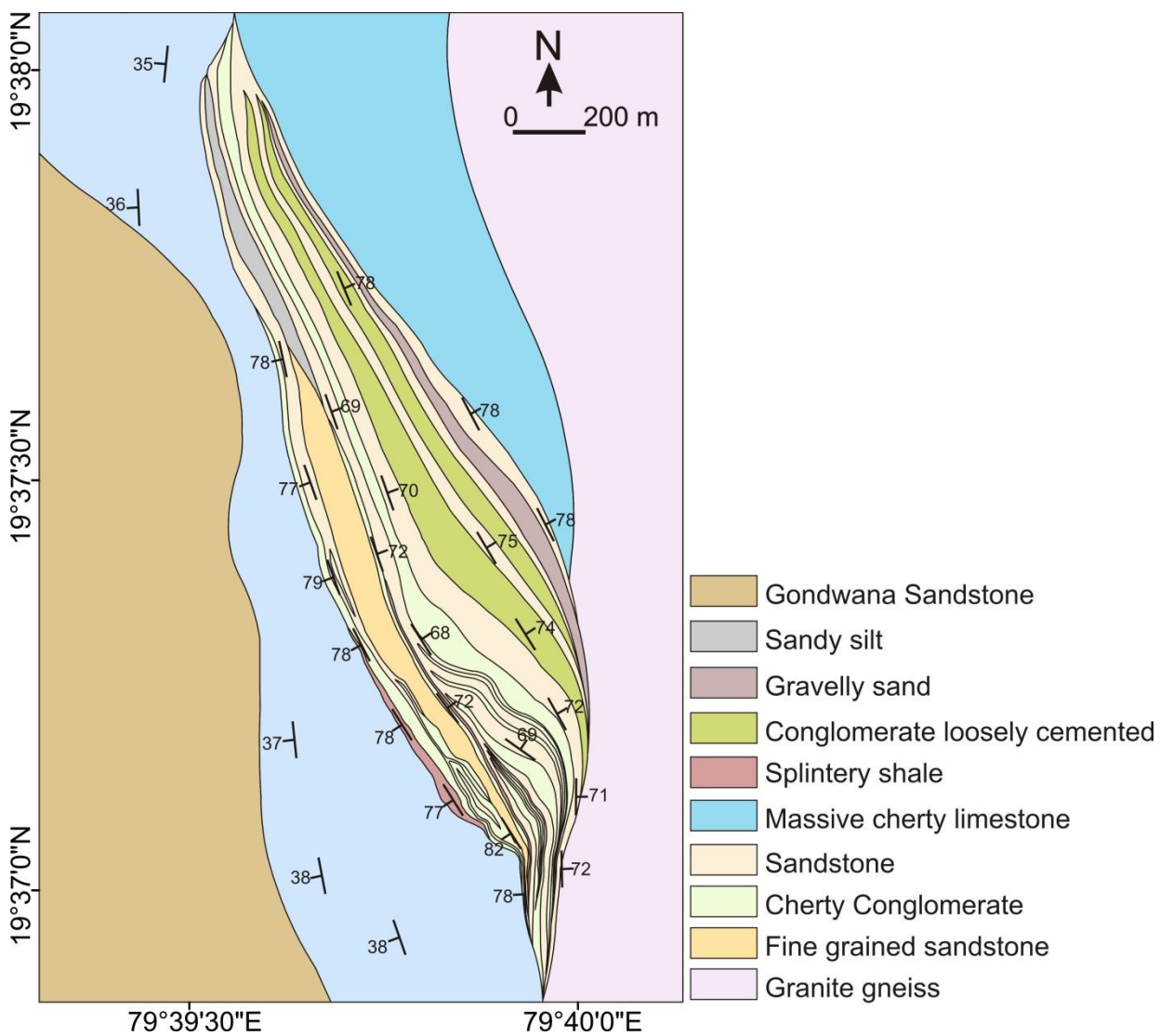


Figure 4.28: Large scale geological map of the Dongargaon fan delta at 1:1000 showing lithological distribution.

The structural controls and depositional environments with the association of drainage and allogenic and autogenic parameters define the system settings in any fan-delta system. Similar parameters are observed in the lower part of the study area in the basin margin and its proximity near Dongargaon. Therefore, an attempt has been made to describe the Dongargaon fan-delta system (Fig. 4.28) in the present study which is required to assemble the whole tectonic and palaeo-geomorphological scenario in the region to establish its evolutionary history and stratigraphy.

4.2.7 Facies and fan setting

Some of the basins are small and others are large in terms of few kilometers to a few tens of square kilometers and usually have within them several different local depositional environments. Physical, chemical, biological and other factors influence these environments, and the conditions that they produce largely determine the nature of the sediments that accumulate. Several local environments may also exist side by side within single basin as conditions change laterally (Flugel, 2012). Therefore, various facies developed within the fan delta from the proximal to the distal part are described below.

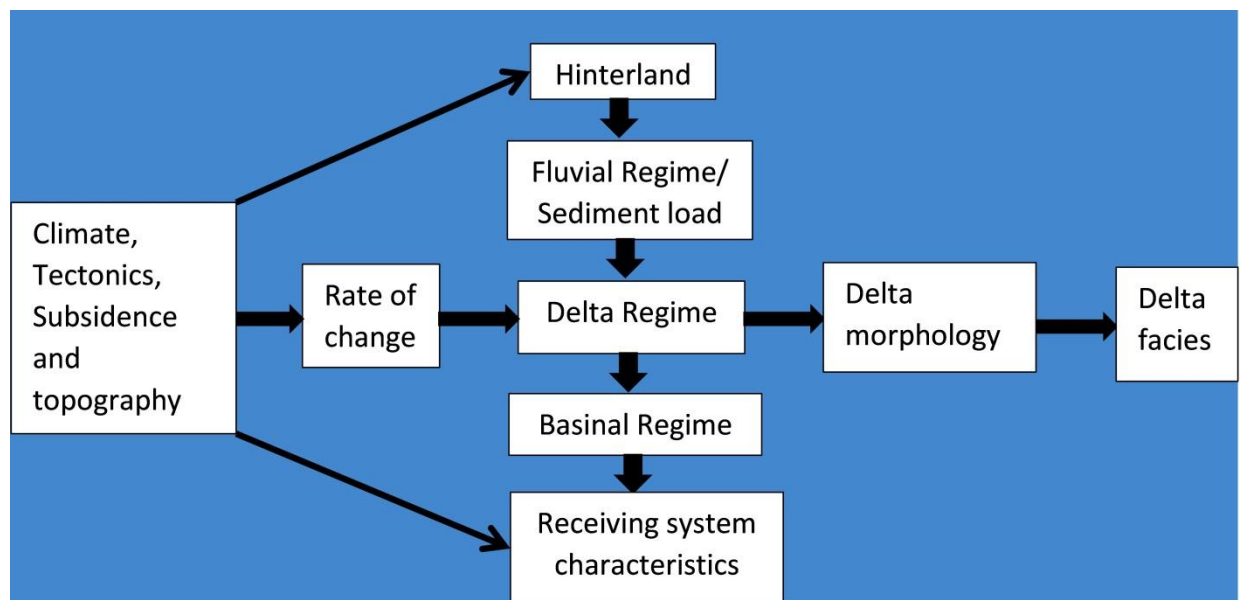


Figure 4.29: Some important parameters given by Postma (1995) to explain the formation of fan delta.

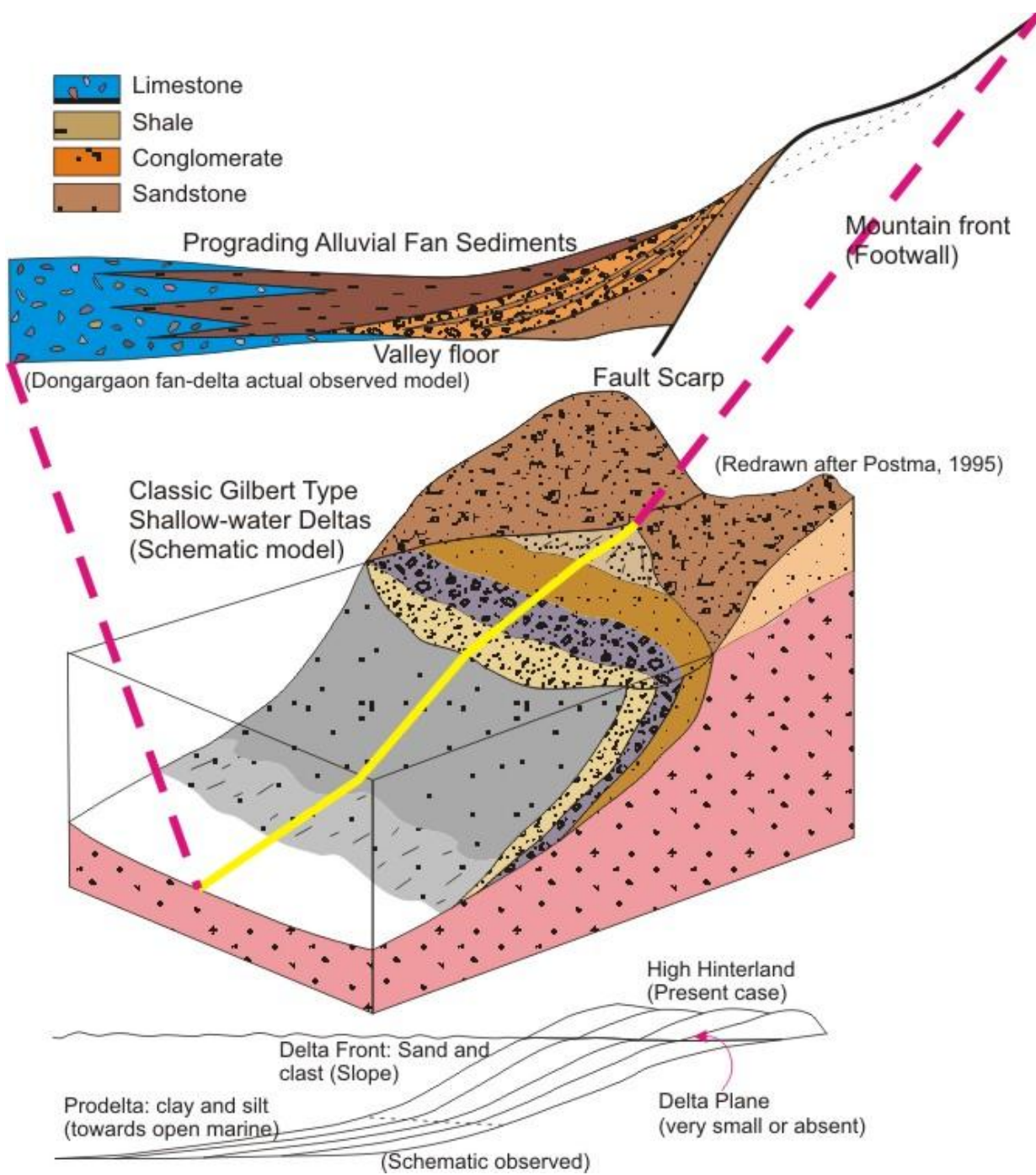


Figure 4.30: Structurally controlled architecture of the Dongargaon fan delta with classic gilbert type fan delta (redrawn from Postma, 1995) and observed schematics of Dongargaon.

There are certain parameters which decide the morphology and facies composition of the fan delta. Also, fan deltas are the basin marginal manifestations of high terrain and tectonically controlled fluvial system. They show subsidence evidences and rate of change of sediment supply also visible through various facies compositions. These parameters are explained by Postma (1995) shown in Fig. (4.29).

Postma (1990) described that, it is very imperative to have sufficient transport of bed-load to mouth with a sufficiently large water depth immediately seaward of the mouth and turbulent discharge of stream into that for Gilbert type fan delta where slip-face processes dominate. Also, the interbedded conglomerates show cycles of sedimentation with intervals of change in tectonic styles and discharge. Therefore, Dongargaon fan-delta (Fig. 4.30) architecture was the result of structurally controlled basin margin and bimodal feeder system i.e. sediment laden stream and the sediment gravity flow from the hills.

The redrawn schematic with the observational settings has been shown (Fig 4.30). However, since the basin floor is deeper than 3° , it allows the formation of Gilbert type delta where lower angles allow formation of mouth bar type deltas (Dunne and Hempton, 1984; Postma, 1990) which may be destructed later due to subsidence activity along the basin margin. Seeing the present conditions of this delta it can be classified under the classic Gilbert type delta under type A of Postma (1990) shown in the figure (4.30). The facies association in the Dongargaon fan-delta has been shown in the schematic of figure (4.30) and discussed below.

4.2.7.1 Fine grained sandstone facies

A typical vertical sequence of a prograding fan-delta will comprise a fine-grained basinal facies (marine or lacustrine mudstones) conformably overlain by a coarse-grained alluvial-fan facies (interbedded sheet flood, debris-flow, and stream-channel conglomerates and sandstones) (McPherson et al., 1987).

Hence, the deposition of fine grained sandstone of considerable thickness initially took place in the basin (Fig 4.33a). It was a comprehensive activity of streams as well as the prograding fan into the shallow marine waters of the basin. The rounded quartz grains as seen in the photomicrographs (Fig. 4.31) show its reworking level due to the waves and tides along the margin of sea and the prograding fan.

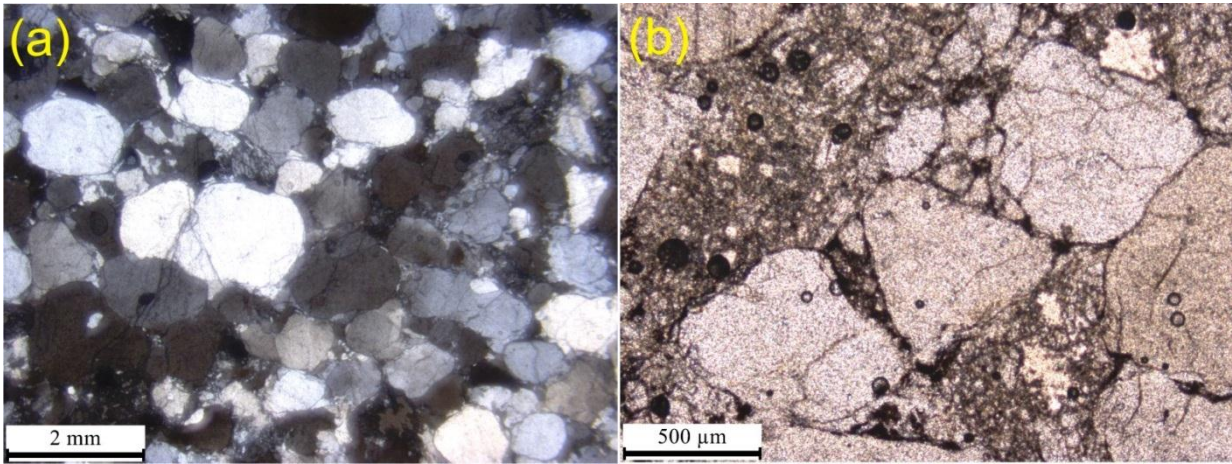


Figure 4.31: The rounded quartz in the photomicrographs show the level of reworking in the sediments of fine grained sandstone which is the initial stage of its formation.

Presence of well crystallized quartz crystals within this fine grained sandstone are indications of deformation and compaction with further solution movement during the latter phase of deposition. Reddish tint of the sandstone indicates presence of Fe in the basin margin which is supported by the photomicrographs as one of the component of cementing material is showing reddish tint (Fig. 4.32).

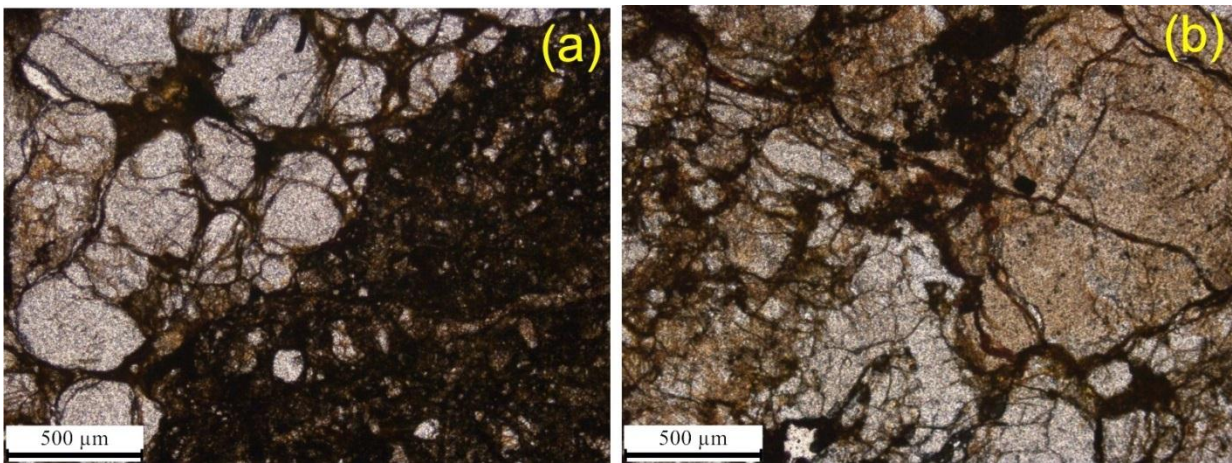


Figure 4.32: Fe content in the sandstone can be observed with the grain to grain mutual cementing in the photomicrographs.

A delta can only be classified as fluvial dominated if the degree of reworking in that is found negligible (Galloway, 1975; Nemec, 1990) and that in the Dongargaon fan

delta, it is moderate because firstly, the grains are found well rounded in the thin section and secondly, the matrix content of the overlying conglomerate sequence is in between 45-50%. However, it is intercalated with sandstone beds.

Therefore, the basin marginal fan-delta processes was initially dominated by river sediments which later on, due to upliftment, got interrupted by sea level changes and climatic activities.

4.2.7.2 Clast supported conglomerate with intercalating sandstones facies

The conglomerates in the front part of the fan delta are mainly clast supported and matrix content is < 30% indicating high energy condition. Since it is a coarse grained sedimentary system, and they are in general, associated with tectonic activities and show evolution patterns resulting from complex pattern of sea-level change (Postma, 1984). Therefore, from a purely matrix supported conglomerate in the proximal end to a clast supported conglomerate in the distal part of the fan-delta shows the change in the energy sequence of the fluvial environment with the subsiding basin including wave action in the later stages (Fig. 4.33 e, f).

The incoming stream as soon diminished into the sea, the change in the current directions and increase in the turbulence within the deltaic margin had affected the matrix content of the conglomerate. The subsidence and the sea level fluctuation also helped the accommodation for the sediments in the distal part of the fan-delta. Because for a steady state delta system, the constraints like sea-level fluctuation and climate should remain constant whereas the influx of sediments and discharge may vary (Postma, 1984). As the sediment supply and basin dynamics essentially govern the fluvial and basinal regimes, mix types of settings were developed in the Dongargaon fan-delta where tectonic disturbances had caused changes in the sediment influx.

Variations in bed attitude and clast composition also suggest syndepositional tectonic movement as suggested by Hwang et al. (1995). Therefore, comparatively slight increase in the grain size with matrix content also indicates the same. Bed attitude has been changed since Proterozoic as the deformation pattern in the form of a fold is visible on the outcrop scale (Fig. 4.33b).

According to Orton (1988), wave reworking and grain size variation in sediment yield are best defined by processes dominating in the delta front. Hence, cyclicity of

fine sediment swarm deposition in the form of thin lenses caused alternating sandstone conglomerate sequence (Fig.4.33c, d).



Figure 4.33: (a&b) Deposition of initially deposited thick fine grained sandstone facies which later went a deformation phase and folded (c&d) Conglomerate and sandstone intercalatory relation showing intermittent fluvio-marine energy variations due to tectonism (e&f) Matrix supported and clast supported conglomerate in the proximal and distal end of the fan delta.

Where, pebble to gravel size of clast in the conglomerate bed alternating with sandstone indicates towards the tectonic disturbances causing the cyclic shift of drainage and reducing its surficial traversing distance.

4.2.7.3 Shale facies

Disruption after the deposition of clast supported conglomerate has shown a state of non-deposition or quiet environment which can be supported by initiation of carbonate deposition in the form of precipitation in the distal part of prodelta or shale facies (Fig 4.34).

The distal slope and basinal facies are mainly silty and muddy (Dabrio, 1990). Therefore, progressing from clast supported conglomerate towards progressively thickening shale member of fan-delta sequence of Dongargaon gave rise to the prodelta sequence in the slightly deeper part of the isolated basin.

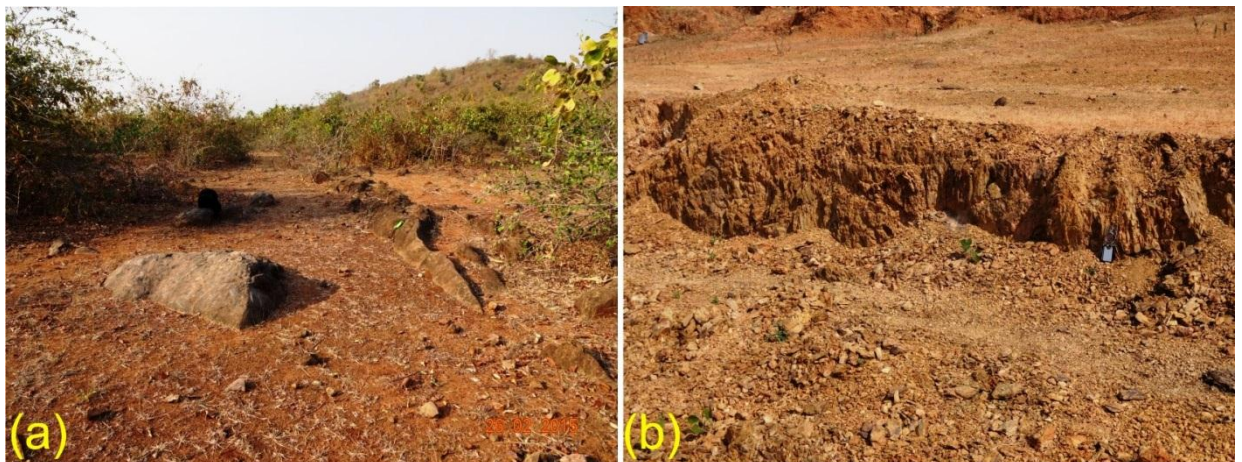


Figure 4.34: (a) Shale facies can be observed with splintery shale (b) limestone without any laminations which is in the prodelta region beyond the deposition of shale.

However, quiet environment and warm waters in this region had generated the limestone sequence in the distal part of prodelta. Gradation from shale to limestone definitely marks the break in deposition which can be visualized from a schematic (Fig. 4.35).

Absence of any lamination in the limestone deposits are clearly shows slow quiet precipitation in the later stages and transgression of the sea within the basin. Lesser impact of the global eustatic changes in the basin were due to only one sided

connection with the larger sea precluded it from making much disturbances and allowing slow deposition of limestone within the distal fan-delta sequence. Present day topography is just the consequence of comprehensive tectonics and sea-level play along the basin margin in the Pranhita-Godavari valley.

4.2.8 Controls and evolutionary pattern of dongargaon fan delta

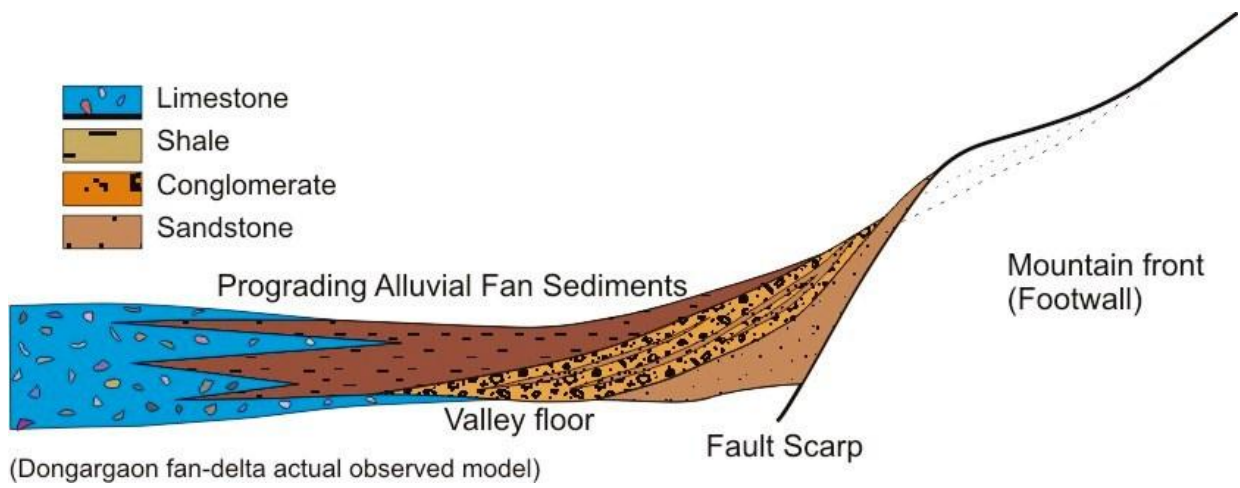


Figure 4.35: Schematic shows the presence and disposition of various facies and gives the overview about the morphology of the delta with structural control.

The location and dimension of the fan-delta systems are analogous to those of few basins which experienced orthogonal extension (e.g. Leeder et al., 1988; Gawthorpe and Colella, 1990). Here, orthogonal extension has been observed by previous workers in the Pranhita-Godavari valley where Penganga group of rocks has been deposited which contains the Dongargaon fan-delta setting (Pati, 2010; Dora et al., 2011). Rapid subsidence of the basin and high rate of sediment supply resulted in the progradation of Gilbert-type fan deltas (Postma, 1984). Therefore, analogy can be observed in presently studied fan-delta setting.

Alluvial fans are controlled by climate and tectonics on a long time scale (Rust and Koster, 1984) because tectonics describe the slope gradient which is responsible for the feeder system such as discharge rate, flow velocity and density of river effluent

(Leeder et al., 1988; Gawthorpe and Colella, 1990; Postma, 1990). Therefore, steep slope on the delta front is observed as compared to the hinterland gentle slope. However, smaller alluvial fans with high debris-flow deposits commonly occur along the basin margins with short drainage systems and steeper slopes, whereas larger fans with less steep slope and large scale drainage system (Steel, 1976; Gloppen and Steel, 1981). Hence, small scale drainage and small scale fan could be up to the mark of understanding. Another imperative process that assisted in the formation of present fan-delta is sediment dispersal in subaqueous environment which varied from time to time during its development due to other factors.

Controls on the evolution and morphology of the fan delta system are mainly given by sediment and water mixture supply towards the upstream end of the system, available for transport and deposition. And accommodation space available which is filled in relation to the sea level fluctuations. Since, the boundary conditions are given by allogenic controls where another process like autogenic processes acts internally.

These autocyclic processes had acted intermittently limiting the erosion and character of the deposition in the system (Maurits van Dijk, 2009). Generally, during the base level rise the gravel-sand transition moves upstream (Parker et al., 2004). Therefore, the extent of the fan delta sequence has been followed along the basin margin.

4.3 Depositional environments in the basin margin

Certainly variation in types of lithology in the join between the Bastar and Dharwar cratonic nuclei indicates towards the presence of various kinds of depositional environments. Since the formation of these environments is the manifestation of interplay between many geological and geochemical parameters along with tectonics which causes the deposition of sediments. These allogenic and autogenic processes lead to the formation of various rocks along the basin margin which has been studied at present. The climatic conditions were cold and basin conditions were shallow marine along the margin and the potash rich granite exposure in the western Bastar craton also added to the sediment influx to the basin in addition to other provenances.

4.3.1 Shallow marine environment: marginal swash zone detached, anoxic and cold

Along the marginal region of the basin during the Neoproterozoic not much of the free oxygen were developed as it just began to develop. Therefore, most of the areas are devoid of it. Similarly, in Dubarpet along the faulted region due to subsidence and sediment accommodation the slope was a changing parameter. However, basin remained shallow and the formation of paleosol took place during the marine regression and because of the subsiding adjustment towards the footwall side of the region. The incoming streams bringing the sediments accumulated in the form of a miniature fan-delta. Drainage condition of that particular part was poor and the ambit was of epeiric sea framework (Chakraborty et al., 2012). Due to poor drainage basin conditions the salinity of the closed basin was on a higher side which was taken into consideration in the explanatory part.

4.3.2 Shallow marine environment: Supratidal to near shore warm and alkaline

Limestone deposited in the basin margin near Gojoli and surrounding area was mainly due to warmer and alkaline ambit because only then the limestone precipitation can take place from the marine waters. Since the deposition was well below the wave base therefore it can be said that it was a low energy hydrodynamic regime (Wilson, 1975; Geel, 2000). The larger clasts with the fine matrix are transported towards the deep-marine region. Also, when minimal external clastic supply takes place, deposition of carbonate takes place along the shore (Pettijohn, 1975). Due to juxtaposed igneous activity (felsic volcanism, Sarbani P. Deb, 2003) climate was warmer in that particular part of basin.

Shallow and quiescent alkaline environment helped in the precipitation of carbonate. Mg induction took place lately by the substitution of Ca in lieu of Mg in the interstitial spaces. In the same environment, due to the presence of juxtaposed felsic volcanism numerous small subsurface splays acted as the injection for the formation of lensoidal bodies of iron ore within the limestone through the hydrothermal fluid channelization (see Fig 4.19c, d). Therefore, it can be found near Gojoli area within the limestone.

4.3.3 Continental shelf environment: Near shore to deep coast line warm and alkaline, below active wave base

For the three mass flows main components responsible were gradient, gravity and tectonic impulse. After initial development of massive compact dolomitic limestone first flow took place and then due to brief freeze in the local tectonism in the basin it rejoined and compacted before next flow. Thereafter, development of algal mats which remained fixed to one end by these limestones. Algal mats indicate the initiation of oxygen containing mid-continental shelf environment where hydrothermal fluidal activity was alone enough to make the environment warmer.

Thus, the limestone finds itself not dissolvable and bounded by the bacterial activity over the sediments and linked to enhance their colonization. Distension of gases within the algal mats and creation of voids caused the occurrence of oxygen formation and calcite precipitation within them (Martindale et al., 2015).

4.3.4 Shallow marine continental shelf: Intertidal deltaic environment

Environments associated with the fan-delta are more or less similar to the major deltaic environmental sequences. In broader sense, deltas are defined on the basis of aqueous and subaqueous, formed by fluvial sediments and strongly modified by the marine forces such as waves, currents and tides therefore display a high degree of variability. But, in fan delta separate conditions prevail because instead of deltaic sediments there is an influx of sediments from the mountain slope which slowly progrades into the marine waters with tidal currents.

The mud particles were carried into the suspension. The reworking of the sediments due to shore currents make the sediments well rounded. Therefore, the formation of sandstone shows more or less structure less and massive in general kind of sandstone. However, shale is probably the dominant product of sedimentation in ideal conditions but in conditions like Dongargaon fan-delta it is one of the last depositing products due to the suspension carriage towards the prodeltaic part of the basin.

4.3.5 Moderately deep marine continental shelf: Subtidal deltaic environment

In the moderately deep sea basin which is the part of continental shelf towards the prodelta side of deposition. Suspension load brought forward by turbidites as well as other suspension particles and broken gravelly matrix of the mass flow regime creates most of the activity in this region. Eh and pH conditions of the sea remaining the same but it goes beyond the zone of dolomitization and before the shelf break region.

In Dongargaon, similar kinds of deposits were found like shale due to the suspensions carried forward by the current and the turbidity disturbances. But in the same settings due to the presence of limestone beyond the deposition of shale indicates that the warmness and alkalinity of water was dominant and the turbidity currents were very weak. Therefore, the shale member encountered after the conglomerate member in the outcrop was not found considerably thick and it was enveloped in the limited prodelta regime of the fan-delta sloping towards the shelf break.

5.1 Introduction

Ground Penetrating Radar (GPR) is a non-destructive geophysical surveying tool which helps to study the subsurface stratigraphy where near-continuous, high resolution profiles may help in determining subsurface strata, sand body geometry, correlation and quantification of other sedimentary structures and shallow subsurface faults (Bhatt et al., 2006; Desai et al., 2016). With suitable ground conditions (sediments with high resistivity e.g. sand and gravels), GPR profiles can help to get the idea of subsurface geology and significant sedimentary bodies or structural features (Jol and Bristow, 2003).

GPR detects electrical discontinuities in the shallow sub-surface (typically < 50 m) by generation, transmission, propagation, reflection and reception of discrete pulses of high-frequency electromagnetic energy. GPR has been used by sedimentologists to reconstruct past depositional environments and the nature of sedimentary processes in a variety of environmental settings, aid hydrogeological investigations (including groundwater reservoir characterization), and also assist in hydrocarbon reservoir analogue studies.

Although the rise in use of GPR in sedimentological studies can be attributed to its wider availability since the 1980s, its use by the research community is also related to the ease and rapidity of data collection, the ability to collect sub-surface information away from outcrops or boreholes, and the apparent familiarity of the images, due to GPR's analogy with the established seismic reflection technique.

With respect to interpretation, the basic assumption in both techniques is that, at the resolution of survey and after appropriate data processing, reflection profiles will contain accurate information regarding the nature of a sediment body's primary depositional structure. In other words, the form and orientation of bedding and sedimentary structures in the plane of the survey will be adequately represented by recorded reflections, and any non-geological reflections can be readily identified and removed by data processing, or by simply discounting them from the interpretation. Low magnitude faults from igneous or sedimentary terrains having more or less same

lithology on both the sides of fault plane can be easily observed by GPR (Bhatt et al., 2006; Bhatt, 2003).

Although this assumption is a seemingly simple basis for the interpretation of radar reflection profiles, the degree to which it can be assumed to be true is dependent upon a wide range of factors. These include the nature of the sediment body under investigation, the groundwater regime, the type of terrain immediately adjacent to the survey line, the nature and appropriateness of any data processing undertaken, the interpretation techniques employed, and the overall understanding and experience of the researcher(s) with respect to GPR, and hence their appreciation of the other factors.

High resolution images of the shallow subsurface can be obtained through GPR survey which cannot be derived by any other non-destructive method. GPR helps in identifying active faults along the basin boundary, depositional unconformities etc. along the fault planes, the lithological contrast, significant amount of slip and up dip or down dip nature of slip produce ample reflections on GPR profile (Bhatt et al., 2006).

5.2 Basic Principles of GPR data collection

The working principle of GPR is given in Fig. 5.1. It consists of two antennas: one transmitter which transmits electromagnetic waves to subsurface and the other one is receiver which receives the returned (reflected and refracted) waves. The type of survey depends upon the position of these two antennas and the way in which they interact with the ground. If the position of the source and receiver or just the receiver is varied, the data contains the information on the spatial variation of the subsurface.

The visualization of the GPR profile is the time–space representation of the subsurface, but the time is converted to depth by using measured wave velocity. In this geophysical method radar pulses in the form of electromagnetic waves are ground down to a depth of few tens of meters and detect the signals from the subsurface structures. It can be used in a variety of media including rock, soil and ice.

The depth range of the GPR is somewhat limited by the electrical conductivity of the ground, the transmitted center frequency and the radiated power. With increase in electrical conductivity, penetration depth decreases. This is because the electromagnetic waves are dissipated in the form of heat causing a fall in signal strength at depth. Higher frequencies do not penetrate as far as lower frequencies, but

give better resolution. Optimal depth penetration is achieved in sandy soils where penetration can be achieved up to a hundred meter.

The antennas are oriented perpendicular to the profile direction. The main record parameters are 1000 ns time range, 1024 samples/scan, 16 bits/sample, and 32-fold vertical stacking. The data was processed using automatic gain control (AGC) function, band pass-filter, migration, velocity analysis and time to depth conversion and elevation correction. Also, the data processing is a fairly long and complex affair and it has weight induced logistic problems associated with it. However the accuracy of the data depends on the parameters selected and the ground conditions like material and roughness etc.

Van Dam et al. (2003) suggested that few sub centimeter scale structures are composites of interfering signals and show some tuning effect, which causes reflections which may vary with radar frequency. Also, the influence of iron oxides, organics and sediment character concluded that the changes in water content associated with small scale textural changes in sediments are responsible for the dielectric property changes which produce radar reflections (Van Dam and Schlager, 2000). It is mainly used for imaging faults in the subsurface with varying degrees of success.

Depth penetration depends upon the dielectric constant of the matter which is the ability of material to hold or pass the electric charge, where the reflected signal has information on how quickly the signal travelled and how much was attenuated. Different materials have different dielectric constant which are given as follows: (table of dielectric constants, Table 8)

Table 5.1: Dielectric values for common materials used for various terrains (Desai et al., 2016)

Material	Dielectric constant	Velocity (mm/ns)
Air	1	300
Water (fresh)	81	33
Granite	5-8	106-120
Limestone	7-9	100-113
Sand (dry)	3-6	120-170
Sand (wet)	25-30	55-60
Silt (wet)	10	90
Clay (wet)	8-15	86-110

Geophysical reflection data are of four main types: common offset, common mid (or depth) point, common source and common receiver (Fig. 5.1).

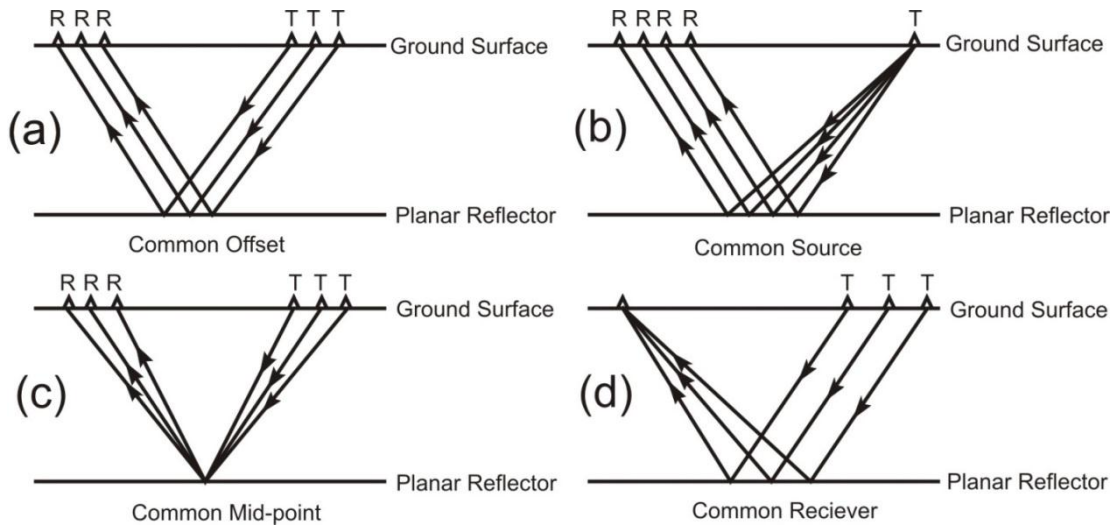


Figure 5.1: Four main types of geophysical survey. T=Transmitter, R= Receiver, (Neal, 2004; Daniels, 1996)

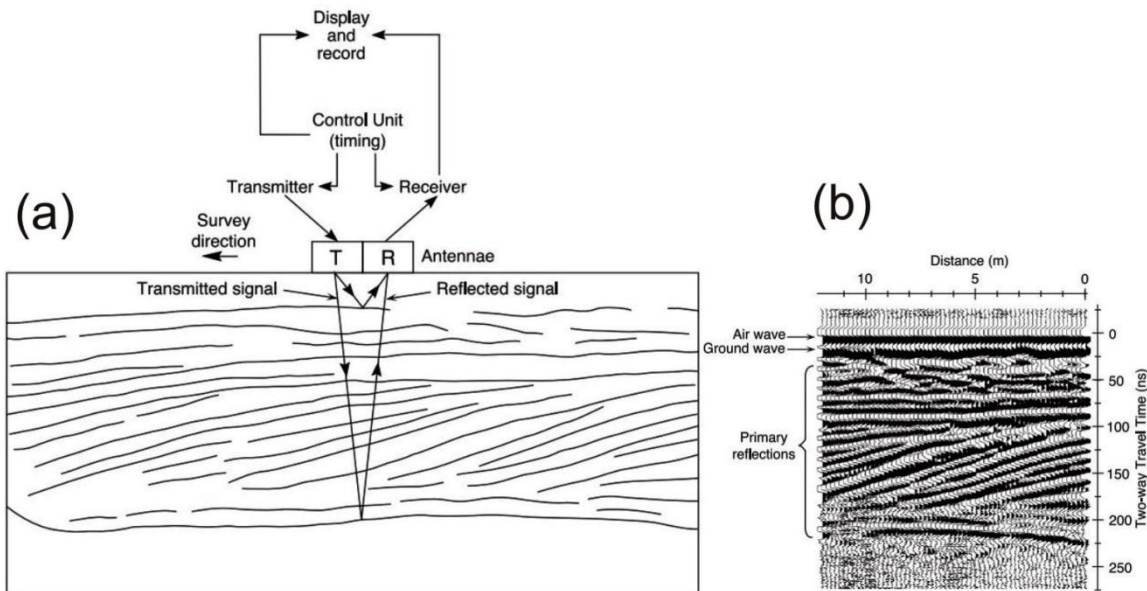


Figure 5.2: GPR data acquisition and the resulting radar reflection profile (a) Data acquisition at a single survey point, showing GPR system components and subsurface reflector configuration. (b) Radar reflection profile resulting from sequential plotting of individual traces from adjacent survey points. Positions of air-wave, ground wave and primary reflections are indicated (Neal, 2004).

Common-offset surveys (Fig. 5.1a,) are most frequently used in GPR studies. The GPR system mainly comprises of three main elements: The control unit, antenna and the survey encoder (Fig. 5.2).

Fig. 5.2 showing the above quoted things where data acquisition at an individual survey point, showing GPR system components and subsurface reflector configuration and radar reflection profile resulting from sequential plotting of individual traces from adjacent survey points. Positions of the air-wave, ground wave and primary reflections are indicated in different diagrams (b), (c) and (d) of figure 5.1 in different acquisition settings (Neal, 2004; Neal and Roberts, 2000).

5.3 Methodology

To carry out the desired profile data acquisition work following methodology has been adopted.

5.3.1 Site Selection



Figure 5.3: Google earth image showing the location and path of profile various profiles.

GPR survey was carried out after deciding the purpose and selecting the best suitable site for the study. The exact locations where contacts between different lithounits exposed to the surface, along the basin boundary were identified during the field

mapping and study and their locations were transferred to the Survey of India topographic sheets and Google Earth images were identified (Fig. 5.3).

In order to trace the unconformities, GPR traces are chosen such that they cut across the general trend of strikes of lithological units of the area, so that variations in the lithology can be recorded. To trace the faults or palaeochannels in the region, GPR traces were chosen across the low lying areas, which makes them the probable sites for the occurrence of faults or palaeochannels.

5.3.2 Instrumentation and data acquisition

As observed by Bristow and Jol (2003), 100 MHz antennae provide the best trade-off between the two aspects of depth of penetration and resolution, this frequency antennae were used in our investigations. The system comprises five main components (1) control unit, (2) transmitter, (3) receiver, (4) survey wheel, and (5) interface, data storage, and display module (Fig. 5.4).



Figure 5.4: Image showing various parts of GPR.

Shielded antennae were used to avoid ringing inherent in the hardware (Audru et al., 2001). Data were collected in distance mode using a survey wheel (model 620, GSSI) along a profile. Data transfer from the antennae to control unit was through fiber optic cables. Automatic Gain Control (AGC) was applied while collecting the data, as it is the best way of acquiring data in a sedimentary terrain (Neal, 2004). Two basic types of data collection i.e. Common Mid-Point method (CMP) for point data and Common Offset Method (CO) for line scan were used. In most of profiles, we practiced Common offset method which provides good results for sedimentological studies in the subsurface (Neal, 2004).

As the average velocity of profiles varies commonly from 0.0768 to 0.0671 m/ns with 100 MHz, resolution of the GPR survey comes to 25.6 cm to 20.3 cm. assuming the spatial resolution as a quarter of wave length (Reynolds, 1997). Precautions were taken while acquiring the data; avoided acquiring data near hyper-tension lines or electrical poles, avoided acquiring data in heavy traffic areas as vibrations from running vehicles can contribute a good amount of noise in the data, mobile phones and other such instruments were switched off as they use electromagnetic energy like GPR, made sure that GPR antennae were moved or towed on the plain ground without any cobbles or pebbles as they add noise to the data.

5.3.3 Data acquisition in Point mode

Point mode allows us to collect data at one point at one time. For a profile building at a stretch, number of data has to be collected at number of point in a stretch. Deciding the step size plays an important role in point data collection.

Step size (the distance between each data collection point, also known as station spacing) is extremely important and should be included in survey design process. In sedimentary studies, a maximum step size of 1 meter should be used to provide detailed horizontal resolution of sedimentary structures.

CMP technique involves conducting a survey in which the spacing between the transmitter and receiver is successively increased or decreased with each step. CMP soundings are generally considered more precise as the antennae are always centered on the same point. As the available cable connecting the antennae was 100

meters long, we started with the maximum antennae separation of 100 meters and moved each antenna in every 1 meter until they meet at a common point in the center.

5.3.4 Data processing

GPR data processing is similar to seismic data processing technique (Fisher et al., 2000). The GPR data collected from sedimentary terrains do not need much processing (Jol and Bristow, 2003), as the sediment bed geometries in sedimentary terrain are simple and the layers or beds are almost horizontal in nature. Collected data were processed and plotted, using GPR data processing software RADAN 5.0 supplied by GSSI using Infinite Impulse Response (IIR) filter, Finite Impulse Response (FIR) filters, 2-D spatial Fast Fourier Transform filters, gain control, surface normalization, deconvolution, band pass filtering and hyperbola migration as per the requirement.

Filter band width 40/50 and 150/180 MHz were chosen for data processing as suggested by Fisher et al. (2000) for 100 MHz antenna.

5.3.5 Profiles and Interpretation

Interpretation of GPR profiles involves the deciphering of interference patterns of discrete reflections and diffractions (Gawthorpe et al., 1993). In the present study, interpretation was made through reflections caused by the waves while traveling through the air and the road materials were identified and removed from the main trace and origin of the reflections were identified; i.e. whether the interfaces obtained in the traces are real matching the changes expected in the subsurface, since such interfaces can be produced due to the noise and repeated reflections.

The two direct waves (air and ground) observed at the top of the profile are often the strongest return signals. As a result of the high velocity and low attenuation of radar energy in air, the direct air wave is the first to arrive, travelling at the speed of light. The direct ground wave usually follows the air wave with an arrival time that is the function of the ground propagation velocity.

5.3.5.1 Profile AB



Figure 5.5: Google earth image showing the location and path of profile A-B

Parameters used:

Range: 700

Dielectric: 7.5

Rate: 64

Sample: 512

Format : 16 bit

Scan/unit: 40

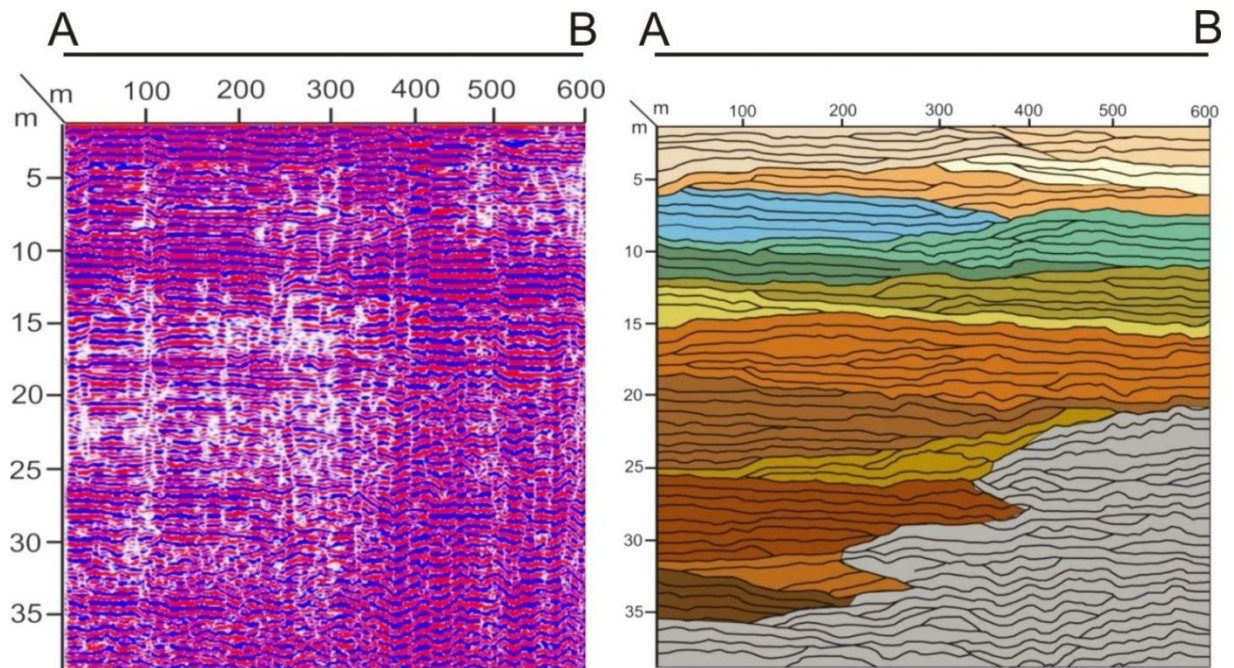


Figure 5.6 (a&b): Reflection profile of path AB and indicating the bounding surfaces of sedimentary package on Archaean gneiss

This profile was collected from the Old Gojoli to the New Gojoli village. The reflection profiling was done by the CMP method. The profile is 600 m long. Step size for the CMP survey was 1 m.

The AB profile represents the clear contact between the Archaean gneiss (B side) and the limestone (A side). The profile shows discrete reflections demarcating the discontinuity.

5.3.5.2 Profile XY



Figure 5.7: Google earth image showing the location and path of profile X-Y

This profile was chosen such that it cut across the different facies of limestone which trend north-south. Common mid-point technique was used to acquire the data. Profile length is 700 m. Seven 100 m profiles were collected through CMP method and appended to get a full 700 m profile which was interpreted and various inferences were taken out accordingly.

In this profile, the stratigraphic sequences can be identified by onlap and offlap patterns visible in the profile which are in abundance.

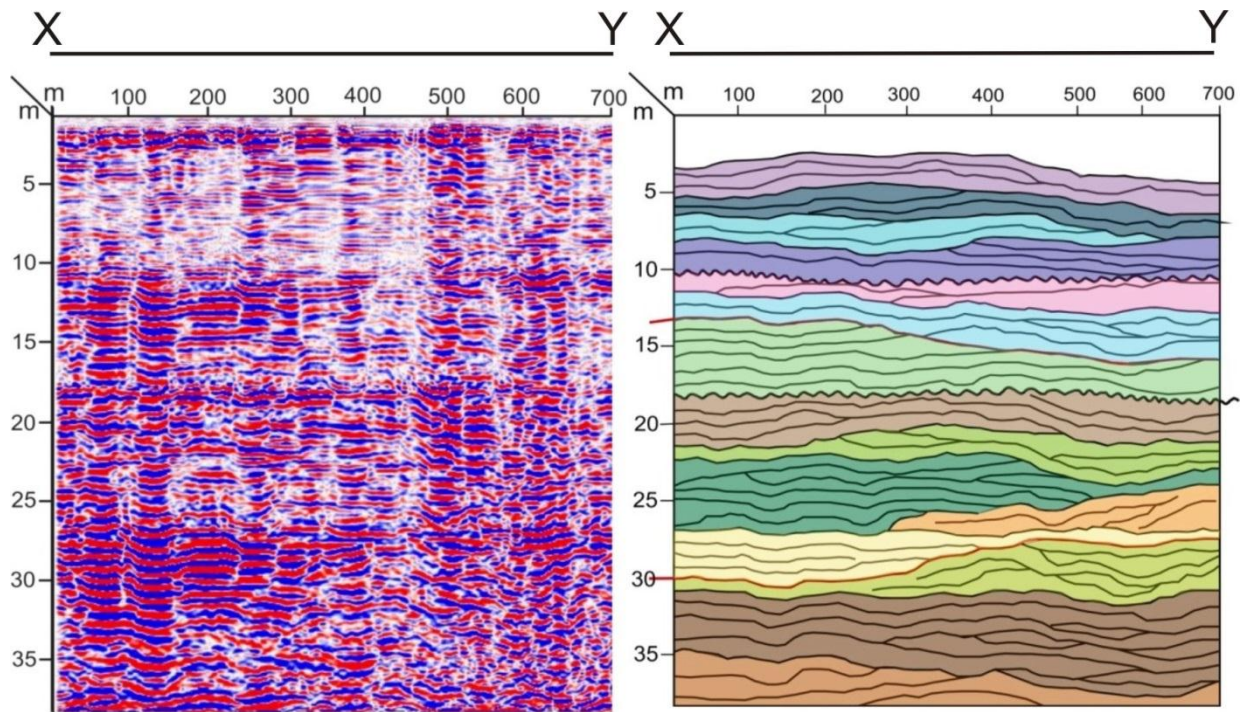


Figure 5.8 (a&b): Reflection profile of path XY and Positive reflections from GPR profile of path XY indicating cross-stratifications and bounding surfaces

Few unconformable surfaces are identified in the profile X-Y which is presented by a zig-zag line respectively and two offlap sequences can be seen in the top and lower part of the profile excluding the unconformable surfaces. At 18 m depth, probably an erosional surface has been detected. At 13 m, another dipping erosional surface can be seen.

Path PQ was selected for GPR such that line PQ cut across the limestone facies which trend N-S. Path PQ is 350 m long. The following GPR profile is obtained by appending three 100 m profiles and one 50 m profile. All three profiles were collected by CMP method with the step size of 1 m.

5.3.5.3 Profile PQ



Figure 5.9: Google earth image showing the location and path of profile P-Q

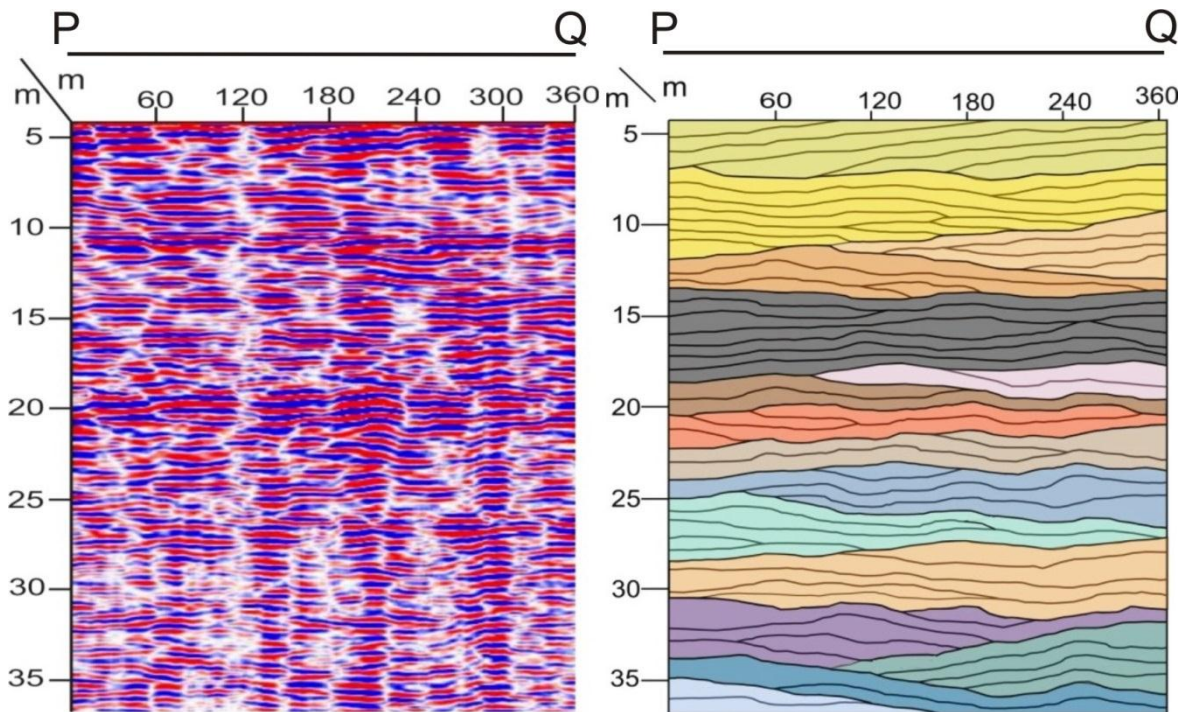


Figure 5.10 (a&b): Reflection profile of path P-Q and positive reflections from GPR profile of path PQ indicating cross-stratifications and bounding surfaces

The bounding surfaces and the cross strata have been traced on the GPR profile. Orientation of these cross strata and the bounding surfaces will be useful in the transgression regression scenario in the region. In this profile, till 28 m depth, the steady basin conditions seem to be existed, represented by the sub horizontal layers. For the sedimentary package between 28-25 m basinward propagation of strata indicates the regression event i.e. sea level might have decreased. Another period of regression must have been occurred when the sediments between 13-11 m were deposited in the basin, which might be because of the sea level decline or the tectonic uplift of the block.

Event of transgression must have occurred after this, indicated by the landward propagation of layers where the sedimentary package pinch outs at 90 m distance from P end.

5.3.5.4 Profile RS



Figure 5.11: Google earth image showing the location and path of profile R-S

The path of the profile RS is chosen such that it cut across the different limestone facies trending NS direction. The length of the profile is 350 m.

This profile is obtained by appending two 100 m and one 80 m profiles, all collected by CMP technique. Lines traced from the GPR profile (Fig 5.12) along path R-S to obtain the traces of strata and the surfaces bounding them. These traces were used to interpret the depositional processes that might have taken place in the past. Sea level fluctuation pattern can be observed.

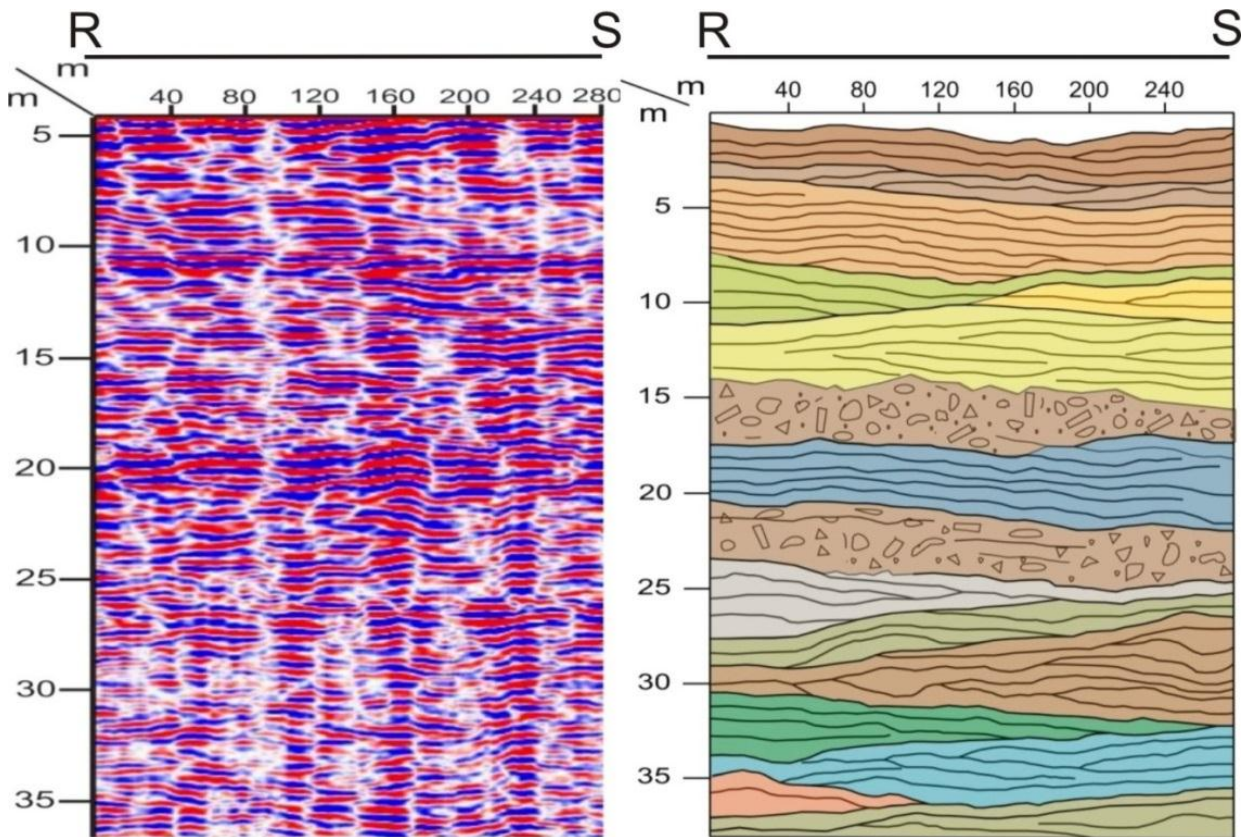


Figure 5.12 (a&b): Reflection profile of path R-S and Positive reflections from GPR profile of path R-S indicating cross-stratifications and bounding surfaces

Strata between 35-34 m shows a landward propagation, which means the transgression might have taken place. Layers between 28-24 m seem to be moving towards basin, which is a case of regression. Between 34-30 m the strata are relatively horizontal. This indicates that the basin was stable due the deposition of this sedimentary package. The water level was rising or decreasing at the constant rate.

The layers within the bounding surfaces at 30 and 28 m seem to be propagating landward i.e. transgression.

Region between 24- 20 m surfaces in figure is somewhat scattered and not continuous. This is because of the fragments of rocks of different physical properties. Fragmented rock is the characteristic of the erosional event.

The Pranhita-Godavari basin was formed in the mid-northern latitude (Torswik et al., 2001; Gregory et al., 2009; Valdiya, 2010) during the existence of the Rodinia Supercontinent when India, East Antarctica, Madagascar, Australia were connected together along the Eastern Ghat Granulite Belt (EGGB) (Sarkar and Gupta, 2012). At present, the western Bastar and the eastern Dharwar cratons meet at the junction in the Pranhita-Godavari fossil rift. The granitic crust of 3.3 Ga in the form of Tonalite-Tronjhemite-Granodiorite (TTG) forms the basement for accommodating Proterozoic sediments. As it is a fossil rift, lithological variations pertaining to tectonics and different kind of depositional environments are well preserved in the basin. A series of tectonic events are manifested as faulting and folding which have modified the basin configuration during and after the deposition. Sedimentological aspect related parameters have shown a major evolutionary trend in the region due to frequent change in basin configuration. Similarly, geology and geomorphology of the area can be properly analyzed through careful and stepwise analysis of the available proxies from the field. Also, the paleogeography and its relation to tectonics, palaeoclimate and palaeoweathering trends can be defined by the analytical field and laboratory methods as well as proper appraisal of the region.

In the same context, initially drainage network and its relation to the slope as well as with the lithology of the region have been established. However, drainage in the study area is mainly affected by the slope and lithology because slope characterizes the runoff speed and resistant rocks decide the amount of erosion. These two factors will be assisted by the amount of precipitation which, if higher in resistant rocks, will create more streams and the drainage density will be higher than the average and since, precipitation is low, therefore, this case is not applicable. Whereas, in vice-versa situation, less influx of precipitation causes a lesser number of streams and reduced stream flow while some part of the remaining water will also get infiltrated downward penetrated in the grain boundaries of the rock. So, drainage density will be moderate to low. But in case the slope is higher in some areas as seen in present case, may increase the drainage density in those areas like near Wardha River or Maleri sandstone etc. However, in the southern part and along the central

region where the passive basin margin exists near the village Gojoli and Dhaba, parallel to sub parallel drainage also exists.

Parameters like drainage texture shows a higher value of 18.65 indicates towards fine drainage texture which means relative spacing of the drainage is medium to sparse, depending upon the climate, rainfall, vegetation, lithology, infiltration, and relief aspect of the terrain (Smith 1950). In the regions where granite gneiss are present still showing high infiltration or higher drainage texture shows development of joints and thick weathering profile.

Stream frequency of any region is the count of all stream segments per unit area of the basin describing the texture of stream network and the bedrock properties such as infiltration, fractures or permeability or porosity etc. In the present study, stream frequency of $2.01/\text{km}^2$ shows a low which can be compared to the medium drainage density of 2.30 of the overall region. However, the infiltration number, which is a product of drainage density and stream frequency, is 4.62 indicating moderate infiltration and medium to low run off. This shows correspondence of infiltration number with drainage density and stream frequency where such behavior of the later in the basin is due to variable gradient and lithology in the region near basin-margin area. Hence, this indicates that gradient and the lithology of the region the regionally play dominant role with the drainage characteristics. Therefore, lesser tectonic disturbances or any other crustal perturbation can be inferred from the study area. This may be due to the diminishing effect of the same in the late stages after the cycles of rift fossilization.

This inference is also assisted by the bifurcation ratio, which is the ratio of the streams of a given order to the next higher order (Strahler, 1964), in the study area ranges between 0.82 to 2.54 with a mean R_b value of 1.88. This indicates that the geologic structure and tectonics does not exercise dominant influence on the drainage pattern because bifurcation is not dominant. Hence, lower order streams have dominated the study area and the drainage been modified by various processes of denudation after the Precambrian with small intervals of tectonic disturbances. In the similar manner while the region has an evolutionary upgraded geomorphology and structure various environments were developed along the basin margin.

The Pranhita-Godavari basin shows several basin openings and rejuvenation processes during the Palaeo-Neoproterozoic time (Conrad et al., 2011; Ghosh and Saha, 2003) as evidenced by the litho-association. Deposition of conglomerates, pebbly sandstones, arkosic sandstones, with intercalated quartz arenites and intermittent paleosol development took place during the terminating depositional time due to the interaction of various environmental factors. This validates it to be a fan-delta environment prevailing at the basin margin. Thereafter, shifting of shore line and exposure of marine sediments at the basin boundary promoted the exposure and development of the paleosol within the sandstone sequence and the unconformity surface within the Neoproterozoic stratigraphic sequence. Field study of litho-association, mineralogy and texture of the sandstone indicate its deposition in a continental shelf environment in a fan-delta setting (Fig. 6.1, Pati, 2010).

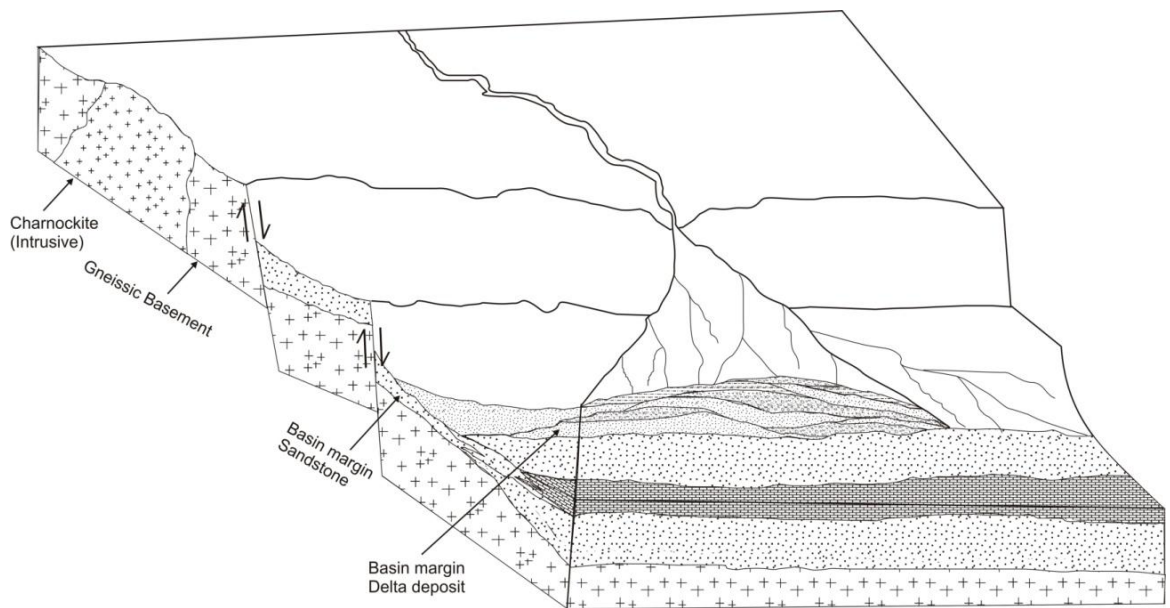


Figure 6.1 Fan-delta model at Dongargaon (not to scale, after Pati, 2010)

Rifting and fluctuation of sea level is inferred by transgressive and regressive sequences at basin margin (Chaudhuri and Deb, 2004; Chaudhuri et al., 2002). The sandstone close to the basin margin is fluviially influenced to certain extent as evidenced by the grain gradient (Pati, 2010). The regressive events and the exposure

of shelf promote paleosol development in the fan-delta setting. Magnetic susceptibility trend is also decreasing with the depth indicates that leaching of Fe containing components were not effectively reached towards the depth which can be compromised sometimes due to burial gleization (Retallack et al., 2003). Still it can be applied for Precambrian paleosols for confirmation (Retallack et al., 2003). The paleosol horizon has less lateral extent and overlain by a transgressive litho-package. Less horizontal extend and little vertical thickness of paleosol horizon may be attributed by weathering. However, feeble presence of sedimentary structure (lamination) and less degree of development of pedo-features at depth, as seen in the petrographic studies (see Fig. 4.9), do suggest relatively less time of exposure for pedogenesis. Glauconite in the paleosol bounds its conditions to shallow marine environments with slow rates of sediment deposition since it develops as a consequence of diagenetic alteration of sedimentary deposits. Therefore, it can be said that the glauconite forms under above mentioned conditions due to high concentrations of K, Na and Ca cations in the sediment influx and found along the near shore sands at the basin boundary.

Values obtained from Chemical Index of Alteration (CIA), Clayeness, and Paleotemperature reveals that the paleo-temperature was about 12°C in which physical weathering was dominating over chemical weathering, which is expected generally in such prevailing colder climate. This is also supported by the presence of illite in the XRD peaks. Illite and Glauconite present in the sample containing K, Na, and Fe indicate that chemical weathering was moderate to low. Cations such as K, Ca, and Mg are leached away as the weathering progressed. Their dominance shows its formation in a poorly drained environment under the reducing conditions. This indicates the deposition in fault-bounded isolated basins in form of grabens along the basin boundary. Therefore, the lower temperatures attested by the presence of glauconite and illite in the sediments during the formation of paleosol and sea level fluctuation due to local tectonics, which must be the manifestation of the regional tectonics, shows the poorly drained basin probably in the shallow marine shelf conditions which sometimes forms due to local detachment from the main water body. As we move towards the central region of the study area along the basin margin there is a drastic difference in the depositional environments.

Certainly presence of autoclastic conglomeratic limestone in the central region shows that climate has been changed to warm and alkaline during the deposition of limestone along the basin margin. The formation of autoclastic conglomeratic limestone in the basin margin along the Pranhita-Godavari valley within the join of western Bastar craton and the Dharwar craton is observed and addressed in all possible manners to get the detailed analysis of the environmental and tectonic aspect of the region.

The evolution of the various flows of the limestone was developed in the Pranhita-Godavari basin is an oscillatory cratonic rift (Sloss, 1984), extensional tectonic derived subsidence and upliftment at different intervals was affecting the accommodation space available for sedimentation (Chaudhuri et al., 2002; Chaudhuri et al., 2012). Extensive partial melting at lower crustal levels led to localized stretching and rifting (Deb, 2003). The retrogradational and progradational facies association along the basin-margin records the transgression and regression events, respectively (Ghosh and Saha, 2003). Shoreline movement had facilitated the development of various types of depositional environments for carbonates besides the cratonic margin like warm and alkaline in shallow marine conditions which supports the formation of limestone. Basin-margin faulting produced steeper slope which assisted the carbonates to acquire prompt mass movements in the region. As earlier the basin was shallow and isolated in nature (as most of the Proterozoic basin in the Indian peninsula), close venue marine activity confined the carbonate deposition to basin margin. During rifting, the smaller or major series of landslides triggered the momentum to the whole plug from the basin margin into the interior. However, intermittently freezing of the movements for a considerable duration promoted settle down of the plug for cementation.

Initially the massive cherty limestone (facies 'A') was juxtaposed to the Archaean granite gneiss and later influenced by potash alteration due to felsic volcanism (Deb, 2003) and hydrothermal K- alteration (Dora and Randive, 2015). The earliest mass flow occurred at the basin margin has left little or no *in-situ* facies probably due to later phase faulting and mass movements. Alternative argument can be made about the steep slope of the basin margin due to the boundary faults the facies is completely buried under the later flow sequences at greater depth. Long-axis

orientation and high degree of roundness (Facies H) of the clasts representing this mass flow event suggests it to be a slow mass movement due to constant clast influx forming a plug along the basin margin which was sliding and rolling along the slope.

The second and third phases of mass flow deposits are extensively exposed and various facies changes have been reported here. However, there is a sudden closing of second flow has been encountered may be due to its complete destruction and stromatolites formation in the later stages. The similarity of facies assemblages (except a few) clearly indicates the similarity in flow nature, slope, sediment supply and fluid dynamics within the flow. Eastward restriction of the flows by the basin margin fault (see fig. 4.17) suggests that the flows were triggered by the activity along the fault and the basin-margin slope provided the momentum for basin-ward

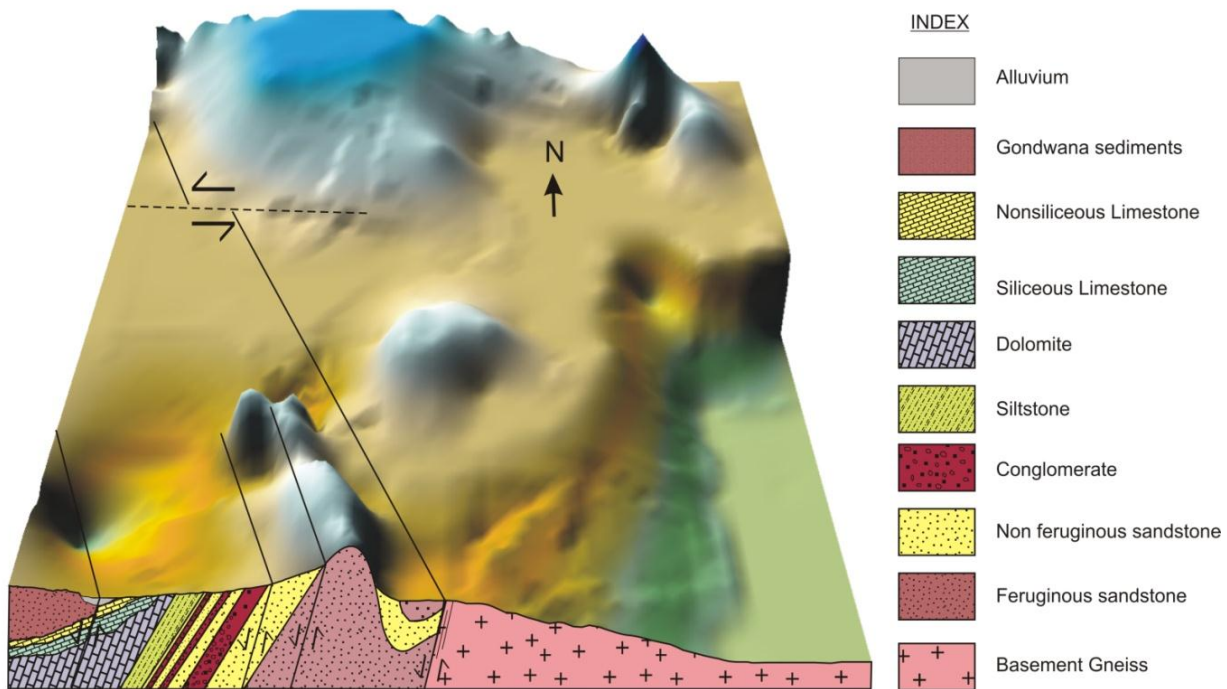


Figure 6.2 Faulting and folding in Dongargaon fan-delta (not to scale)

advancing the mass. In such subsiding basin margin with subaqueous settings where sedimentation was predominantly fault controlled, constant overwhelming influx of the coarser clast caused initial movement. Sometimes, surge type flow depositing at short

sequences also took place (Middleton, 1967) in overall waning flows providing momentum.

Comparing the basin-margin processes interpreted along the eastern margin with that of the western margin suggests closely spaced steeping faults were developed along the eastern margin, which has also been reported earlier (Lakshminarayana, 1997). The southern margin of the study area is represented by the Dongargaon fan-delta. The fan delta was deformed by various folding and faulting activities (Fig. 6.2) and up to one phase of deformation has been identified in the field (see fig. 4.33).

Morphology of this fan-delta is likely to generate varied associations of facies and better understanding of the basin-dynamics can be obtained from facies analysis (Dabrio, 1990). The pebbly-gravelly matrix supported conglomerate towards the delta slope is the manifestation of short distance traversing of streams due to tectonics and debris avalanching in the pebble and cobble streams. The debris avalanches were short and over the cone shaped fan, therefore, we can see these conglomeratic beds in the present day. The development of alluvial or colluvial fan points towards tectonism (Thakkar et al., 2001) which converts to fan deltas on progradation due to addition of marine action and other processes whether past or present.

Since each fan preserves its own combination of process signatures with complex tectonic and paleogeographic framework, which results in the great varieties of fan-delta architectures. Because continued underwater fan development as well as the stream brought sediments and clast reduces gradients below those needed to maintain widespread avalanching, therefore, helped by the subsidence processes intermittently due to extensional regime which had caused short term reductions in the sediment supply too. Hence, thin intercalating beds of sandstone within the conglomerate can be observed. However, Initial phase has only the fine grained sandstone which is due to the simple river brought load and the fine sized material of the prograding fan delta. Such formation is the indication of quiet environment in the initial phase and a continuous sediment supply to the basin margin.

The facies associations record the deposition on a tectonically active basin margin and the differential subsidence (accommodated along faults) is responsible for

the symmetry (Dabrio, 1990). Therefore, the proposed sedimentary model (see fig. 4.35) along the basin-margin fault, along which the major tectonic activities and subsidence took place, with a narrow sloping shelf was distally connected to a steep slope system. Off the mouth of the sloping mountain valleys drainage helping the formation of Dongargaon fan delta developed prograding upon the steep shelf region in the sea. Development of the channelized flow or the sheet flow which may be a part of single flow cause the formation of radial spokes over the delta surface (Maurits van Dijk et al., 2009; Schumm, et al., 1987; Ashworth et al., 2007). In the Dongargaon fan-delta, presence of elongated long furrows on the sandstone surface indicates towards such flow during its conception. Sheet flow along with sea fluctuations caused the aggradation, progradation and backfilling together in the slope region. Therefore, slope variation took place during delta evolution (Kim et al., 2006). The fan delta system experienced subsidence and flash floods with mass transport component in addition to a lesser extent. Detailed mapping and analysis suggests that the radius of the clast supported conglomeratic facies generated is ranged from 2-2.5 km. However, the sediment input surpassed this distance mostly as gravity flows and turbidity currents as well. These gravity flows were mainly fed by partial destruction of shallow-water, shelf and fan-delta slope deposits.

The non-deposition or quiet period of the deeper shelf region shows the presence of carbonate precipitation which attributes the rift fossilization. Since Roep and Kleverlaan (1983) suggests that the edge of the basin should be formed by small cliffs related to active faults. Here, in the Pranhita-Godavari rift margin, since, numerous active faults are present (Biswas, 2003) of which one major fault is passing through fan-delta margin which is acting as the basin margin with its supplementary splays causing sliding of the coarse grained masses to form the fan-delta.

Based on the remote sensing studies, morphometric analysis, field studies of facies association, GPR studies and laboratory analysis of selected samples, the whole work can be concluded as discussed below. The conclusions of this work can be categorized in different themes such as based on geomorphology, various lithological assemblages and tectonic activities.

In the study area geomorphology and tectonics have played significant roles in shaping the present geography. Topographic reversal has been well established by analyzing the lithological disposition and the associated sedimentary structures from the Proterozoic to Recent. During Proterozoic, a basin was existing (PG basin) to the west in which the rivers were debouching their sediments. This is supported by the westward dipping foresets of the cross bedding of the associated sandstone body. However, the present drainage system is south-flowing which indicates topographic reversal.

Analyzing the drainage density, infiltration number and other morphometric parameters, the middle zone (fault affected zone, hydrothermally effected) can be well distinguished. The western part (Gondwana sandstone) and the eastern part (Archaean gneiss) show similar morphometric characteristics. This is because of the intense weathering of the gneissic basement it forms a thick weathering profile and hence shows similar morphometric characteristics as the sandstone. However, in the middle part of the study area, due to hydrothermal activity, significant porosity reduction in the associated litho-units have been noticed. As a result, the middle zone serves as an impervious lithology and shows abnormal morphometric parameters especially the infiltration number.

Major rivers are following the regional faults and lineaments and hence show parallel to sub-parallel drainage. However, the fault-bounded blocks show dendritic to sub-dendritic drainage pattern. This suggests, though the faults and lineaments are of Proterozoic and Paleozoic origin, still they influence the present day drainage pattern which in turn indicates whatever topographic inversion has been taken place, there originated along these faults and lineaments, keeping those active in later times.

The study area is a mosaic of different lithounits of various origins. Upper and lower parts of the area are fluvial dominated representing sandstone and conglomerates of fan-delta environments. However, the middle part of the area is dominated by limestone of marine origin and later affected by various phases of faulting and mass movements. Intermittent marine transgression and regression events are well recorded in the fan-delta environment by the shift of strand line and change in litho-assemblage.

In the northern part of the area, a paleosol horizon has been observed developed on the sandstone. Petrographic analysis, geochemical analysis, magnetic susceptibility study of the paleosol suggests that it was formed in a confined shallow water environment. It indicates local regression events followed by a period of non-deposition. Presence of glauconite and illite in the same paleosol revealed through petrographic studies and XRD analysis suggests the presence of shallow marine environment at the basin boundary in isolation. The Chemical Index of Alteration (CIA) attests to the colder climate of about 12°C.. Abundance of cations in the partially detached basin indicates that basin margin in that zone had a poorly drained local basin probably in a shallow shelf marine environment cut-off from the main water body.

Middle part of the study area represents massive cherty limestone along with stromatolite (Penganga limestone) in which three mass flow sequences have been identified due to rift-related faulting. The sedimentation and mass flow events continued from Mid- to Neo-Proterozoic indicates consistency of rifting processes for a long time. Out of the three mass flow sequences, the earliest one is represented as boulders and the latter two are present in-situ. Occurrence of stromatolite in between the latter two flows indicates intermittent quiescent period in between the rifting processes. Similarity of the latter two flows is indicated by their facies assemblage and texture.

Comparing the facies assemblages and flow characteristics with the western margin, it is concluded that, both margins were responding similarly to the ongoing rifting processes in the Proterozoic time. However, the lateral continuity of different facies from margin to the basin interior were controlled by the initial slope and later modified by the dip angle of the faults associated.

In the lower part of the study area, fluvio-marine depositional setting was prevailing which formed the Dongargaon fan–delta. This depositional setting was constantly being affected by strandline fluctuation and basin-margin tectonism as evident from the facies assemblage. Temporal change in energy sequence is well observed in vertical facies variations. The fan-delta has is interfingred with the limestone at the periphery. Post depositional tectonism has affected the fan-delta to great extent resulting folding of at least two generations and deep seated faulting. As a result the whole litho-package shows steep dip towards the basin.

As a whole the present work can be concluded that, the area was tectonically vary active during Meso to Neoproterozoic times due to development of the rift basin, which had affected the litho-assemblage. Later tectonic activity were initiated along the basin-margin faults and the associated lineaments for which their impression still persists and effecting the Quaternary geomorphic process as well.

BIBLIOGRAPHY:

1. Amarasinghe, U., Chaudhuri, A., Collins, A.S., Deb, G. and Patranabis-Deb, S., 2015. Evolving provenance in the Proterozoic Pranhita-Godavari Basin, India. *Geoscience Frontiers*, 6(3), pp.453-463.
2. Amorosi, A., 1997. Detecting compositional, spatial, and temporal attributes of glaucony: a tool for provenance research. *Sedimentary Geology*, 109(1-2), pp.135-153.
3. Arndorff, L., 1993. Lateral relations of deltaic palaeosols from the Lower Jurassic Ronne formation on the island of Bornholm, Denmark. *Palaeogeography Palaeoclimatology Palaeoecology*, 100, pp.235–250.
4. Ashworth, P.J., Best, J.L. and Jones, M.A., 2007. The relationship between channel avulsion, flow occupancy and aggradation in braided rivers: insights from an experimental model. *Sedimentology*, 54(3), pp.497-513.
5. Audru, J.C., Bano, M., Begg, J., Berryman, K., Henys, S., Niviere, B., 2000. GPR investigations on active faults in urban areas: the Georise-NZ project in Wellington, New Zealand. *Earth and Planetary Science Letters*, 333, pp. 447-454.
6. Bagnold, R.A., 1954. Experiments on a gravity-free dispersion of large solid spheres in a Newtonian fluid under shear. In *Proceedings of the Royal Society of London A: Mathematical, Physical and Engineering Sciences*, 1160(225), pp.49-63.
7. Bandopadhyay, P.C., 1996. Facies associations and depositional environment of the Proterozoic carbonate-hosted microbanded manganese oxide ore deposit, Penganga Group, Godavari Rift basin, India. *Journal of Sedimentary Research*, 66(1), pp.197-208.
8. Basumallick, S., 1967. Problems of the Purana stratigraphy of the Godavari valley with special reference to the type area in Warangal district, Andhra Pradesh, India. *Quarterly Journal Geological, Mining and Metallurgical Society (India)*, 39, pp.115-127.
9. Beukes, N.J. and Lowe, D.R., 1989. Environmental control on diverse stromatolite morphologies in the 3000 Myr Pongola Supergroup, South Africa. *Sedimentology*, 36(3), pp.383-397.

10. Bhatt, N. and Bhonde, U., 2006. Geomorphic expression of late Quaternary sea level changes along the southern Saurashtra coast, western India. *Journal of Earth System Science*, 115(4), pp.395-402.
11. Bhatt, N. and Bhonde, U.A., 2003. Quaternary fluvial sequences of south Saurashtra, western India. *Current Science-Bangalore-*, 84(8), pp.1065-1071.
12. Bhatt, N., Patidar, A.K., Maurya, D.M. and Chamyal, L.S., 2006. Delineation of three shallow subsurface faults using GPR in south Saurashtra, western India. In 11th International Conference on GPR, Columbus, OH.
13. Bhosle, B., Parkash, B., Awasthi, A.K. and Pati, P., 2009. Use of digital elevation models and drainage patterns for locating active faults in the Upper Gangetic Plain, India. *International Journal of Remote Sensing*, 30(3), pp.673-691.
14. Birkeland, P.W., 1999. *Soils and Geomorphology*, (3rd Ed.). Oxford University Press, New York. 448 pp.
15. Biswas, S.K., 2003. Regional tectonic framework of the Pranhita–Godavari basin, India. *Journal of Asian Earth Sciences*, 21(6), pp.543-551.
16. Bose, P.K. and Sarkar, S., 1991. Basinal autoclastic mass flow regime in the Precambrian Chanda Limestone Formation, Adilabad, India. *Sedimentary geology*, 73(3-4), pp.299-315.
17. Bourrouilh, R., 1987. Evolutionary mass flow-megaturbidites in an interplate basin: example of the north Pyrenean basin. *Geo-marine letters*, 7(2), pp.69-81.
18. Bristow, C.S. and Jol, H.M., 2003. An introduction to ground penetrating radar (GPR) in sediments. Geological Society, London, Special Publications, 211(1), pp.1-7.
19. Brookfield, M.E., 1998. The evolution of the great river systems of southern Asia during the Cenozoic India-Asia collision: rivers draining southwards. *Geomorphology*, 22(3), pp.285-312.
20. Buchbinder, B., Benjamini, C., Mimran, Y. and Gvirtzman, G., 1988. Mass transport in Eocene pelagic chalk on the northwestern edge of the Arabian platform, Shefela area, Israel. *Sedimentology*, 35(2), pp.257-274.
21. Buol, S.W., Hole, F.D., McCracken., R.J., Southard, R.J., 1997. *Soil Genesis and Classification*. Iowa State University Press, Ames, Iowa. 527 pp.

22. Castelltort, S., Goren, L., Willett, S.D., Champagnac, J.D., Herman, F. and Braun, J., 2012. River drainage patterns in the New Zealand Alps primarily controlled by plate tectonic strain. *Nature Geoscience*, 5(10), pp.744-748.
23. Chakraborty, P.P., Sarkar, S. and Patranabis-Deb, S., 2012. Tectonics and sedimentation of Proterozoic basins of Peninsular India. *Proceedings of the Indian National Science Academy*, 78, pp.393-400.
24. Chakraborty, T. and Chaudhuri, A.K., 1993. Fluvial-aeolian interactions in a Proterozoic alluvial plain: example from the Mancheral Quartzite, Sullavai Group, Pranhita-Godavari Valley, India. *Geological Society, London, Special Publications*, 72(1), pp.127-141.
25. Chakraborty, T., 1991a. Sedimentology of a Proterozoic erg: the Venkatpur Sandstone, Pranhita-Godavari Valley, south India. *Sedimentology*, 38(2), pp.301-322.
26. Chakraborty, T., 1991b. Stratigraphy and sedimentation of the Proterozoic Sullavai Group in the south-central part of the Pranhita-Godavari Valley, Andhra Pradesh, India. Unpublished Ph. D. thesis, Jadavpur University.
27. Chakraborty, T., 1999. Reconstruction of fluvial bars from the Proterozoic Mancheral Quartzite, Pranhita–Godavari Valley, India. In: Smith, N. D. & Rogers, J. (eds.) *Fluvial sedimentology VI*, International Association of Sedimentologists, Special Publications, pp.451-466.
28. Chaudhuri, A. and Howard, J.D., 1985. Ramgundam Sandstone: a middle Proterozoic shoal-bar sequence. *Journal of Sedimentary Research*, 55(3), pp.392-397.
29. Chaudhuri, A., 1977. Influence of eolian processes on Precambrian sandstones of the Godavari valley, South India. *Precambrian Research*, 4(4), pp.339-360.
30. Chaudhuri, A., 1985. Stratigraphy of the Purana Supergroup around Ramgundam, Andhra Pradesh. *Journal of the Geological Society of India*, 26(5), pp.301-314.
31. Chaudhuri, A.K. and Deb, G.K., 2004. Proterozoic rifting in the Pranhita-Godavari Valley: implication on India-Antarctica linkage. *Gondwana Research*, 7(2), pp.301-312.

32. Chaudhuri, A.K., 1970. Precambrian stratigraphy and sedimentation around Ramgundam, Andhra Pradesh (Doctoral dissertation, PhD thesis, Calcutta University).
33. Chaudhuri, A.K., 2003. Stratigraphy and palaeogeography of the Godavari Supergroup in the south-central Pranhita-Godavari Valley, south India. *Journal of Asian Earth Sciences*, 21(6), pp.595-611.
34. Chaudhuri, A.K., Dasgupta, S., Bandyopadhyay, G., Sarkar, S., Bandyopadhyay, P.C. and Gopalan, K., 1989. Stratigraphy of the Penganga Group around Adilabad, Andhra Pradesh. *Geological Society of India*, 34(3), pp.291-302.
35. Chaudhuri, A.K., Deb, G.K. and Patranabis-Deb, S., 2015. Conflicts in stratigraphic classification of the Puranas of the Pranhita–Godavari Valley: review, recommendations and status of the ‘Penganga’ sequence. *Geological Society, London, Memoirs*, 43(1), pp.165-183.
36. Chaudhuri, A.K., Deb, G.K., Patranabis-Deb, S. and Sarkar, S., 2012. Paleogeographic and tectonic evolution of the Pranhita-Godavari Valley, Central India: a stratigraphic perspective. *American Journal of Science*, 312(7), pp.766-815.
37. Chaudhuri, A.K., Saha, D., Deb, G.K., Deb, S.P., Mukherjee, M.K. and Ghosh, G., 2002. The Purana basins of southern cratonic province of India—a case for Mesoproterozoic fossil rifts. *Gondwana Research*, 5(1), pp.23-33.
38. Chopra, R., Dhiman, R.D. and Sharma, P.K., 2005. Morphometric analysis of sub-watersheds in Gurdaspur district, Punjab using remote sensing and GIS techniques. *Journal of the Indian Society of Remote Sensing*, 33(4), pp.531-539.
39. Conrad, J.E., Hein, J.R., Chaudhuri, A.K., Patranabis-Deb, S., Mukhopadhyay, J., Deb, G.K. and Beukes, N.J., 2011. Constraints on the development of Proterozoic basins in central India from $^{40}\text{Ar}/^{39}\text{Ar}$ analysis of authigenic glauconitic minerals. *Geological Society of America Bulletin*, 123(1-2), pp.158-167.
40. Cook, H. E., 1979, Ancient continental slope sequences and their value in understanding modern slope development, in L. J. Doyle and O. H. Pilkey eds., *Geology of continental slopes: SEPM Special Publication*, 27, p. 287-305.

41. Cook, H.E., McDaniel, P.N., Mountjoy, E.W. and Pray, L.C., 1972. Allochthonous carbonate debris flows at Devonian bank ('reef') margins Alberta, Canada. *Bulletin of Canadian Petroleum Geology*, 20(3), pp.439-497.
42. Crookshank, H., 1963. Geology of southern Bastar and Jeypore from Bailadila range to Eastern Ghats. *Geological Survey of India, Memoir*, 87, pp.96-108.
43. Dabrio, C.J., 1990. Fan-Delta Facies Associations in Late Neogene and Quaternary Basins of Southeastern Spain. *Coarse-grained deltas*, pp.91-111.
44. Daniels, D.J., 1996. *Surface Penetrating Radar*, The Institute of Electrical Engineering. London.
45. Das, A.K. and Mukherjee, S., 2005. Drainage morphometry using satellite data and GIS in Raigad district, Maharashtra. *Geological Society of India*, 65(5), pp.577-586.
46. Das, D.P., Chakraborty, D.K. and Sarkar, K., 2003. Significance of the regional lineament tectonics in the evolution of the Pranhita–Godavari sedimentary basin interpreted from the satellite data. *Journal of Asian Earth Sciences*, 21(6), pp.553-556.
47. Deb, G.K., 2003. Deformation pattern and evolution of the structures in the Penganga Group, the Pranhita–Godavari Valley, India: probable effects of Grenvillian movement on a Mesoproterozoic basin. *Journal of Asian Earth Sciences*, 21(6), pp.567-577.
48. Deb, S.P., 2003. Proterozoic felsic volcanism in the Pranhita–Godavari valley, India: its implication on the origin of the basin. *Journal of Asian Earth Sciences*, 21(6), pp.623-631.
49. Desai, L., Jadhav, G., Shinde, V., Patil, S., 2016. Ground Penetrating Radar (GPR). *Imperial Journal of Interdisciplinary Research (IJIR)*, Vol. 2(6), pp. 1508-1511.
50. Dora, M.L. and Randive, K.R., 2015. Chloritisation along the Thanewasna shear zone, Western Bastar Craton, Central India: Its genetic linkage to Cu–Au mineralisation. *Ore Geology Reviews*, 70, pp.151-172.
51. Dora, M.L., Nair, K.K.K. and Shasidharan, K., 2011. Occurrence of platinum group minerals in the Western Bastar Craton, Chandrapur district, Maharashtra. *Current Science (Bangalore)*, 100(3), pp.399-404.

52. Driese, S.G., Medaris Jr, L.G., Ren, M., Runkel, A.C. and Langford, R.P., 2007. Differentiating pedogenesis from diagenesis in early terrestrial paleoweathering surfaces formed on granitic composition parent materials. *The Journal of geology*, 115(4), pp.387-406.
53. Driese, S.G., Srinivasan, K., Mora, C.I. and Stapor, F.W., 1994. Paleoweathering of Mississippian Monteagle Limestone preceding development of a lower Chesterian transgressive systems tract and sequence boundary, middle Tennessee and northern Alabama. *Geological Society of America Bulletin*, 106(7), pp.866-878.
54. Dżułyński, S. and Sanders, J.E., 1962. Current marks on firm mud bottoms. *Transactions of the Connecticut Academy of Arts and Sciences*, 42, pp.57-96.
55. Eberli, G.P., 1987. Carbonate turbidite sequences deposited in rift basins of the Jurassic Tethys Ocean (eastern Alps, Switzerland). *Sedimentology*, 34(3), pp.363-388.
56. Ekdale, A.A. and Bromley, R.G., 1988. Diagenetic microlamination in chalk. *Journal of Sedimentary Research*, 58(5), pp.857-861.
57. Eliet, P.P. and Gawthorpe, R.L., 1995. Drainage development and sediment supply within rifts, examples from the Sperchios basin, central Greece. *Journal of the Geological Society*, 152(5), pp.883-893.
58. Eyles, N., Clark, B.M. and Clague, J.J., 1987. Coarse-grained sediment gravity flow facies in a large supraglacial lake. *Sedimentology*, 34(2), pp.193-216.
59. Faniran, A., 1968. The index of drainage intensity-A provisional new drainage factor. *Australian Journal of Science*, 31, pp.328-330.
60. Fastovsky, D.E., McSweeney, K., 1987. Paleosols spanning the Cretaceous-Paleogene transition, eastern Montana and western North Dakota. *Geol. Soc. Am. Bull.* 99, pp.66-77.
61. Feakes, C.R., Retallack, G.J., 1988. Recognition and chemical characterization of fossil soils developed on alluvium; a Late Ordovician example. In: Reinhardt, J., Sigleo, W.R. (Eds.), *Paleosols and Weathering through Geologic Time; Principles and Applications*. Geological Society of America Special Paper, 216, pp.35-48.

62. Fedo, C.M., Nesbitt, H.W. and Young, G.M., 1995. Unraveling the effects of potassium metasomatism in sedimentary rocks and paleosols, with implications for paleoweathering conditions and provenance. *Geology*, 23(10), pp.921-924.
63. Fisher, C.S., Stewart, R.R., Jol, H.M., 2000. Processing ground penetrating radar. In: *Proceedings of Eighth International Conference on Ground Penetrating Radar*, vol. 4084. University of Queensland. SPIE.
64. Fisher, R.V., 1971. Features of coarse-grained, high-concentration fluids and their deposits. *Journal of Sedimentary Research*, 41(4), pp.916-927.
65. Flügel, E., 2012. *Microfacies analysis of limestones*. Springer Science & Business Media.
66. Gajbhiye, N.G., 1965. A note on the occurrence of Barytes in Phutana area, Chandrapur District, Maharashtra in toposheet 56 M/9. GSI report, GSI Portal, 2010.
67. Galán, E., 2006. Genesis of clay minerals. *Developments in clay science*, 1, pp.1129-1162.
68. Galloway, W.E., 1975. Process framework for describing the morphologic and stratigraphic evolution of deltaic depositional systems, pp.87-98.
69. Galloway, W.E., 1976. Sediments and stratigraphic framework of the Copper River fan-delta, Alaska. *Journal of Sedimentary Research*, 46(3), pp.726-737.
70. Gawthorpe, R.L. and Colella, A., 2009. Tectonic controls on coarse-grained delta depositional systems in rift basins. *Systems in Rift Basins. Coarse-Grained Deltas: Special Publication 10 of the International Association of Sedimentologists*, 27, p.113.
71. Gawthorpe, R.L., Collier, R.L., Alexander, J., Bridge, J.S. and Leeder, M.R., 1993. Ground penetrating radar: application to sandbody geometry and heterogeneity studies. *Geological Society, London, Special Publications*, 73(1), pp.421-432.
72. Geel, T., 2000. Recognition of stratigraphic sequences in carbonate platform and slope deposits: empirical models based on microfacies analysis of Palaeogene deposits in southeastern Spain. *Palaeogeography, Palaeoclimatology, Palaeoecology*, 155(3), pp.211-238.

73. Ghosh, G. and Saha, D., 2003. Deformation of the Proterozoic Somanpalli Group, Pranhita–Godavari valley, South India—implication for a Mesoproterozoic basin inversion. *Journal of Asian Earth Sciences*, 21(6), pp.579-594.
74. Gloppen, T. G., and Steel, R. 7., 1981, The deposits, internal structure, and geometry in six alluvial fan-fan delta bodies (Devonian-Norway)—A study in the significance of bedding sequence in conglomerates, in Ethridge, F. G., and Flores, R. M., eds., *Recent and ancient nonmarine depositional environments: Models for exploration: Society of Economic Paleontologists and Mineralogists Special Publication 31*, pp. 49-69.
75. Gregory, L.C., Meert, J.G., Bingen, B., Pandit, M.K. and Torsvik, T.H., 2009. Paleomagnetism and geochronology of the Malani Igneous Suite, Northwest India: implications for the configuration of Rodinia and the assembly of Gondwana. *Precambrian Research*, 170(1), pp.13-26.
76. Grimley, D.A. and Vepraskas, M.J., 2000. Magnetic susceptibility for use in delineating hydric soils. *Soil Science Society of America Journal*, 64(6), pp.2174-2180.
77. Hallows K.A.K., 1923. Basic and ultrabasic members of the series in the Central Provinces. *G, F, 1. Rec.v.55, pt. 3*.
78. Hamer, J.M.M., Sheldon, N.D., Nichols, G.J., Collinson, M.E., 2007. Late Oligocene–Early Miocene palaeosols of distal fluvial systems, Ebro Basin, Spain. *Palaeogeography, Palaeoclimatology, Palaeoecology* 247, pp.220-235.
79. Hein, F.J., 1982. Depositional mechanisms of deep-sea coarse clastic sediments, Cap Enrage Formation, Quebec. *Canadian Journal of Earth Sciences*, 19(2), pp.267-287.
80. Hempton, M.R. and Dunne, L.A., 1984. Sedimentation in pull-apart basins: active examples in eastern Turkey. *The Journal of Geology*, 92(5), pp.513-530.
81. Heron, A.M., 1949. Synopsis of Purana formation of Hyderabad. *Journal of Hyderabad Geological Survey* 5 (2), pp.14-17.
82. Hiscott, R.N. and Middleton, G.V., 1979. Depositional mechanics of thick-bedded sandstones at the base of a submarine slope, Tourelle Formation (Lower Ordovician), Quebec, Canada. *The Society of Economic Paleontologists and Mineralogists Special Publication*, 27, pp.307-326.

83. Hobbs, W.H., 1904. Lineaments of the Atlantic border region. *Geological Society of America Bulletin*, 15(1), pp.483-506.
84. Hobson, J.P., Caldwell, C.D. and Toomey, D.F., 1985. Early Permian deep-water allochthonous limestone facies and reservoir, west Texas. *AAPG Bulletin*, 69(12), pp.2130-2147.
85. Holland, H.D., 1984. *The chemical evolution of the atmosphere and oceans*. Princeton University Press, Princeton, New Jersey, USA. 583 pp.
86. Holland, H.D., 1994. Early Proterozoic atmospheric change. In *Early Life on Earth: Nobel Symposium, 84*, Columbia University Press.
87. Holland, H.D., Feakes, C.R. and Zbinden, E.A., 1989. The Flin Flon paleosol and the composition of the atmosphere 1.8 BYBP. *American Journal of Science*, 289(4), pp.362-389.
88. Holland, T.H., 1906. Classification of the Indian strata. Presidential Address, *Transaction Mining and Geological Institute, India* 1, pp.1-17.
89. Hornung, J. and Hinderer, M., 2011. Depositional dynamics and preservation potential in a progradational lacustrine fluvio-deltaic setting: Implications for high-resolution sequence stratigraphy (Upper Triassic, Northwestern China). *From River to Rock Record: The Preservation of Fluvial Sediments and Their Subsequent Interpretation*, pp.281-310.
90. Horton, R.E., 1932. Drainage basin characteristics. *Transactions of American Geophysical Union*, v.13, pp.350–361.
91. Horton, R.E., 1945. Erosional development of streams and their drainage basins; hydrophysical approach to quantitative morphology. *Geological society of America bulletin*, 56(3), pp.275-370.
92. Howard, A.D., 1967. Drainage analysis in geologic interpretation: a summation. *American Association of Petroleum Geologists bulletin*, 51(11), pp.2246-2259.
93. Hughes, T.W.H., 1877. Wardha valley coal fields. *Geological Society of India Memoir*. 13. pp.1-154.
94. Hwang, I.G., Chough, S.K., Hong, S.W. and Choe, M.Y., 1995. Controls and evolution of fan delta systems in the Miocene Pohang Basin, SE Korea. *Sedimentary Geology*, 98(1-4), pp.147-179.

95. Jol, H.M. and Bristow, C.S., 2003. GPR in sediments: advice on data collection, basic processing and interpretation, a good practice guide. Geological Society, London, Special Publications, 211(1), pp.9-27.
96. Kalaivanan, K., Gurugnanam, B. and Suresh, M. 2014. GIS based morphometric analysis of gadilam river basin, Tamil Nadu, India, International Journal of Advanced Research, 2014; 7(2), pp.1015-1022.
97. Kim, W., Paola, C., Swenson, J.B. and Voller, V.R., 2006. Shoreline response to autogenic processes of sediment storage and release in the fluvial system. Journal of Geophysical Research (Earth Surface), pp.111.
98. King, W., 1881, Geology of the Pranhita-Godavari Valley: Geological Survey of India Memoir 19, pp. 151–311.
99. Klein, C. and Dutrow, B., 2008. Mineral Science. Hoboken.
100. Kraus, M.J. and Aslan, A., 1993. Eocene hydromorphic paleosols: significance for interpreting ancient floodplain processes. Journal of Sedimentary Research, 63(3), pp. 453-463.
101. Kraus, M.J. and Aslan, A., 1999. Palaeosol sequences in floodplain environments: a hierarchical approach. Palaeoweathering, palaeosurfaces and related continental deposits, pp.303-321.
102. Kulkarni, A.M., 1964. Geology of a portion of Chanda District in toposheet 56 M/9 and geochemical prospecting for copper mineralization near Thanewasna, Chanda District, Maharashtra. . GSI report, GSI Portal-2010, pp.1963-64.
103. Lander, R.H., Bloch, S., Mehta, S. and Atkinson, C.D., 1991. Burial diagenesis of Paleosols in the giant Yacheng gas field, People's Republic of China; bearing on illite reaction pathways. Journal of Sedimentary Research, 61(2), pp.256-268.
104. Lakshminarayana, 1997. Proterozoic intracratonic Godavari rift development at right angle to the Eastern Ghat Mobile Belt: An example for collision-induced rifting in SE India. Current Science, 73(5), pp.444-450.
105. Leeder, M.R., 1988. Development of alluvial fans and fan deltas in neotectonic extensional setting: implications for the interpretation of basin-fills. Fan Deltas: Sedimentology and Tectonic Setting, pp.173-185.

106. Li, Y.H., 2000. *A Compendium of Geochemistry*. Princeton University Press, Princeton. 475p.
107. Liivamägi, S., Somelar, P., Vircava, I., Mahaney, W.C., Kirs, J. and Kirsimäe, K., 2015. Petrology, mineralogy and geochemical climofunctions of the Neoproterozoic Baltic paleosol. *Precambrian Research*, 256, pp.170-188.
108. Lin, Z. and Oguchi, T., 2004. Drainage density, slope angle, and relative basin position in Japanese bare lands from high-resolution DEMs. *Geomorphology*, 63(3), pp.159-173.
109. Logan, B.W., Rezak, R. and Ginsburg, R.N., 1964. Classification and environmental significance of algal stromatolites. *The Journal of Geology*, 72(1), pp.68-83.
110. Martindale, R.C., Strauss, J.V., Sperling, E.A., Johnson, J.E., Van Kranendonk, M.J., Flannery, D., French, K., Lepot, K., Mazumder, R., Rice, M.S. and Schrag, D.P., 2015. Sedimentology, chemostratigraphy, and stromatolites of lower Paleoproterozoic carbonates, Turee Creek Group, Western Australia. *Precambrian Research*, 266, pp.194-211.
111. Maynard, J.B., 1992. Chemistry of modern soils as a guide to interpreting Precambrian paleosols. *The Journal of Geology*, 100(3), pp.279-289.
112. McCarthy, S. M.; Powell, C. A.: and Rogers, J. J. W., 1983, A relative residual study of the southern peninsula of India using the Gauribidanur seismic array, in Naqvi, S. M., and Rogers, J. J. W., eds., *Precambrian of South India: Geological Society of India Memoirs 4*, pp.525-552.
113. McLaughlin, R.J. and Nilsen, T.H., 1982. Neogene non-marine sedimentation and tectonics in small pull-apart basins of the San Andreas fault system, Sonoma County, California. *Sedimentology*, 29(6), pp.865-876.
114. McPherson, J.G., Shanmugam, G. and Moiola, R.J., 1987. Fan-deltas and braid deltas: Varieties of coarse-grained deltas. *Geological Society of America Bulletin*, 99(3), pp.331-340.
115. McRae, S.G., 1972. Glauconite. *Earth-Science Reviews*, 8(4), pp.397-440.
116. Middleton, G.V., 1967. Experiments on density and turbidity currents: III. Deposition of sediment. *Canadian Journal of Earth Sciences*, 4(3), pp.475-505.

117. Middleton, G.V., 1967. The orientation of concavo-convex particles deposited from experimental turbidity currents. *Journal of Sedimentary Research*, 37(1), pp.229-232.
118. Mitchum, R.M., Jr., Vail, P. R. and Thompson, S. III., 1977. Seismic stratigraphy and global changes of sea-level, part 2, the depositional sequence as a basic unit for stratigraphic analysis. In: Clayton, C. E. (ed.) *Seismic Stratigraphy – Applications to Hydrocarbon Exploration*. American Association of Petroleum Geologists, *Memoirs*, 26, pp.53–62.
119. Montgomery, D.R. and Fofoula-Georgiou, E., 1993. Channel network source representation using digital elevation models. *Water Resources Research*, 29(12), pp.3925-3934.
120. Mountjoy, E.W., Cook, H.E., Pray, L.C. and McDaniel, P.N., 1972. Allochthonous carbonate debris flows—worldwide indicators of reef complexes, banks or shelf margins. In *Reports of the 24th International Geological Congress*, Montreal (pp. 172-189).
121. Munsell Color., 2005. *Munsell Soil Colour Charts: Matte Collection*. Macbeth Division of Kollmorgen Corporation, Baltimore.
122. Muravchik, M., Bilmes, A., D'Elia, L. and Franzese, J.R., 2014. Alluvial fan deposition along a rift depocentre border from the Neuquén Basin, Argentina. *Sedimentary Geology*, 301, pp.70-89.
123. Nageswara Rao, C., 1964. Pakhals and Sullavais around Ramagundam Railway Station, Karimnagar District., *AP Journal of the Indian Geological Scientists Association*, 4, pp.63-67.
124. Narain, H., 1973. Crustal structure of the Indian subcontinent. *Tectonophysics*, 20(1-4), pp.249-260.
125. Neal, A. and Roberts, C.L., 2000. Applications of ground-penetrating radar (GPR) to sedimentological, geomorphological and geoarchaeological studies in coastal environments. *Geological Society, London, Special Publications*, 175(1), pp.139-171.
126. Neal, A., 2004. Ground-penetrating radar and its use in sedimentology: principles, problems and progress. *Earth-science reviews*, 66(3), pp.261-330.

127. Nemec, W., 1990. Deltas-Remarks on terminology and classification. In: A. Collela and D.B. Prior (Editors), Coarse Grained Deltas. International Association of Sedimentology, Special Publication, 10, pp.29-73.
128. Nesbitt, H. W. and Young, G.M., 1982. Early Proterozoic climates and plate motions inferred from major element chemistry of lutites. *Nature*, 299, pp.715-717.
129. Nordt, L.C., Driese, S.G., 2012. New weathering index improves paleorainfall estimates from vertisols. *Geology*, 38, pp.407-410.
130. O'Callaghan, J.F. and Mark, D.M., 1984. The extraction of drainage networks from digital elevation data. *Computer vision, graphics, and image processing*, 28(3), pp.323-344.
131. Odin, G.S. and Fullagar, P.D., 1988. Geological significance of the glaucony facies. *Marine Clays*. Amsterdam: Elsevier, pp.295-332.
132. Odin, G.S. and Matter, A., 1981. De glauconiarum origine. *Sedimentology*, 28(5), pp.611-641.
133. Orton, G.J., 1988. A spectrum of Middle Ordovician fan deltas and braidplain deltas, North Wales: a consequence of varying fluvial clastic input. *Fan deltas: Sedimentology and tectonic settings*, pp.23-49.
134. Parker, G., Akamatsu, Y., Muto, T. and Dietrich, W., 2004. Modeling the effect of rising sea level on river deltas and long profiles of rivers. In *Proceedings July*, pp. 27-28.
135. Pati, 2010 (Un Pub.). Large Scale Geological Mapping of Archaean-Proterozoic Boundary Zone around Sukwasi, Southeast of Heti PGE Prospect, Chandrapur District, Maharashtra. Geological Survey of India, Central Region, Nagpur.
136. Pati, P., Parkash, B., Awasthi, A.K., Acharya, V. and Singh, S., 2011. Concealed thrusts in the Middle Gangetic plain, India—A ground penetrating radar study proves the truth against the geomorphic features supporting normal faulting. *Journal of Asian Earth Sciences*, 40(1), pp.315-325.
137. Pettijohn, F.J., 1984. *Sedimentary Rocks*. 3rd edn. CBS Publishers and Distributors, New Delhi, 628 p.
138. Planavsky, N., Rouxel, O., Bekker, A., Shapiro, R., Fralick, P. and Knudsen, A., 2009. Iron-oxidizing microbial ecosystems thrived in late Paleoproterozoic

- redox-stratified oceans. *Earth and Planetary Science Letters*, 286(1), pp.230-242.
139. Postma G., 1990. Depositional architecture and facies of a river and fan deltas: a synthesis. In: A. Collela and D.B. Prior (Editors), *Coarse Grained Deltas*. Special Publication, International Association of Sedimentology, 10, pp.13-27.
140. Postma, G. and Cruickshank, C., 1988. Sedimentology of a late Weichselian to Holocene terraced fan delta, Varangerfjord, northern Norway. *Fan deltas: Sedimentology and tectonic settings*, pp.144-157.
141. Postma, G., 1984. Mass-flow conglomerates in a submarine canyon: Abrioja fan-delta, Pliocene, southeast Spain. *Canadian Society of Petroleum Geologists, Memoir*, 10, pp.237-258.
142. Postma, G., 1995. Sea-level-related architectural trends in coarse-grained delta complexes. *Sedimentary Geology*, 98(1-4), pp.3-12.
143. Prochnow, S.J., Nordt, L.C., Atchley, S.C. and Hudec, M.R., 2006. Multi-proxy paleosol evidence for middle and late Triassic climate trends in eastern Utah. *Palaeogeography, Palaeoclimatology, Palaeoecology*, 232(1), pp.53-72.
144. Prothero, D.R. and Schwab, F., 2004. *Sedimentary geology*. Macmillan.
145. Radhakrishna, B.P. and Naqvi, S.M., 1986. Precambrian continental crust of India and its evolution. *The Journal of Geology*, 94(2), pp.145-166.
146. Rajesham, T., Bhaskar Rao, Y. J. and Murli, K. S. 1993. The Karimnagar granulite terrane – a new sapphirine bearing granulite province, south India. *Journal of the Geological Society, India*, 41, pp.51–59.
147. Ramachandra, H.M., Mishra, V.P., Roy, A. and Dutta, N.K., 1998. Evolution of the Bastar Craton—a critical review of gneiss-granitoids and supracrustal belts. In *MS Krishnan Centenary Commemorative National Seminar, Calcutta*, pp.144-50.
148. Ramachandra, H.M., Roy, A., Mishra, V.P. and Dutta, N.K., 2001. A critical review of the tectonothermal evolution of the Bastar Craton. *Geological Survey of India Special Publication*, 55, pp.161-180.
149. Rao, K.S., Rao, T.S. and Nair, S.R., 1979a. Stratigraphy of the upper Precambrian Albaka belt, east of the Godavari River in Andhra Pradesh and Madhya Pradesh. *Geological Society of India*, 20(5), pp.205-213.

150. Rao, K.S., Subbaraju, M., Rao, T.S., Immamalikhan, M. and Silekar, V.S., 1979b. Tectonic evolution of the Godavari graben. In IVth International Gondwana Symposium Vol.2, pp.889-900.
151. Rao, V.V. and Reddy, P.R., 2002. A Mesoproterozoic supercontinent: evidence from the Indian shield. *Gondwana Research*, 5(1), pp.63-74.
152. Reid, R.P., Visscher, P.T., Decho, A.W., Stolz, J.F., Bebout, B.M., Dupraz, C., Macintyre, I.G., Pearl, H.W., Pinckney, J.L., Prufert-Bebout, L. and Steppe, T.F., 2000. The role of microbes in accretion, lamination and early lithification of modern marine stromatolites. *Nature*, 406(6799), pp.989-992.
153. Retallack, G., 1986. Reappraisal of a 2200 Ma-old paleosol near Waterval Onder, South Africa. *Precambrian Research*, 32(2-3), pp.195-232.
154. Retallack, G., 1997. *A Colour Guide to Paleosols*. JohnWiley and Sons, New York.
155. Retallack, G.J., 1988. Field recognition of Paleosols, Geological Society of America, Special Paper, 29, pp.1-20.
156. Retallack, G.J., 1991. Untangling the effects of burial alteration and ancient soil formation. *Annual Review of Earth and Planetary Sciences*, 19(1), pp.183-206.
157. Retallack, G.J., 1992. How to find a Precambrian paleosol. In: Schidlowski, M., Golubic, S., Kimberley, M.M., McKirdy, D.M., Trudinger, P.A. (Eds.), *Early Organic Evolution and Mineral and Energy Resources*. Springer, Berlin, pp.16–30.
158. Retallack, G.J., 1998. Fossil Soils and Completeness of the Rock and Fossil Records, in: *The Adequacy of the Fossil Record*. pp.133-163.
159. Retallack, G.J., 2000. Depth to pedogenic carbonate horizon as a paleoprecipitation indicator? Comment and reply. *Geology* 28, pp.572-573.
160. Retallack, G.J., 2001. Cenozoic expansion of grasslands and climatic cooling. *The Journal of Geology*, 109(4), pp.407-426.
161. Retallack, G.J., Grandstaff, D., Kimberley, M., 1984. The promise and problems of Precambrian paleosols. *Episodes* 7, pp.8–12.
162. Retallack, G.J., Sheldon, N.D., Cogoini, M. and Elmore, R.D., 2003. Magnetic susceptibility of early Paleozoic and Precambrian paleosols. *Palaeogeography, Palaeoclimatology, Palaeoecology*, 198(3), pp.373-380.

163. Reynolds, J.M., 1997. Ground penetrating radar. An introduction to applied and environmental geophysics. John Wiley & Sons, Chichester, UK, pp.681-749.
164. Rezak, R., 1957. Stromatolites of the Belt series in Glacier National Park and vicinity, Montana (No. 294-D). United States Geological Survey.
165. Robinson, P.L., 1971. A problem of faunal replacement on Permo-Triassic continents. *Palaeontology*, v. 14, pp. 131-153.
166. Roep, T., and Kleverlaan, K., 1983. Excursion to a sub-marine fan complex of Tortonian age and geology of Tabernas Basin. Almeria, SE Spain, University of Amsterdam. pp.13.
167. Rogers, J.J., 1986. The Dharwar craton and the assembly of peninsular India. *The Journal of Geology*, 94(2), pp.129-143.
168. Rust, B.R. and Koster, E.H., 1984. Coarse alluvial deposits. In *Facies models*. Toronto: Geological Association of Canada. Vol. 1, pp.53-69.
169. Ruxton, B.P., 1968. Measures of the degree of chemical weathering of rocks. *The Journal of Geology*, 76(5), pp.518-527.
170. Saha, D. and Chaudhuri, A.K., 2003. Deformation of the Proterozoic successions in the Pranhita–Godavari basin, south India—a regional perspective. *Journal of Asian Earth Sciences*, 21(6), pp.557-565.
171. Saha, D. and Ghosh, G., 1987. Tectonic setting of Proterozoic sediments around Somanpalli, Godavari valley. *Journal Indian Association of Sedimentologists*, 7, pp.29-46.
172. Saha, D. and Patranabis-Deb, S., 2014. Proterozoic evolution of Eastern Dharwar and Bastar cratons, India—an overview of the intracratonic basins, craton margins and mobile belts. *Journal of Asian Earth Sciences*, 91, pp.230-251.
173. Saha, D. and Ghosh, G. 1998. Lithostratigraphy of deformed Proterozoic rocks from around the confluence of Godavari and Indravati Rivers, South India. *Indian Journal of Geology*, 70, pp. 217–230.
174. Sarkar, A., Sarkar, G., Paul, D.K. and Mitra, N.D., 1990. Precambrian geochronology of the central Indian shield—a review. Geological Survey of India, Special Publication, 28, pp.353-382.

175. Sarkar, G., Corfu, F., Paul, D.K., McNaughton, N.J., Gupta, S.N. and Bishui, P.K., 1993. Early Archean crust in Bastar Craton, Central India—a geochemical and isotopic study. *Precambrian Research*, 62(1-2), pp.127-137.
176. Sarkar, S. and Bose, P.K., 1992. Variations in Late Proterozoic stromatolites over a transition from basin plain to nearshore subtidal zone. *Precambrian research*, 56(1-2), pp.139-157.
177. Sarkar, S., Bose, P.K. and Friedman, G.M., 1993. Ordered, stoichiometric and sucrosic dolomitization: A result of prolonged exposure to warm sea water: Proterozoic Chanda Limestone, Adilabad, India. *Carbonates and Evaporites*, 8(1), pp.109-117.
178. Sarkar, S.C. and Gupta, A., 2012. *Crustal evolution and metallogeny in India*. Cambridge University Press.
179. Sarma, B.S.P. and Rao, M.K., 2005. Basement structure of Godavari basin, India—Geophysical modelling. *Current Science*, 88(7), pp.1172-1175.
180. Schumm, S.A., 1963. Sinuosity of alluvial rivers on the Great Plains. *Geological Society of America Bulletin*, 74(9), pp.1089-1100.
181. Schumm, S.A., Mosley, M.P. and Weaver, W., 1987. *Experimental fluvial geomorphology*.
182. SenGupta, S., 1966. Studies on orientation and imbrication of pebbles with respect to cross-stratification. *Journal of Sedimentary Research*, 36(2), pp.362-369.
183. Shahid, S., Nath, S. and Roy, J., 2000. Groundwater potential modelling in a soft rock area using a GIS. *International Journal of Remote Sensing*, 21(9), pp.1919-1924.
184. Sheldon, N.D., 2006. Precambrian paleosols and atmospheric CO₂ levels. *Precambrian Research*, 147(1), pp.148-155.
185. Sheldon, N.D., Retallack, G.J. and Tanaka, S., 2002. Geochemical climofunctions from North American soils and application to paleosols across the Eocene-Oligocene boundary in Oregon. *The Journal of geology*, 110(6), pp.687-696.
186. Sheldon, N.D., Tabor, N.J., 2009. Quantitative paleoenvironmental and paleoclimatic reconstruction using paleosols. *Earth Science Reviews*, 95, pp.1–52.
187. Singh, R., Kroes, J.G., Van Dam, J.C. and Feddes, R.A., 2006. Distributed ecohydrological modelling to evaluate the performance of irrigation system in

- Sirsa district, India: I. Current water management and its productivity. *Journal of Hydrology*, 329(3), pp.692-713.
188. Sloss, L.L., 1984. Comparative anatomy of cratonic unconformities. pp.1-6.
189. Smith, K.G., 1950. Standards for grading texture of erosional topography. *American Journal of Science*, 248(9), pp.655-668.
190. Sreenivasa Rao, T. 1994. The Godavari Valley – a rift or raft. In: Guha, P. K. S., Sengupta, S., Ayyasami, K. & Ghosh, R. N. (eds) *Gondwana Nine V*. Oxford and IBH, New Delhi and Kolkata, 2.
191. Sreenivasa Rao, T., 1985. A note on the stratigraphy of the upper Precambrian sediments around Ramagundam, Andhra Pradesh. *Indian Minerals*, 39(3), pp.9-11.
192. Sreenivasa Rao, T., 1987. The Pakhal basin: A perspective. *Purana basins of Peninsular India*. Geological Society of India, Bangalore, *Memoirs*, (6), pp.161-187.
193. Sreenivasa Rao, T., 2001. The “Purana” formations of the Godavari Valley: a conspectus. *Geological Survey of India Special Publication, Serial, 55*, pp.67-76.
194. Steel, R.J., 1976. Devonian basins of western Norway-sedimentary response to tectonism and to varying tectonic context. *Tectonophysics*, 36(1-3), pp.207-224.
195. Stein, H.J., Hannah, J.L., Zimmerman, A., Markey, R.J., Sarkar, S.C. and Pal, A.B., 2004. A 2.5 Ga porphyry Cu–Mo–Au deposit at Malanjkhand, central India: implications for Late Archean continental assembly. *Precambrian Research*, 134(3), pp.189-226.
196. Strahler, A.N., 1956. Quantitative slope analysis. *Geological Society of America Bulletin*, 67(5), pp.571-596.
197. Strahler, A.N., 1956. The nature of induced erosion and aggradation. *Man's Role in Changing the Face of the Earth*. Univ. Chicago Press, Chicago, pp.621-638.
198. Strahler, A.N., 1964. Quantitative geomorphology of drainage basin and channel networks. *Handbook of applied hydrology*.
199. Subba Raju, M., Sreenivasa Rao, T., Setti, D.N. and Reddy, B.S.R., 1978. Recent advances in our knowledge of the Pakhal Supergroup with special reference to

- the central part of the Godavari Valley. Records of Geological Survey of India, 110(2), pp.39-59.
200. Tandon, S.K., Gibling, M.R., 1997. Calcretes at sequence boundaries in upper carboniferous cyclothems of the Sydney Basin, Atlantic Canada. *Sediment. Geol.* 112, pp.43–67.
201. Tandon, S.K., Sood, A., Andrews, J.E., Dennis, P.F., 1995. Palaeoenvironments of the dinosaur-bearing Lameta Beds. *Palaeogeography Palaeoclimatology Palaeoecology* 117, pp. 153–184.
202. Thakkar, M.G., Maurya, D.M., Rachna Raj and Chamyal, L.S., 2001. Morphotectonic analysis of Khari drainage basin in Mainland Kachchh: Evidence for neotectonic activity along transverse faults. In *Structure and Tectonics of Indian Plate*, Gupta, L.N., Kumar, R. and Gill, G.S., (eds.), pp.205-220.
- 203.** Thakkar, M.G., Maurya, D.M., Raj, R. and Chamyal, L.S., 1999. Quaternary tectonic history and terrain evolution of the area around Bhuj, Mainland Kachchh, western India. *Journal-Geological Society of India*, 53, pp.601-610.
204. Torsvik, T.H., Carter, L.M., Ashwal, L.D., Bhushan, S.K., Pandit, M.K. and Jamtveit, B., 2001. Rodinia refined or obscured: palaeomagnetism of the Malani igneous suite (NW India). *Precambrian Research*, 108(3), pp.319-333.
205. Tucker, G.E. and Bras, R.L., 1998. Hillslope processes, drainage density, and landscape morphology. *Water Resources Research*, 34(10), pp.2751-2764.
206. Valdiya, K.S., 2010. *The making of India: Geodynamic Evolution*. Macmillan Publishers India Ltd, New Delhi (pp. 816).
207. Van Dam, R.L. and Schlager, W., 2000. Identifying causes of ground-penetrating radar reflections using time-domain reflectometry and sedimentological analyses. *Sedimentology*, 47(2), pp.435-449.
208. Van Dam, R.L., Van Den Berg, E.H., Schaap, M.G., Broekema, L.H. and Schlager, W., 2003. Radar reflections from sedimentary structures in the vadose zone. *Geological Society, London, Special Publications*, 211(1), pp.257-273.
209. Van Dijk, M., Postma, G. and Kleinhans, M.G., 2009. Autocyclic behaviour of fan deltas: an analogue experimental study. *Sedimentology*, 56(5), pp.1569-1589.
210. Van Loon, A.T., Dechen, S., Yuan, W. and Min, L., 2013. Deformed stromatolites in marbles of the Mesoproterozoic Wumishan Formation as evidence for

- synsedimentary seismic activity. *Journal of Palaeogeography*, 2(4), pp.390-401.
211. Viaplana-Muzas, M., Babault, J., Dominguez, S., Van den Driessche, J. and Legrand, X., 2015. Drainage network evolution and patterns of sedimentation in an experimental wedge. *Tectonophysics*, 664, pp.109-124.
212. Vinogradov, A., Tugarinov, A.L., Zhykov, C., Stapnikova, N., Bibikova, E. and Khorre, K., 1964. Geochronology of Indian Precambrian. In Report of the 22nd International Congress, New Dehli, 10, pp.553-567.
213. Walker, R.G., 1975. Generalized facies models for resedimented conglomerates of turbidite association. *Geological Society of America Bulletin*, 86(6), pp.737-748.
214. Walker, R.G., 1978. Deep-water sandstone facies and ancient submarine fans: models for exploration for stratigraphic traps. *American Association of Petroleum Geologists Bulletin*, 62(6), pp.932-966.
215. Walter, M.R., Buick, R. and Dunlop, J.S.R., 1980. Stromatolites 3,400–3,500 Myr old from the North Pole area, Western Australia. *Nature*, 284(5755), pp.443-445.
216. Weaver, C.E., 1968. Relations of composition to structure of dioctahedral 2: 1 clay minerals. *Clays and Clay Minerals*, 16, pp.51-61.
217. Webb, G.E., 1994. Paleokarst, paleosol, and rocky-shore deposits at the Mississippian-Pennsylvanian unconformity, northwestern Arkansas. *Geological Society of America Bulletin*, 106(5), pp.634-648.
218. Wilson, P.D.J.L., 1975. The lower carboniferous Waulsortian facies. In *Carbonate Facies in Geologic History*. Springer, New York, pp. 148-168.
219. Wolman, M.G., Miller, J.P. and Leopold, L.B., 1964. *Fluvial processes in geomorphology*. San Francisco.
220. Wright, V.P., 1994. Paleosols in shallow marine carbonate sequences. *Earth Science Reviews*, 35, pp.367–395.
221. Wright, V.P., Platt, N.H., 1995. Seasonal wetland carbonate sequences and dynamic catenas: a re-appraisal of palustrine limestones. *Sedimentary Geology*, 99, pp.65–71.

222. Zbinden, E.A., Holland, H.D., Feakes, C.R. and Dobos, S.K., 1988. The Sturgeon Falls paleosol and the composition of the atmosphere 1.1 Ga BP. *Precambrian Research*, 42(1-2), pp.141-163.
223. Zernitz, E.R., 1932. Drainage patterns and their significance. *The Journal of Geology*, 40(6), pp.498-521.